

**Vibration absorption in the tennis grip and the effects on  
racquet dynamics**

*Submitted in fulfilment of the requirements for the degree of Doctor of  
Philosophy*

**By**

**Nicholas James Savage BSc.**

**Supervisor**

**Professor Aleksandar Subic**

**School of Aerospace, Mechanical and Manufacturing Engineering**

**RMIT University**

**Submitted August 2006**

## Declaration

I certify the work presented in the thesis is that of the candidate alone, except where due acknowledgement is given, and has not previously been submitted, in whole or in part, to qualify for any other academic awards. The content of the thesis is the result of the work carried out since the official commencement date of the approved research program. Any editorial work, paid or unpaid, carried out by a third party contribution is acknowledged.

Signed

Nicholas James Savage

Date

# Acknowledgements

I would like to thank everyone who has contributed to my research. This thesis has been a long and difficult adventure that has taught me much more than I expected. The work presented in this thesis would not have been possible without the help and advice of many people.

I would firstly like to thank my family for supporting me throughout my PhD. My father, Neil Savage, has been instrumental in helping me complete my thesis, for which I am eternally grateful. His knowledge and support have helped me conquer the challenges I have faced during my candidature. My mother has also been incredibly supportive during my PhD and this has helped me keep my feet on the ground and achieve my best. Grandparents are great people and should be treated as such. My grandparents (Edith, Joan and George) have shared their knowledge, experience and support with me throughout my research, and it has proven invaluable for helping me complete my work. To my family and friends in England and Australia, I thank you all.

My supervisor, Prof. Aleksandar Subic, proved to be one of the best mentors a researcher could ask for. His technical knowledge and determination were an invaluable help to me in achieving my goals throughout my PhD. The support provided by Aleks throughout my research drove the project and allowed me to achieve my objectives. I would like to take this opportunity to thank him for his patience and belief in me.

*“If I have seen further it is by standing on the shoulders of giants.”*

-Sir Isaac Newton

# Table of contents

<b>Declaration</b> .....	<b>i</b>
<b>Acknowledgements</b> .....	<b>ii</b>
<b>Table of contents</b> .....	<b>iv</b>
<b>List of figures</b> .....	<b>viii</b>
<b>List of tables</b> .....	<b>xii</b>
<b>Nomenclature</b> .....	<b>xiii</b>
<b>Publications</b> .....	<b>xiv</b>
<b>Summary</b> .....	<b>1</b>
<b>1 Introduction</b> .....	<b>4</b>
1.1 Rationale .....	7
1.2 Literature review .....	8
1.2.1 <i>Overview of lateral epicondylitis</i> .....	9
1.2.2 <i>Dynamic behaviour of tennis racquets</i> .....	12
1.2.3 <i>Mechanics of the tennis grip</i> .....	20
1.2.4 <i>Active damping technology</i> .....	28
1.2.5 <i>Summary of relevant body of knowledge</i> .....	29
1.3 Research objectives and scope .....	33
1.3.1 <i>General objectives</i> .....	34
1.3.2 <i>Specific objectives</i> .....	34
1.4 Thesis overview .....	35
1.4.1 <i>Chapter 2</i> .....	36
1.4.2 <i>Chapter 3</i> .....	36

1.4.3	Chapter 4.....	37
1.4.4	Chapter 5.....	37
1.4.5	Chapter 6.....	38
<b>2</b>	<b>Comparing the structural dynamic properties of two tennis racquets .....</b>	<b>39</b>
2.1	Methodology .....	43
2.1.1	Experimental set-up.....	44
2.1.2	Test racquets.....	48
2.2	Experimental results .....	50
2.2.1	Racquet A .....	51
2.2.2	Racquet B .....	55
2.3	Discussion of results.....	58
2.3.1	Effect of racquet strings.....	61
2.3.2	Vibration excitation.....	63
2.4	Conclusions and significance .....	64
<b>3</b>	<b>Characterisation of tennis grip pressure distributions .....</b>	<b>67</b>
3.1	Identification of locations in the tennis grip with the greatest contact pressure .....	71
3.1.1	Instrumentation .....	72
3.1.2	Testing protocol.....	73
3.1.3	Results and discussion.....	75
3.2	Use of strain gauge cantilever system grip characterisation .....	80
3.2.1	Experimental set-up.....	83
3.2.2	Testing protocol.....	83
3.2.3	Results and discussion.....	87
3.3	Real time analysis of tennis grip pressure distribution characteristics .....	96
3.3.1	Experimental set-up.....	98
3.3.2	Testing protocol.....	102
3.3.3	Results and discussion.....	104

3.4	Conclusions and significance .....	127
<b>4</b>	<b>Experimental investigation of damping in tennis racquets.....</b>	<b>130</b>
4.1	Experimental set-up.....	133
4.2	Results and discussion.....	137
4.2.1	<i>Time based damping estimation .....</i>	<i>149</i>
4.2.2	<i>Signal processing .....</i>	<i>153</i>
4.2.3	<i>Quantifying the effectiveness of the piezoelectric damping system .....</i>	<i>160</i>
4.3	Conclusions and significance .....	163
<b>5</b>	<b>The effect of grip pressure distribution on racquet frame vibrations damping.....</b>	<b>167</b>
5.1	Establishing correlations between grip pressure and racquet vibration damping .....	169
5.1.1	<i>Data Exclusion .....</i>	<i>176</i>
5.1.2	<i>Defining an appropriate grip pressure.....</i>	<i>178</i>
5.2	Grip damping results .....	181
5.2.1	<i>Grip damping with respect to mode shapes.....</i>	<i>182</i>
5.3	Grip damping model.....	188
5.4	Discussion of findings .....	191
<b>6</b>	<b>Conclusions and recommendations .....</b>	<b>194</b>
6.1	Conclusions .....	195
6.1.1	<i>General outcomes.....</i>	<i>196</i>
6.1.2	<i>Specific outcomes .....</i>	<i>199</i>
6.2	Recommendations .....	202
<b>7</b>	<b>References.....</b>	<b>205</b>
<b>8</b>	<b>Appendices.....</b>	<b>214</b>

8.1	Appendix 1 .....	214
8.1.1	<i>Development of a strain gauge cantilever system for the measurement of tennis gripping forces..</i>	214
8.2	Appendix 2 .....	223
8.2.1	<i>Locations of hydrocell pressure sensor attachments on the racquet handle .....</i>	223
8.3	Appendix 3 .....	226
8.3.1	<i>Half power bandwidth damping calculation .....</i>	226
8.4	Appendix 4 .....	230
8.4.1	<i>Subjective Gripping data.....</i>	230

## List of figures

Figure 1. Anatomical diagram of lateral epicondylitis (Source: med.umich.edu).....	10
Figure 2. Sweet spot and other important locations on the tennis racquet (Source: Brody <i>et al.</i> 2002; Kotze <i>et al.</i> 2000).....	14
Figure 3. Mode shapes for clamped and freely suspended racquet condition (Source: Kotze <i>et al.</i> 2000) .....	15
Figure 4. Example of node lines and locations of a tennis racquet (Source: Cross 2001).....	16
Figure 5. Wave propagation from the centre of percussion along the racquet strings shown at different time intervals (Source: Brannigan and Adali 1981).....	19
Figure 6. Example of tennis gripping force traces for the forehand stroke (Source: Knudson and White 1989).....	22
Figure 7. Forces in the tennis grip resulting from the tennis ball impact (Brody <i>et al.</i> 2002).	23
Figure 8. Schematic of tennis racquet modal test set-up .....	45
Figure 9. Racquet geometry showing excitation points (response measured at point 31).....	46
Figure 10. Racquet dimensions.....	48
Figure 11. Frequency response measurements for racquet A (with strings).....	51
Figure 12. Frequency response measurements for racquet B (with strings).....	55
Figure 13. Node location associated with the first bending mode for racquets A and B.....	58
Figure 14. Comparison of average FRF's for racquets A and B .....	60
Figure 15. Comparison of average FRF's for racquet B with and without strings.....	62
Figure 16. Pressure film layout.....	72
Figure 17. Continental gripping technique .....	73
Figure 18. Developed pressure film attached to racquet handle.....	75

Figure 19. Pressure film results for a forehand stroke for the metacarpals and thumb .....	77
Figure 20. Pressure film results for a forehand stroke for the MP joint and phalanges.....	78
Figure 21. Strain gradient: <i>a)</i> relationship between strain and distance from load applied to the beam; <i>b)</i> measurement locations on the cantilever beam .....	82
Figure 22. Location of cantilever beams with respect to the gripping hand for a)distal phalanx; b) proximal phalanx; c) MP joints and distal metacarpals; d) metacarpals .....	85
Figure 23. Diagram of drop test set-up .....	86
Figure 24. Threshold calculation .....	89
Figure 25. Sample of measured strain gauge for a visual test at: a) distal phalanx; b) proximal phalanx; c) MP joints and distal metacarpals; d) metacarpals.....	94
Figure 26. Schematic of hydrocell sensor data collection set-up.....	101
Figure 27. Accelerometer locations .....	102
Figure 28. Experimental set-up on a tennis court .....	103
Figure 29. Racquet handle: a) upper and b) lower gripping sections .....	105
Figure 30. Sample of right-handed forehand stroke handle section pressure variation measurements during impact .....	108
Figure 31. Pre-impact pressure distribution in a forehand stroke for: a) upper handle and b) lower handle.....	110
Figure 32. Post-impact pressure distribution in a forehand stroke for: a) upper handle and b) lower handle.....	112
Figure 33. Sample of service stroke handle section pressure variation measurements during impact.....	113

Figure 34. Pre-impact pressure distribution for the service stroke at: a) upper handle and b) lower handle.....	115
Figure 35. Post-impact pressure distribution for the service stroke at: a) upper handle and b) lower handle.....	116
Figure 36. Sample of backhand slice stroke handle section pressure variation measurements during impact .....	118
Figure 37. Pre-impact pressure distribution for the backhand slice stroke at: a) upper handle and b) lower handle.....	120
Figure 38. Post-impact pressure distribution for the backhand slice stroke at: a) upper handle and b) lower handle.....	121
Figure 39. Free suspension racquet-ball impact experiment: a) front view; b) side view .....	134
Figure 40. Schematic diagram of hand-held ball drop test .....	136
Figure 41. Average frequency response of freely suspended tennis racquet (B) for tennis and golf ball impacts.....	138
Figure 42. Average frequency response of hand-held tennis racquet (B) for tennis and golf ball impacts .....	139
Figure 43. Comparison of racquet frequency responses for different gripping conditions ...	140
Figure 44. Damping and gripping correlations for racquet A.....	147
Figure 45. Damping and gripping correlations for racquet B.....	147
Figure 46. Decaying vibration .....	150
Figure 47. Sample of raw acceleration data.....	154
Figure 48. Sample of acceleration data after frequency filtering.....	155
Figure 49. Sample of acceleration data after smoothing (Savitzky and Golay, 1964) .....	156

Figure 50. Damping ratio box-plots for freely suspended and hand held racquets .....	159
Figure 51. Definition of vibration ( $a$ ) and pressure ( $p$ ) peak parameters .....	172
Figure 52. Frequency response of a tennis racquet with nodal and non-nodal impacts .....	177
Figure 53. Mode shape of tennis racquets 1 <sup>st</sup> bending mode .....	179
Figure 54. Damping correlations using the total pressure applied to the racquet handle .....	181
Figure 55. Damping correlation using the pressure applied to the racquet handle in the z direction .....	184
Figure 56. Damping correlations using the grip pressure applied to the upper handle section .....	187
Figure 57. Linear damping correlations using the grip pressure applied to the lower handle section .....	187
Figure 58. Non-linear damping correlation using the grip pressure applied to the lower handle section .....	189
Figure 59. Schematic of the cantilever beam and circuit diagram.....	215
Figure 60. Full Wheatstone bridge orientation on a cantilever beam .....	216
Figure 61. Wheatstone bridge circuit diagram.....	217
Figure 62. Test racquet handle butt (end view dimensions) .....	219
Figure 63. Test racquet handle butt (side view dimensions) .....	220
Figure 64. Hand grip cantilever test system.....	221
Figure 65. Calibration chart for beams A: D .....	222
Figure 66. Racquet handle side configuration .....	223
Figure 67. Half power damping parameter identification.....	227
Figure 68. Example of half power damping parameter identification .....	228

## List of tables

Table 1. Summary of existing knowledge relevant to this investigation .....	33
Table 2. Racquet mass and centre of mass location.....	49
Table 3. Modal analysis results for racquet A .....	53
Table 4. Modal analysis results for racquet B.....	56
Table 5. Outline of experimental investigation of tennis gripping pressure.....	71
Table 6. “Visual” drop test gripping time results .....	90
Table 7. “Blind” drop test gripping time results .....	90
Table 8. Evaluation of response parameters of racquet A for tennis ball impacts.....	145
Table 9. Evaluation of response parameters of racquet B for tennis ball impacts.....	145
Table 10. Logarithmic decrement calculations for a hand held racquet .....	157
Table 11. Logarithmic decrement calculations for a freely suspended racquet.....	158
Table 12. Logarithmic decrement and damping ratio of racquet A .....	161
Table 13. Logarithmic decrement and damping ratio of racquet B .....	161
Table 14. Vibration and pressure measurements used for grip damping correlations.....	173
Table 15. Hydrocell attachment locations for the continental forehand grip .....	224
Table 16. Hydrocell attachment locations for the service and backhand slice grips .....	225
Table 17. Response data of racquet A for tennis ball impacts .....	230
Table 18. Response data of racquet B for tennis ball impacts .....	231

## Nomenclature

$F$  - Force

$a$  - Acceleration

$k$  - Stiffness

$m$  - Mass

$t$  - Time period

$\omega_n$  - Natural frequency

$\omega_d$  - Damped natural frequency

$\tau$  - Period of oscillation

$\tau_d$  - Damped period of oscillation

$\delta$  - Logarithmic decrement

$\zeta$  - Damping ratio

## **Publications**

Savage, N. & Subic, A. (2006). Relating grip characteristics to the dynamic response of tennis racquets. In: Moritz, E.F. & Haake, S.J. ed. **6<sup>th</sup> International Conference on the Engineering of Sport, 2006, Munich**, pp.155-160.

## Summary

The modern game of tennis has changed in recent years as a result of lightweight, stiffer racquets. The evolution of the tennis racquet, with respect to both design and materials, has increased the speed of the game but also the levels of stress placed on the player's bodies. Larger racquet heads generate greater top spin on the ball, allowing the player to strike the ball harder and still be able to place the ball in court. However, by striking the ball harder the strains on the player's upper extremities caused by the transmission of ball-racquet impact energy are increased. Injuries such as lateral epicondylitis (tennis elbow) are thought to be both instigated and aggravated by the transfer of racquet shock and vibration. Therefore, it is important to manage the levels of shock and vibration transmission to the player, in order to reduce the associated performance inhibiting effects.

Racquet energy that causes upper extremity injuries is transferred to the tennis player via the tennis grip in the form of shock and vibration. Parameters defining the degree of shock and vibration transmission are the inherent properties of the racquet and the mechanics of the tennis grip. This thesis presents an experimental investigation into the transmission of racquet vibration to the player's hand and forearm. Experimental techniques have been used to quantify the main parameters defining the transmission of vibration via the tennis grip.

The mechanics of grip damping show precisely how the transfer of racquet vibration to the player occurs. The tennis grip has been experimentally quantified using various sensing equipment. Gripping devices used in previous research have been modified,

manufactured and used in conjunction with pressure sensitive film and hydrocell sensors. Each of the experimental techniques used in this research has been designed to examine different aspects of the tennis grip. Manufactured strain gauge cantilever systems have been utilised for a real-time analysis of the grip tightness variations during impact. The cantilever technique enabled estimations of anticipation times, allowing for a description of the tennis grip regarding the time of maximum grip force and the initial increase in grip force with respect to the time of impact. Specialised pressure sensitive film has also been utilised to identify important contact locations within the tennis grip where the magnitudes of pressure are greatest. These two primary laboratory tests provided information for further experiments, allowing for the analysis of grip pressure distribution during different stroke types using real-time data acquisition.

Variations in the distribution of grip pressure during impact for three stroke types have been measured by attaching hydrocell pressure sensors to the racquet handle at multiple contact locations. Calculated pressure distributions show the magnitudes of gripping pressure at multiple contact locations in the tennis grip. These pressure distribution characteristics have been used to analyse the applied gripping pressure of the player's hand together with the reactions force imparted on the player's hand, generated by racquet rotation during impact.

Correlations between racquet vibrations and grip pressure distribution could only be made if the degree to which the vibrations are dampened could be quantified. The half-power bandwidth method (Quality factor) has been applied to estimate the magnitude of racquet damping in the frequency domain. Racquet damping estimations have been

correlated with the grip pressure characteristics to show the mechanics of the grip damping phenomena. Estimates of logarithmic decrement have been utilised to relate variations in grip pressure distribution to the damping of racquet vibrations. Using the modal properties of the racquet (also established in this thesis) the mechanics by which the tennis grip absorbs racquet vibrations, have been described.

Previous research has shown the hand to have a profound effect on the dynamic response of the tennis racquet in terms of frame vibration damping. It has been shown that the tighter a tennis grip, the greater the level of vibrations transferred to the player's hand and forearm. This research has investigated the grip damping phenomena and built upon the current body of knowledge by interpreting the mechanics of grip damping, showing precisely how the tennis grip dampens tennis racquet frame vibrations, and how they are absorbed by the player at contact locations on the hand. Future racquet designs can now incorporate the findings of the present research to optimise the vibration attenuation systems (whether they are passive or active) to aid in the management of upper extremity injuries such as lateral epicondylitis.

# **Chapter 1**

## **Introduction**

Over recent years the dramatic evolution of tennis racquet design has led to an increase in game speed that has resulted in increased physical forces being imparted on the player. These increased forces are thought to have given rise to increases in the development and aggravation of injuries. The most common injuries are those that involve the player's upper extremities, and are believed to come primarily as a result of the forces transmitted to the player during racquet - ball impact. The most common injury resulting from such impact forces is lateral epicondylitis (tennis elbow). Tennis elbow is not the only upper extremity injury encountered by players, but with tennis elbow affecting 40-50% of recreational players (Roberts *et al.* 1995; Nirschl 1986), the injury inhibits player performance on a large scale. Recent surveys have shown that 55.6% of recreational players occasionally suffer from symptoms of tennis elbow, and 42.2% of those injured said that tennis elbow reduced the amount of tennis they played (Sports Marketing Surveys 2003). The management of tennis elbow is therefore in high demand.

Although tennis elbow represents an acute problem for many players across the world, additional upper extremity injuries, such as wrist and shoulder strains, also affect the players. Upper extremity injuries are thought stem from the transfer of large impact forces in a repetitive manner, to the player via the racquet-hand interface known as the tennis grip. Injuries, such as tennis elbow, can be better managed only if the causes can be better understood. This in turn means that the transmission of racquet forces to the player needs to be better understood.

The impact forces transmitted to the player are in the form of impact shock and post-impact racquet vibrations. However, the degree of racquet shock and vibration

transmission is determined by a number of contributing factors. Specific stroke types, such as the backhand, allow for a greater degree of energy transfer to the player as they biomechanically isolate the susceptible forearm tendons during the stroke. Backhand strokes require the use of wrist extensors that develop the symptoms of tennis elbow if they are overused or placed under great strain. The large strain on the wrist extensor muscles and tendons arises from the transfer of energy generated by the impact. Correlations between racquet vibration levels and grip pressure characteristics need to be made before a comprehensive understanding of energy transfer to the player can be established. It is important that the transfer mechanics be described in detail in order to gain a greater insight into the effects of racquet impact forces on the player. Racquet design can evolve based on the understanding of the racquet-hand interface mechanics, which affect the racquet's dynamic behaviour.

Optimisation of racquet design currently focuses on the inherent structural properties such as mass distribution, stiffness and additional damping materials. However, the dynamic properties of the racquet (i.e. natural frequencies etc.) will not be the same under the hand-held conditions during a match. Extra mass is added in the hand-held racquet in the form of the hand as it becomes part of the system. This added mass will alter the dynamic response of the racquet, in terms of natural frequencies and vibration damping. Therefore optimisation of racquet design (in terms of vibration attenuation) can only be achieved by incorporating the effects of the hand, with respect to its damping mechanics.

## **1.1 Rationale**

The tennis elbow injury is thought to be caused by the transfer of shock and vibration from the racquet to the player's hand and arm via the tennis grip. Efforts have been made in equipment manufacturing to attenuate the levels of racquet shock and vibration transmitted to the player. However, the shock and vibration attenuation equipment (such as active/passive damping systems and additional damping materials) is less than optimal and has often been manufactured without the underlying knowledge of the mechanics involved in the transfer of the energy to the player. The specific knowledge regarding the damping mechanics of the tennis grip would be valuable as it would describe the transfer of racquet energy (in the form of shock and vibration) to the player.

The investigation of grip damping parameters can aid the development of more appropriate design solutions for shock and vibration attenuation in racquet and bat-based sports. Sports such as cricket, baseball, squash and golf all have racquets, bats or clubs that can be thought of as hand-held simple beam structures. Therefore damping theories used to aid optimisation in one type of racquet/bat sport may be applicable/ transferable to other bat/racquets sports.

This research aims to describe the damping mechanics in the tennis grip and more specifically to determine the degree of vibration absorption by the tennis grip. The transfer of racquet shock to the player is also of concern when researching upper extremity injuries (due to the large loads involved); however it is racquet vibration that will be the main focus of this research. Experimental data will be obtained in this research to analyse the tennis grip damping phenomena. In order to do this, the research

will investigate the effects of varying grip tightness in relation to the associated vibration absorption levels in the tennis grip. With respect to investigating grip tightness, this research aims to analyse the effect of grip pressure changes on the dynamic response of the tennis racquet during and after impact. This will be achieved by giving a comprehensive characterisation of tennis grip pressure distributions for a range of tennis strokes, such as the forehand and the problematic backhand. The tennis grip has been quantified to show the distribution of pressure across the racquet handle and identify pressure variations during impact. Experimental quantification of racquet damping is achieved and discussed with respect to controlling parameters such as the tennis grip. With the knowledge of the tennis gripping pressures, correlations are made with the structural damping of the racquet.

The overall research objective was to investigate the underlying parameters that contribute to the transfer of shock and vibration to the player. The injury of tennis elbow itself needed to be reviewed before specific research objectives could be made in order to achieve the overall research objective. It was important to understand the injury and its associated symptoms if the research was to add to current knowledge and aid the management of tennis elbow. It is also important to understand the kind of biomechanical characteristics that instigate and aggravate injuries such as lateral epicondylitis.

## **1.2 Literature review**

This section provides a comprehensive overview of the existing body of knowledge relating to the present research problem. The key areas of concern for the present research needing to be reviewed are as follows:

- Understanding of upper extremity tennis injuries such as lateral epicondylitis in order to understand the contributing effects of racquet shock and vibration transmission.
- Current knowledge regarding the characteristic structural dynamic properties of tennis racquets.
- Findings regarding the damping parameters involved during impact, including the current knowledge concerning the effects of the player's hand and the tennis ball on the damping of racquet frame vibrations.
- Knowledge regarding the mechanics of the tennis grip during impact in terms of gripping tightness variations.

A review of the current body of knowledge covering these key outlined areas is required in order for appropriate research objectives to be formulated for this research

### ***1.2.1 Overview of lateral epicondylitis***

Lateral epicondylitis (tennis elbow) is defined as the pain around the elbow that causes discomfort when playing tennis (Kamien 1990). The pain felt by the player is caused by the overuse of the wrist extensors in the forearm causing tendonitis. The overuse of the wrist extensors causes micro tears at the tendonous origin (lateral epicondyle) of the extensor carpi radialis brevis (wrist extensor) (Ollivierre and Nirschl 1996; Cassel and McGrath 1999). The micro tears are generated in the early stages of the injury and develop into larger lesions over time as the injury is aggravated. Figure 1 shows an anatomical depiction of lateral epicondylitis.

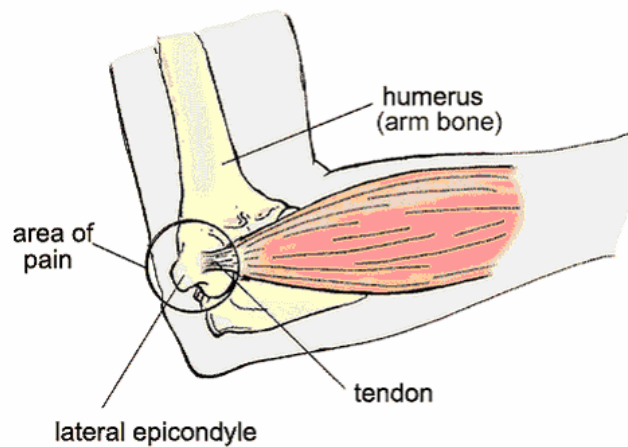


**Figure 1. Anatomical diagram of lateral epicondylitis (Source: med.umich.edu)**

Micro tears in the muscles and tendons in the forearm and surrounding the elbow begin to appear with the overuse of the wrist extensors. The symptoms of lateral epicondylitis can also arise from the tendon origin being placed under excessive loads. The micro tears of tendonitis can vary in their magnitude and, as previously mentioned, they are mainly located at the tendon-bone junction of the elbow (Kamien 1990). The micro tears will continuously heal and re-appear, leaving scar tissue. An accumulation of scar tissue at the lateral epicondyle appears after repeated tears, which then as a result become rough, and calcium deposits begin to appear. Collagen then leaks from the injured area and causes the elbow to become inflamed and painful. In extreme cases tennis elbow can lead to the circulation being cut off to the lower arm and restricting the nerves that control the arm and hand. However, the main causes of the pain felt by a tennis player range from an inflamed synovial fringe of the elbow joint to calcific tendonitis (Kamien 1990). The pain factor caused by tendonitis is the main issue for the tennis player as it leads to increases in fatigue and loss of racquet control during play (Brody 1989). Aggravations of the injury are believed to include excessive strain placed on the insertion of the lateral

tendons at the lateral epicondyle of the humerus, and the absorption of post-impact racquet vibrations by the wrist extensors and tendonous origin. The management of tennis elbow (i.e. injury prevention devices and rehabilitation methods) needs to be optimised to reduce its inhibiting effects. Aggravating causes therefore require research and need to be addressed if injury management is to become optimised.

The elbow injuries are not only found in the sporting world. The person suffering from lateral epicondylitis may have acquired the injury which is then aggravated by the hand gripping actions of everyday life (Cassel and McGrath 1999). If the gripping interfaces of the hand can be better understood, whether it is in tennis or in everyday life, then causes of the tennis elbow pain may be better understood and knowledge for treatment and prevention will be more effective. There needs to be a greater understanding of the loads imparted on the wrist extensors and/or flexors if the inhibiting properties of elbow injuries and other associated upper extremity ailments, are to be alleviated. Although upper extremity ailments can stem from many different activities, this research will focus on those stemming from the sport of tennis.

The transfer of shock and vibration from the tennis racquet occurs when the muscles in the forearm are contracted during the stroke. When the forearm muscles are contracted they have a limited amount of additional movement available to absorb the racquet shock and vibration, resulting in the energy being transferred to the tendon origin at the lateral epicondyle of the elbow. Absorption of racquet shock and vibration by the tendon insertion is thought to produce the symptoms of tennis elbow. The contracted muscles of the forearm also provide the medium for the transfer of racquet frame vibrations. As the

tennis grip becomes tighter the forearm muscles increase in their degree of contraction. The more contracted a muscle the stiffer its properties become. The stiffer the forearm muscles become, the greater the transfer of racquet vibrations to the forearm due to the stiff properties of a contracted muscle. The energy of racquet shock and vibration will be transferred through the forearm muscles and absorbed by the tendon origin (Roberts *et al.* 1995).

Management of lateral epicondylitis requires an understanding of contributing factors, so prevention and treatment techniques may be developed and optimised. The cause and aggravation of the tennis elbow symptoms is thought to be the transfer of racquet energy to the player's forearm and tendon origin. The transfer of racquet energy to the player takes place via the tennis grip, so in order to understand this transfer, the racquet's dynamic behaviour and grip damping mechanics during impact need to be investigated.

### ***1.2.2 Dynamic behaviour of tennis racquets***

The tennis racquet is a complex structure containing many different materials; however the racquet's geometry can be considered a simple beam. The tennis racquet has a number of different sweet spots that have individual attributes, each of which will now be explained in detail. They are located at different locations on the racquet and are shown in figure 2. The sweet spot that relates to the racquet vibrations felt by the player is the nodal sweet spot of the racquet.

The structural analysis of the tennis racquet reveals a number of rigid body modes together with bending and torsional modes, each with their own modal frequency, modal

shape and modal damping. The modal properties of the racquet depend on racquet mass, mass distribution and racquet stiffness. The inherent natural frequencies of the tennis racquet, can be determined using equation (1.1).

$$\omega_n = \sqrt{\frac{k}{m}} \quad (1.1)$$

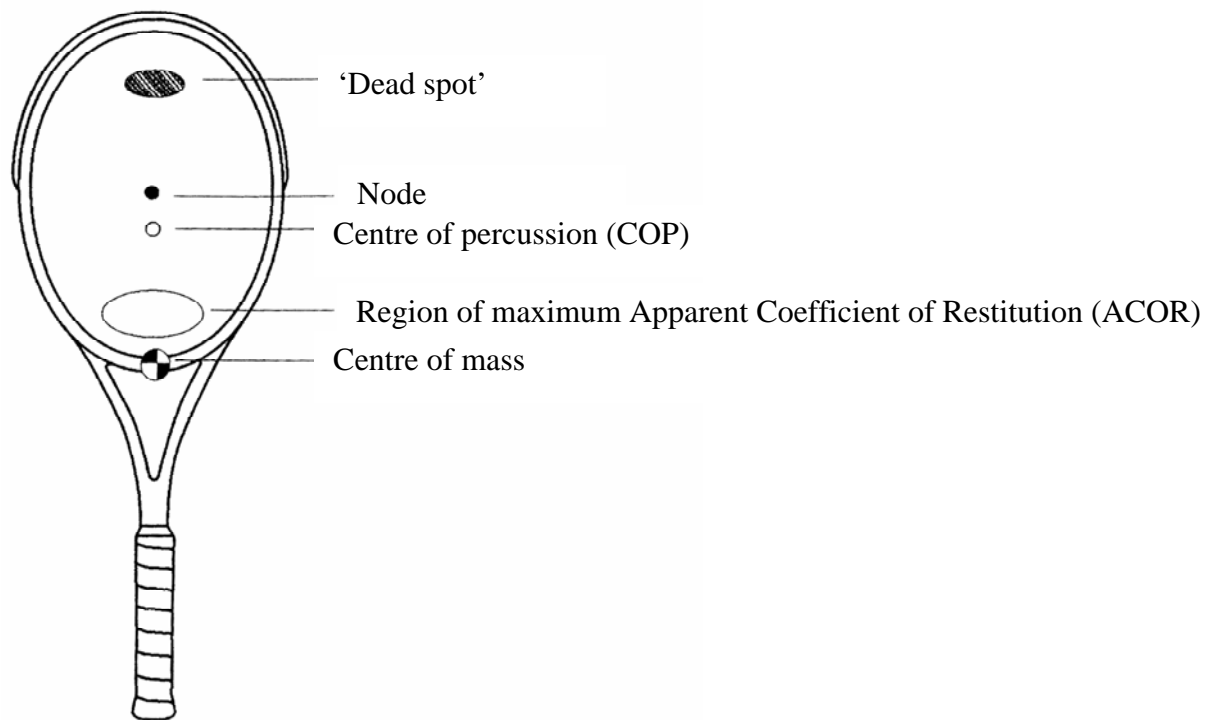
Where:

$\omega_n$  = natural frequency

$k$  = stiffness

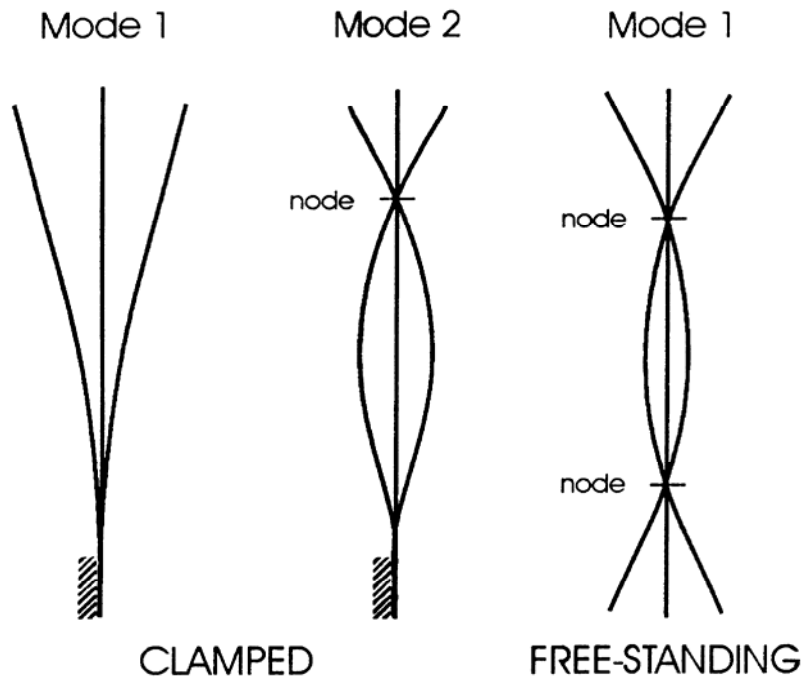
$m$  = mass

Figure 3 displays the important bending shapes and node locations of the racquet's first mode of oscillation (Brody 1987), which produces the vibrations thought to instigate and aggravate the tennis elbow injury. The nodes of the first bending mode are located at the approximate centre of the racquet's head, and the top section of the racquet handle. The node location at the racquet head provides an impact location where the player will feel zero or minimal post-impact vibrations at the associated natural frequency, because the racquet displays zero displacement at the node. This is known as the nodal sweet spot of the tennis racquet. (Excitation of the racquets higher modes of oscillation will be discussed later in the chapter.) Due to the racquet's structural geometry and mass distribution, its node locations are not single points but a curved line across the racquet structure (figure 4).



**Figure 2. Sweet spot and other important locations on the tennis racquet (Source: Brody *et al.* 2002; Kotze *et al.* 2000)**

Figure 3 shows the geometric mode shapes for racquets in clamped and freely suspended conditions. The racquet has a fundamental mode of oscillation in the frequency range 25-40Hz. This mode of vibration displays no nodes and only occurs with clamped racquets. This low mode of oscillation is not identified in hand-held racquets, indicating that the player is not capable of producing the required gripping pressure to give a clamped racquet condition. Clamped racquet analysis is therefore not a true representation of racquet dynamics during hand-held conditions (Brody 1987, 1997; Cross 1997). The first bending mode of the tennis racquet in freely suspended conditions is in the frequency range 100-200Hz (Brody *et al.* 2002; Kotze *et al.* 2000) and is considered the racquet's fundamental mode. It is these modes of vibration at higher frequencies that are undesirable for the player as energy of the racquet at this frequency is thought to contribute to, and aggravate, tennis elbow symptoms (Brody, 1981; Li *et al.* 2004).



**Figure 3. Mode shapes for clamped and freely suspended racquet condition (Source: Kotze et al. 2000)**

Figure 4 shows an example of a racquet analysis and shows the curved node lines for the 1<sup>st</sup> and 2<sup>nd</sup> bending modes of a tennis racquet. If the ball impact location is on a node line the vibrations at the associated natural frequency will not be excited and the player will feel zero vibrations at that frequency. An impact at the fundamental node will not excite vibrations at that frequency. But vibrations the frequency of other modes of oscillation will be excited. The amplitude at which the player will feel the vibrations associated with the next mode depends upon the relationship between the dwell time of the ball on the string bed and the mode period. This relationship and its influence on the amplitude of vibration will be discussed later in the chapter. Off centre impact locations will generate torsional rotation of the racquet, even if the impact is on the node line of the fundamental mode, causing the player to experience uncomfortable forces acting on their hand.

The 1<sup>st</sup> and 2<sup>nd</sup> bending modes of the racquet are at different frequencies (the second modal frequency (373Hz in this case) is normally approximately 3 times that of the 1<sup>st</sup> bending mode (129Hz)). Both modes have node locations in the tennis grip and therefore their vibrations will be felt by the player if they are excited. However, due to ball-racquet interaction properties the first mode is the main mode of interest due to ball damping effects. Ball-racquet interaction properties and their damping effects will be discussed later.

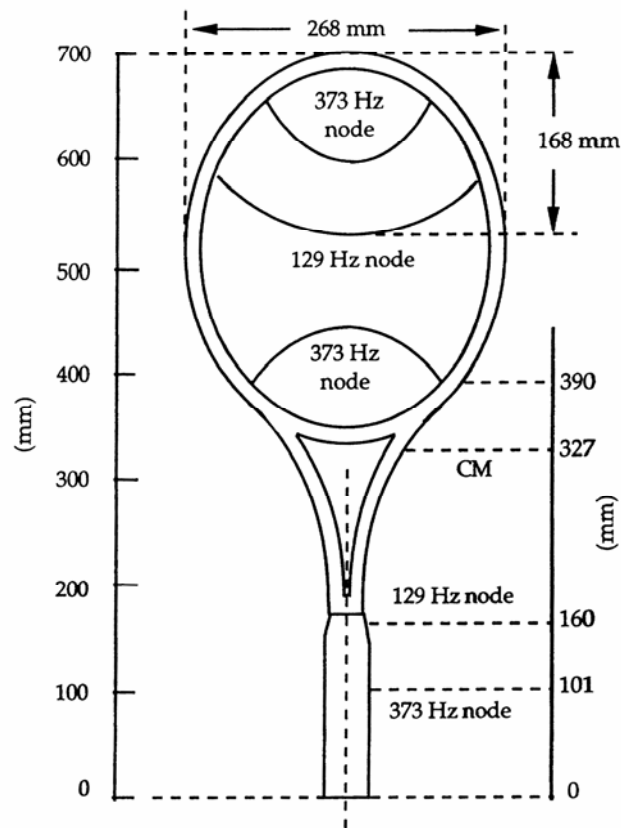


Figure 4. Example of node lines and locations of a tennis racquet (Source: Cross 2001)

Another sweet spot of the tennis racquet relates to the centre of percussion (COP) (figure 2). The COP provides an impact location that results in minimal shock forces felt by the player. This shock force of the racquet is known as its impulse reaction and is the

opposing racquet reaction forces on the player's hand (Kotze *et al.* 2000; Brody 1981). The conjugate relationship between the COP and the axis of rotation in the racquet handle provide a sweet spot where zero impulse force of racquet rotation will be felt by the player (Cross 1998a, 2004). If the racquet-ball impact is located at the COP the forces acting in opposite directions on the players hand, caused by the racquet's rotation in the tennis grip, will be equal to zero (Brody *et al.* 2002). It is the transfer of the racquet's impulse force to the player that places excessive strain on the player's forearm muscles and tendon origins. The racquet's COP will be discussed in greater detail later in the chapter with regards to the acting forces in the tennis grip.

An additional sweet spot relates to the location on the tennis racquet that returns the most energy to the rebound ball, and it is known as the maximum apparent coefficient of restitution (ACOR) (Brody 1979; Brody *et al.* 2002; Kotze *et al.* 2000; Cross 2001). Figure 2 shows the region at the base of the racquet head where the location of the maximum ACOR can be found. Every point on a racquet has a measurable ACOR that is defined by measuring the ratio between the initial ball speed and the rebound speed when the racquet is initially at rest. The location on the tennis racquet that produces the greatest ratio between the two ball speeds is known as the maximum ACOR and is located in the throat region of the racquet. The location of maximum ACOR provides an impact area on the string bed that will return the maximum amount of energy to the ball during impact, creating a faster ball rebound speed.

All three locations on the string bed display sweet spot qualities, with each having their own benefits. A player will feel zero post-impact vibrations if the nodal sweet spot is hit,

while they will feel minimal impulse reaction forces on the hand if the COP sweet spot is hit. In order for the player to hit the ball with maximum rebound velocity, the ball needs to be hit struck at the racquet's ACOR sweet spot. However, as figure 2 shows, the sweet spots reside at different locations on the racquet head and not at a common site. Moreover, each sweet spot needs to be researched individually, complete with an assessment of their contributions to tennis elbow. The injury of tennis elbow has previously been discussed and believed to be caused and aggravated by the post-impact racquet vibration of the racquet's 1<sup>st</sup> mode, although no clinical evidence has been published to date (Brody 1981). These vibrations are directly related to the racquet's 1<sup>st</sup> bending mode and the associated nodal sweet spot. Optimisation of tennis elbow management can only be achieved if the properties of these bending mode vibrations and their interaction with the player are fully understood.

Racquet-ball interaction during impact also plays a key role in the levels of post-impact vibration. The approximate dwell time of the ball (i.e. the time the ball stays in contact with the racquet string bed during impact) is approximately 5ms (Brody 1979; Hatze 1976). The dwell time of the ball can be increased or decreased depending on string tension. The dwell has its own damping effects on racquet vibrations, as the ball itself acts as a string damper. As a result of a 5ms ball dwell time, racquet vibrations exceeding approximately 200Hz are damped before the ball has left the string bed (Brody *et al.* 2002).

The ball impact excites the racquet's modes of oscillation from the impact location. Vibration waves travel from the impact location to the racquet's perimeter where they are

reflected back to the impact location. Figure 5 shows computer-simulated wave propagation across the string bed, generated by a ball impact at the racquet centre of percussion. The wave travels to the outer limits of the racquet, as shown by the different time intervals.

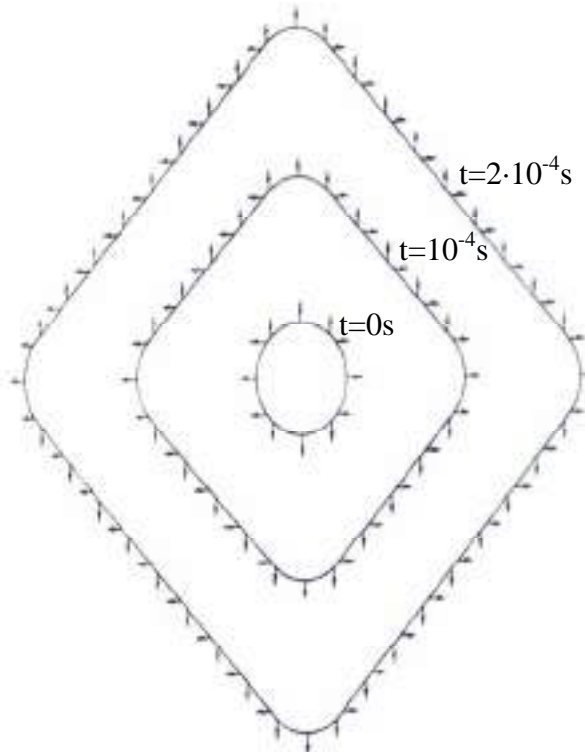


**Figure 5. Wave propagation from the centre of percussion along the racquet strings shown at different time intervals (Source: Brannigan and Adali 1981)**

If the excited wave is reflected back to the impact point after the ball has left the surface, the racquet will vibrate at that frequency. Using the expression  $\frac{1}{t}$ , where  $t$  is the time for the transverse wave to propagate from the impact location to the racquet perimeter and back, the frequency of the vibration waves that will return to the impact location and excite the racquet can be calculated (Cross 1999). Given that the average dwell time of the ball is approximately 0.005s (Brannigan and Adali 1981),  $\frac{1}{t}$  gives 200Hz. If the

frequency of the vibration wave is less than  $\frac{1}{t}$  the reflected wave will reach the impact location after the ball has left the surface and will not be damped by the ball resulting in racquet vibration. If the frequency of the vibration wave is greater than  $\frac{1}{t}$  then the reflected wave will reach the impact site before the ball has left the racquet surface and will be damped out, causing a reduction in the amplitude of racquet vibrations at the associated frequency. This means that vibrations corresponding to the racquet's second bending mode are drastically dampened by the ball, as they are usually associated with a frequency greater than 200Hz.

The vibrations of the racquet's first freely suspended bending mode are thought to be a major cause of upper extremity injuries as they are transferred to the players arm via the tennis grip, although there is no clinical evidence to support this claim (Hennig *et al.* 1992). The tennis grip is the point at which the racquet shock and vibration caused by the ball-racquet impact is transmitted to the players' hand and lower arm. It was therefore important to have understand the current knowledge regarding the tennis grip and its dynamic behaviour during impact.

### ***1.2.3 Mechanics of the tennis grip***

The tennis grip is a dynamic interaction of forces between the player's hand and the racquet handle. Gripping forces are not entirely attributed to the player's gripping tightness, but also the reaction force of the racquet handle as it rotates in the player's hand (Brody *et al.* 2002). Any analysis of the tennis grip will have to take this into consideration when interpreting measured pressures/forces. The gripping pressure has

previously been measured using single point measurements, and hence they have been quoted as gripping force. However, the tennis grip covers the handle area so it can also be quoted as a pressure measurement.

Gripping pressure/force is symmetrical in its increase and decrease in relation to the ball impact. This is due to the player requiring greater grip stiffness during impact to allow for greater racquet control over the rebound ball. The pressure/ force may be symmetrical in relation to the ball impact, however there are two pressure peaks during impact. Figure 6 shows an example of single point gripping dynamics relating to two locations on the hand (*top* handle force at the base of the index finger and the bottom handle force at the *hypothenar* eminence of the hand) during impact, using force measurements (Knudson and White 1989). The symmetrical increase and decrease in relation to the ball impact (0s) can be seen together with two clearly identifiable force peaks.

The initial force peak is created as a combination of two factors. Firstly, the player increases the gripping tightness to generate a greater stiffness of the tennis grip in preparation for the high velocity ball impact. In conjunction with this, the acceleration of the racquet during the swing will also create and increase the forces on the player's hand. If we consider the net force ( $F$ ) on the handle to be given by equation(1.2), the increase in racquet acceleration ( $a$ ) generated by the forearm movements, will consequently result in an increase in the force on the handle. Therefore the increase in the measured grip force is a combination of both player grip tightness and racquet acceleration. Furthermore, the increased force due to racquet acceleration will result in an uneven distribution of force over the racquet handle.

$$F = ma \quad (1.2)$$

The second force peak is created due to the loss of racquet control by the player resulting from the high forces of the ball impact. The second peak relates to the player's attempts to regain control of the tennis racquet after impact (Hatze 1998; Knudson and White 1989). Figure 6 also shows that the force traces for the two locations on the hand follow opposing trends during impact. Both increase before impact but show opposing increases and decreases after the impact. This is evidence of the racquet's rotation in the tennis grip after impact and an effect of the impulse reaction forces it imparts on the hand (Brody *et al.* 2002).

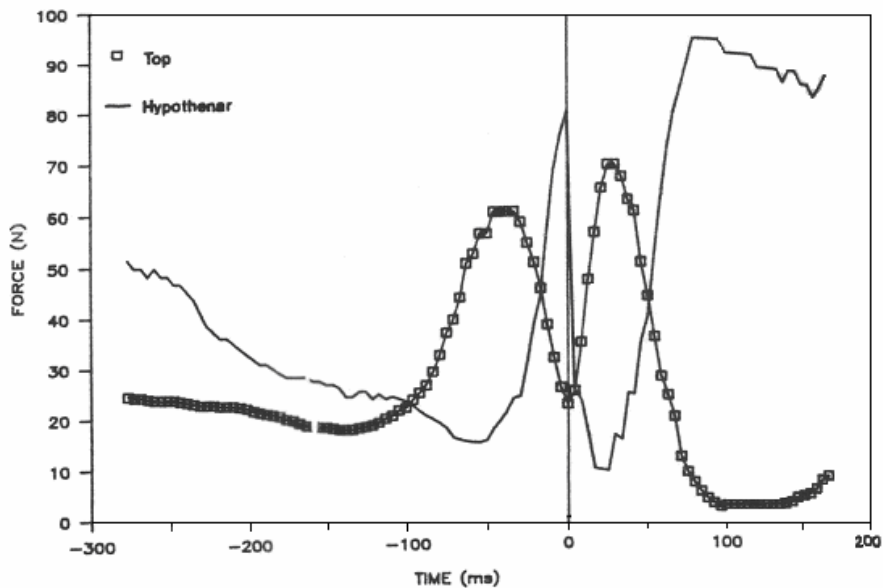


**Figure 6.** Example of tennis gripping force traces for the forehand stroke (Source: Knudson and White 1989)

Figure 7 shows that depending on the location of the ball impact on the racquet face, the forces in the grip and where they are imparted on the hand will be varied. (N.B. The

forces shown in figure 7 represent the forces acting on the hand as a result of racquet rotation.).  $F_3$  represents the overall force acting upon the axis of rotation in the tennis grip. This is known as the impulse reaction force. If the impact location of the ball is above the centre of percussion (i.e. the racquet tip), the overall impulse reaction ( $F_3$ ) causes a forward movement of the axis of rotation. This is known as a pulling effect on the tennis grip and is often called a negative impulse reaction. As figure 7 shows, if the ball impacts the COP, then  $F_3$  is equal to zero and therefore the impulse reaction is reduced to zero. The impulse reaction ( $F_3$ ) will have a pushing effect on the racquet's axis of rotation if the location of the ball impact is lower than the COP (i.e. the racquet throat). The pushing effect on the grip is often called a positive impulse reaction.

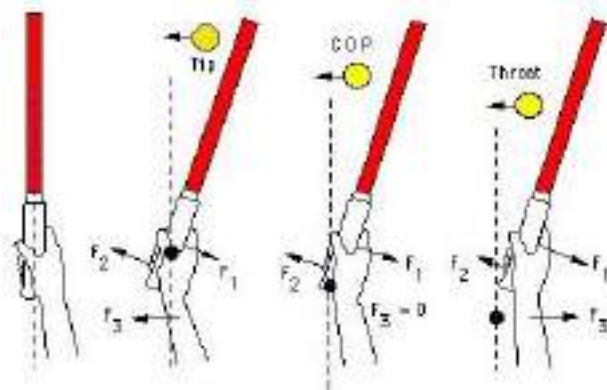


**Figure 7. Forces in the tennis grip resulting from the tennis ball impact (Brody *et al.* 2002)**

The impulse reaction of the racquet ( $F_3$ ) is the overall force the player will feel as a result of the ball impact whether it is positive or negative. The COP provides an impact location that produces equal positive ( $F_1$ ) and negative ( $F_2$ ) racquet rotation forces so the overall impulse reaction is 0 and therefore the player will feel zero overall force on their hand.

The forces within the tennis grip are very subjective and depend on the individual player gripping characteristics and the velocity of the incoming ball, meaning that every stroke will present a different racquet condition. The materials and design of the modern tennis racquet allow for greater top spin and greater swing speeds, generating more powerful strokes. The more powerful shot generated by an increase in swing speed will consequently generate greater levels of racquet shock and vibration. Increasing the grip tightness will result in racquet energy (in the form of shock and vibration) being absorbed at a greater rate by the player's hand (Hatze 1976).

The quantification of the tennis gripping tightness has been achieved to a certain extent, but the analysis has only ever been with subjective gripping conditions (i.e. light, moderate and tight grips). A range of experimental procedures have been used to measure the tennis grip, but they have only been used for subjective gripping tightness (Hatze 1976; Elliot 1982; Brody 1989; Li *et al* 2004). Moreover, previous studies into the tennis grip have failed to use grip tightness measurements for the characterisation of pressure distributions for different strokes. Further still, any previous quantification of the tennis gripping tightness has only been researched in regards to the effect on impulse reaction and ball rebound velocities. The tennis grip needs to be quantified, and related to, the structural damping of the tennis racquet to show the damping mechanics of the player's hand.

When attempting to quantify the tennis grip by measuring tightness, the location where the measurements should be taken are important as they will need to represent the grip and its dynamic behaviour. Previous research has identified important locations in the

tennis grip, and used them as force measurement locations to show the dynamic behaviour of the grip during impact (Li *et al.* 2004; Knudson and White 1989; Cross 1998b). These locations on the hand are the hypothenar eminence and the thenar eminence. They have been deemed important as they exhibit critical gripping forces during the forehand and backhand strokes (Li *et al.* 2004; Knudson and White 1989; Knudson 1991). Once again these force measurements were analysed focusing on ball velocities and not racquet damping. The quantification of the tennis grip has not been used for correlations with quantified racquet damping, although grip tightness has been used to demonstrate its effect on racquet vibration levels (Li *et al.* 2004). The techniques used in previous research to identify locations in the grip with the greatest magnitude of force, have been developed in the present investigation to aid more advanced techniques for real-time measurements of the tennis grip. The tennis grip has also been quantified in relation to the dynamic response of the racquet to enable correlations of grip pressure distribution and racquet damping to be established.

Racquet oscillations are damped out far greater in hand-held racquets than racquets in free suspension. The hand is the most effective means of damping racquet frame vibrations, compared to manufactured attenuators, as it provides a transfer of racquet energy to the player's hand and lower arm. The player's hand and lower arm provide energy absorption to the racquet-hand system, allowing for post-impact vibrations to be damped. The addition of a second hand on the racquet handle (i.e. double-handed strokes) will dampen racquet vibrations more efficiently than with only a single hand. The double handed strokes also provide a second source of vibration attenuation; therefore the total energy absorbed by the player is distributed between the two hands rather than being

fully absorbed by one. Double handed players do not suffer for upper extremity injuries to the same extent as single handed players as the racquet energy is not concentrated on a single hand but is distributed between two. Previous studies have related the effect of the tennis grip to racquet vibrations but have failed to quantify both grip tightness and the magnitude of vibration damping it imparts on the racquet structure (Brody 1987, 1989). Both gripping tightness and racquet damping need to be quantified before correlations between the two factors can be made.

The overuse and excessive straining of the wrist extensors and tendon origins in the forearm is thought to be the major cause of tennis elbow. Overuse of the wrist extensors is caused by the absorption of racquet shock and vibration by the muscles and tendons of the wrist extensors. The contraction of the wrist extensor muscle group occurs mainly in the backhand tennis strokes, and previous studies have focused on the transfer of shock and vibration for these particular stroke types (Hennig *et al.* 1992). The experiments on the backhand stroke have found that the levels of vibration at the player's elbow are significantly lower than those levels measured at the player's wrist (Kawazoe *et al.* 2000; Kawazoe and Yoshinari 2000). This provides evidence that racquet shock and vibration transferred to the player is absorbed largely by the player's forearm muscles, tendons and other soft tissue.

Studies have been carried out to assess the effectiveness of racquet vibration attenuators (Wilson and Davis 1995; Cottey *et al.* 2006). It has been revealed in previous research that vibration attenuation devices such as string dampers do not reduce the magnitude of vibration transferred to the player's forearm. The string damping devices are small in

mass (5-10g), and when compared to the racquet mass (>200g) the device is too light to damp the lower frequency vibrations that are thought to cause tennis elbow (Li *et al.* 2004). String damping devices have been shown to attenuate the higher frequency vibrations of the string bed (Stroede *et al.* 1999). However it is the lower vibration frequencies of the racquet frame that are believed to cause the discomfort of tennis elbow. Vibrations below 180Hz have been shown to produce more discomfort to the forearm than those above 180Hz (Reynolds *et al.* 1977). If the vibration attenuation devices only damp higher frequency string vibrations, the issue of lower frequency frame vibration transfer to the players forearm is not resolved. Tuned vibration attenuation has been investigated based on the inherent structural properties of the tennis racquet and discounting the effect of the tennis grip on its dynamic response (Vethecan and Subic 2002). Optimal locations for the attachment of vibration attenuation devices can only be determined if the dynamics of the tennis racquet in hand-held conditions can be established. The damping of racquet frame vibrations by the tennis grip needs to be fully understood to establish the behaviour of the tennis racquet under hand-held conditions.

Vibration attenuation devices need to be optimised to allow for improved management of tennis elbow injuries (i.e. optimisation of vibration attenuators together with rehabilitation methods and techniques). Knowledge regarding the damping mechanics of the tennis grip will allow for a better understanding of the damping mechanics involved in the transfer of racquet shock and vibration. Knowledge of grip damping mechanics will aid the optimisation of future vibration attenuation devices.

#### ***1.2.4 Active damping technology***

Throughout this thesis two racquets will be used for all the testing carried out. The candidate received two Intelligence i.X16 racquets from Head Sports Company for testing purposes. The racquets are manufactured with the new piezoelectric active damping technology. However, only one of the two racquets had the system active to allow for comparisons to be made regarding the effectiveness of the system. The candidate was unaware of which racquet had the inactive damping system to avoid any bias in the comparisons. The racquets will be compared to show the effectiveness of the piezoelectric system with respect to the damping of racquet frame vibrations.

Piezoelectric materials generate an electric charge when they are deformed by an external force. The charge produced is proportional to the force applied to deform the material (Brody *et al.* 2002; Cottey *et al.* 2006; Reynolds *et al.* 1977; Lammer and Kotze 2003). This technology has been applied to tennis racquets to aid in the alleviation of racquet shock and vibration, by moulding the ceramic fibres to the throat and sides of the racquet. When the racquet has a bending force (either shock or vibration or a combination of both) applied to it during impact with the ball, the frame bends and the piezo fibres generate an electrical charge. This charge is then fed into a self-powered circuit board located in the handle where it is redirected back into the racquet's piezo system. When the electrical charge is redirected back into the piezo fibres on the racquet, they react by increasing their stiffness. This increase in stiffness can reportedly dampen up to 50% of the racquet's vibrations and increase the power of the rebound ball (Lammer and Kotze 2003; Crawford 2000). The system has also been tested in clinical trials to demonstrate its effectiveness when used by players suffering from symptoms of tennis elbow. Trials

showed there to be a significant improvement in both acute and chronic tennis elbow sufferers based on the Mayo Elbow performance index (Cottey *et al.* 2006). It will be one of the additional objectives of this thesis to give an evaluation from a mechanical engineering perspective to determine the magnitudes of vibration attenuation by the active piezo damping system.

### 1.2.5 Summary of relevant body of knowledge

To summarise the most relevant knowledge covered in this literature review, table 1 is used to describe the key findings to date. The table includes a brief description of the publications content together with the findings that are relevant to this investigation. The full details of each publication can be found in the reference section at the end of this thesis.

Number	Publication title	Author & year	Description of content	Summary of findings relevant to this investigation
1	<i>The physics and technology of tennis</i>	Brody, H., Cross, R., and Crawford, L. (2002)	The publication examines the role of physics and technology in the sport of tennis. A wide range of subjects are covered ranging from racquet technology and physics to stroke analysis.	The publication describes the inherent properties of the tennis racquet (including approximate ranges for natural frequencies and mode shapes) and relates them to the different sweet spots of the tennis racquet. The publication also establishes that the addition of the hand to the racquet system results in a dramatic increase in vibration damping. The forces imparted on the hand by the racquet and their relationship with the COP is also discussed.

2	<i>The biomechanics of tennis elbow: An integrated approach</i>	Roberts, P.E., Brody, H., Dillman, J.C., Groppel, J.L. (1995)	The investigation attempts to integrate a number of different approaches to assess the injury of tennis elbow. The approaches include biomechanics, racquet physics and clinic analysis.	Stroke types are related to the different categories of tennis elbow. Forehand and service strokes are linked to medial epicondylitis, with the backhand stroke related to the lateral injuries. The vibrations of the tennis racquet are related to the ball impact location and are said to be transferred to the tendon origins of the forearm via contracted muscles. This thesis aims to utilise this information and build upon it to establish the mechanics by which racquet vibrations are transferred to the player's hand during impact.
3	<i>Impact of a ball with a bat or racket</i>	Cross, R. (1999)	The publication focuses on the collision structural dynamics of a uniform beam as a result of a tennis ball impact.	The investigation shows the propagation of waves through the beam after impact and establishes that not all excited vibration will be felt by the tennis player at the grip. Those higher frequencies are said to be too small in amplitude and heavily dampened by the ball so the player will not feel them. The knowledge acquired in this publication can be utilised to identify the racquet vibration frequencies of greatest importance when discussing the damping effect of the tennis grip.
4	<i>Models of tennis racket impacts</i>	Brody, H. (1987)	The investigation analyses the impact of the tennis ball on the racquet and the response of the racquet under both freely suspended and hand-held conditions.	The influence of the hand is shown and it is determined that the hand is incapable of producing a "clamped" effect. Therefore hand-held racquets are representative of the freely suspended conditions.
5	<i>The role of the racket in high-speed tennis serves</i>	Kotze, J., Mitchell, S.R., and Rothberg, S.J. (2000)	The publication provides a comprehensive literature review of racquet physics and technology.	The common attributes of racquet behaviour are discussed based on extensive literature review. Literature concerning racquet sweet spots and their influence on both ball rebound properties and player injuries is reviewed and compared. This thesis aims to add to this literature base by quantifying the relationship between tennis gripping pressure distribution and the damping of racquet vibration.

6	<i>Forces and duration of impact and grip tightness during the tennis stroke</i>	Hatze, H. (1976)	The motion of the racquet as a result of impact is analysed in this work. The forces within the tennis grip and racquet vibrations are defined and linked to the injury of tennis elbow.	It was concluded that an increase in gripping tightness will result in a more powerful tennis stroke (due to increased swing speed) but will also increase the magnitude of vibration transferred to the tennis player. To reduce the pain felt by the injured player, it was suggested that a looser grip should be used or a redesigned racquet is necessary to alleviate vibration transfer to the player. This research aims to provide new knowledge to aid the redesign of the racquet, by quantifying the effect of the tennis grip on the racquet's response to impact. Racquet optimisation can only be achieved if parameters such as gripping tightness and their influence on racquet vibrations can be quantified.
7	<i>Transfer of tennis racket vibrations onto the human forearm</i>	Hennig, E.M., Rosenbaum, D., and Milani, T.L. (1992)	The investigation focuses on the transfer of racquet vibrations to the player's wrist and elbow to determine the magnitudes of vibration at these locations and relate them to those of the racquet after impact.	It was found that vibrations levels at the player's arm after impact were inversely related to the resonance frequency of the tennis racquet (i.e. the lower the resonance frequency of the tennis racquet, the greater the transfer to the player's arm). It is evident that there is transfer of racquet shock and vibration but this transfer is yet to be quantified, and this is one of the main objectives of this thesis.
8	<i>The centre of percussion of tennis rackets: a concept of limited applicability</i>	Hatze, H. (1998)	This investigation utilised a manusimulator to analysis the effect of ball impacts on reaction forces in the tennis grip.	The investigation identified two force peaks acting on the hand during impact. It is concluded that these forces are a result of the racquet movement within the tennis grip after impact and the player's attempts to regain control. This identification of the grip force patterns will be built upon in a more comprehensive manner to show the distribution of pressure within the tennis grip rather than single point measurements. This can then be utilised to analyse the effect the pressure distribution has on the damping of racquet vibrations.

9	<i>Forces on the hand in the tennis forehand drive: application of force sensing resistors</i>	Knudson, D.V., and White, S.C. (1989)	The publication investigates the forces acting on the hand during the forehand drive, in terms of the variations in magnitudes of force during impact.	Forces acting on the hand at two locations are measured for a range of test subjects. However, gripping forces are subjective in nature and are dependant on the individual player and ball impact properties. Grip force patterns during impact are identified showing the rotation of the racquet within the tennis grip as a result of the impact. This thesis aims to build on this work by utilising subjective grip pressure distributions to quantify the effects on racquet vibration damping.
10	<i>Forces on the hand in the tennis one-handed backhand</i>	Knudson, D. (1991)	The investigation analyses the patterns of forces acting on two locations within the tennis grip during a one-handed backhand stroke.	Magnitudes of forces acting on the player's hand at two locations are measured for a range of players. The grip forces are quantified but not related to the damping of frame vibrations by the hand. This thesis aims to build on this research by establishing the distribution of pressure in the tennis grip and relating it to the damping of racquet vibrations by the player's hand.
11	<i>Tennis racket shock mitigation experiments</i>	Wilson, J.F. and Davis, J.S. (1995)	This publication examines the effectiveness of retrofits in mitigating shock in tennis racquets.	The experiments conducted in this research produced isolines for the COR for test racquets, together with estimations of damping factors based on the racquet's damped natural frequency. The research was focused on assessing the effectiveness of the retrofits using clamped racquet conditions and does not attempt to analysis the effect of grip damping. This research aims to build on this by calculating estimations of racquet vibration damping and relating them to the distribution of grip pressure.

12	<i>The sweet spot of a tennis racket</i>	Cross, R. (1998)	The publication analyses the impact of the racquet with the ball under hand-held conditions.	Forces acting on the hand as a result of ball impact location are investigated and discussed in terms of COP and node locations. Comments are made regarding the influence of the hand on the node location in the tennis grip which is of the utmost importance to this research, as it is the location of vibration transfer to the player. This investigation aims to advance this research by examining the mechanics by which racquet vibrations are absorbed by the player via the tennis grip.
13	<i>Customising a tennis racket by adding weights</i>	Cross, R. (2001)	The publication examines the physics of the tennis racquet and how the racquet can be tuned to suit players. The Sweet spots (including the racquet's nodes, COP and ACOR) are investigated and the effects of added masses are analysed.	The node lines of the racquet are shown to be curved in nature. It was concluded that the location of the node locations on the racquet remain unaltered by stringing the racquet but the natural frequencies significantly decreased (approximately 8.5% reduction).

**Table 1. Summary of existing knowledge relevant to this investigation**

### 1.3 Research objectives and scope

Based on the current body of knowledge, objectives for this investigation have been devised. The overall aim of the investigation is to analyse the absorption of racquet shock and vibration via the tennis grip. This aim encompasses a wide range of both general and specific research objectives which are now outlined:

### **1.3.1 General objectives**

- *Quantify tennis racquet vibration damping* – the magnitude of structural damping needs to be measured in relation to a subjective gripping tightness together with any additional damping factors such as the tennis ball. The damping of racquet vibrations by the tennis grip must be quantified in both the time and frequency domain.
- *Establish the inherent structural dynamic properties of the test tennis racquets and examine the influence of strings on frame modes* – knowledge of the racquet's inherent properties is required if an appropriate assessment of damping parameters (such as the tennis grip) is to be conducted. The effects of racquet strings on the measured frame modes of oscillation will also be investigated.
- *Quantify the tennis gripping tightness* - knowledge concerning the magnitudes of gripping forces is required if the effect of the tennis grip on racquet dynamics is to be assessed.
- *Establish relationships between grip pressure distributions and tennis racquet damping* – correlations between the measured parameters (i.e. grip pressure dynamics and racquet damping) needed to be made so the mechanics of the grip damping phenomena can be fully understood.

### **1.3.2 Specific objectives**

- *Identify key locations in the tennis grip that display the greatest magnitudes of pressure* – by identifying key contact points, the mechanics defining the transfer of racquet frame vibrations to the player's hand can be established and modelled.

- *Evaluate grip pressure distribution characteristics for different stroke types in the time domain* – characterisation of grip pressure distributions for different stroke types is needed if correlations are to be made with racquet damping. Quantifying the distribution of pressure with respect to the contact points of the player's hand will allow for grip damping mechanics to be described.
- *Quantify player perception* – by quantifying and understanding player perception of the incoming ball it will be possible to describe how they prepare the racquet for impact in terms of grip tightness.
- *Relate the transfer of racquet vibration to the contact areas and their associated pressure distributions* – by understanding the distribution of pressure across both the player's hand and the racquet handle, the transfer of frame vibrations to the player's hand can be described in terms of the magnitude of grip damping in relation to the racquet handle.
- *Estimate the effectiveness of the piezoelectric damping system on the Head Intelligence racquet* – develop a systematic technique for establishing the damping capability of individual racquets and use the technique to determine the effectiveness of the piezo system in comparisons of the two test racquets.

#### **1.4 Thesis overview**

Contributions to the current body of knowledge were accomplished by experimentally investigating the research objectives outlined in section 1.3. The research objectives were achieved using deliverable targets leading to integration of data and theoretical principles. The following sections give a brief description of the thesis chapter content and how they approach the research objectives.

### ***1.4.1 Chapter 2***

Chapter 2 utilises modal analysis to identify the inherent structural dynamic properties of the two test tennis racquets. The comparison of the two racquets with respect to their inherent properties is crucial if the damping of racquet vibrations by the tennis grip is to be quantified. Modal analysis conducted in this chapter investigates additional modes of oscillation brought about by the addition of string vibrations to the racquet system.

### ***1.4.2 Chapter 3***

This chapter uses experimental techniques to quantify and characterise the tennis grip. Contact locations displaying the greatest magnitudes of pressure are established using pressure sensitive film. Qualitative magnitudes of pressure are also determined via this method. Using the identified contact points, a real-time data acquisition system is developed to analyse the distribution of grip pressure across the racquet handle during impact. Variations in pressure distribution are quantified and related to locations on the racquet handle and anatomically to the player's hand. Using the pressure distribution measurements, it is possible to hypothesise the movements of the player's hand in order to describe the mechanics by which racquet shock and vibration are transferred to the player's hand and forearm.

In addition to the pressure distribution experiments, the application of a strain gauge cantilever system is conducted to describe the behaviour of the tennis grip in relation to the incoming ball. The system allows for the quantification of gripping forces on the racquet handle and their variations with respect to player perception of the incoming

tennis ball. Player anticipation times are estimated using this system to describe how the player prepares the tennis racquet before impact with respect to the stiffness of the racquet-hand interface.

#### ***1.4.3 Chapter 4***

Chapter 4 investigates the dynamic response of the tennis racquet during a ball impact. The effect of using a ball impact excitation instead of using modal analysis techniques allows for the ball damping effect to be quantified. In addition to this, the effects of subjective gripping tightness on the racquet's dynamic response are also analysed. The half-power and logarithmic decrement damping estimations are both utilised to determine the relationship between grip tightness and the damping of racquet frame vibrations.

#### ***1.4.4 Chapter 5***

Chapter 5 uses the data acquired in chapter 3 (gripping pressures) to establish relationships between the grip pressure distribution and the damping effect it has on racquet vibrations. The chapter establishes quantitative relationships between gripping pressures and racquet vibration damping in terms of overall grip pressure and more specific locations of grip pressure. The analysis considers the dynamic response of the tennis racquet (analysed in chapter 2) and examines the effect of variable grip pressure in relation to the displacement of the racquet's first mode shape. Using these relationships, the transfer of vibration to the player's hand at the contact points within the tennis grip, is described.

### ***1.4.5 Chapter 6***

This is the final chapter of the thesis that concludes the relevant findings of the research. Conclusions regarding the objectives outlined in this chapter are made and the contributions to the current body of knowledge are identified. The chapter contains a discussion regarding the relevance of the thesis for the development of tennis elbow injury management (e.g. vibration attenuation devices). Recommendations for future research are discussed, which is based on the findings of this research and the areas identified requiring further investigation.

## **Chapter 2**

# **Comparing the structural dynamic properties of two tennis racquets**

The research conducted in this thesis investigates the effectiveness of a piezoelectric damping system of the Head© i.X16 Chipsystem racquet. Two tennis racquets are used throughout the research with identical dimensions to assess the damping system, with only one racquet having the system enabled. It was not known which of the two racquets contained the active damping system, termed racquets A and B to distinguish between them. Experimental modal analysis is used in this chapter to identify structural dynamics properties of the two tennis racquets, including natural frequency, mode shapes and damping coefficients. A comprehensive knowledge regarding the dynamic response of the racquet in terms of natural frequencies, inherent damping and mode shapes, is required if appropriate analysis of the racquet's damping system is to be conducted. The effect of the damping system cannot be assessed using modal analysis, because a ball impact is required in order for the test to be realistic. Modal analysis uses impact hammers and shakers and therefore conclusions regarding the effectiveness any damping system can not be based on modal analysis. However, knowledge acquired from the modal analysis is required for the appropriate interpretation of data acquired during the ball impact experiments. Modal analysis of the racquet under freely suspended conditions reveals the inherent structural dynamic properties of the racquet (i.e. natural frequencies and damping coefficients) and therefore the effect variable parameters such as the tennis grip and piezoelectric damping system can be analysed in comparison.

As discussed in the previous chapter, the analysis of the racquet in a clamped state is not representative of the racquets' behaviour when it is hand-held (Brody 1987; Cross 1997). If the racquet is to be analysed in relation to hand held condition, then modal analysis

should be representative of this as well. Free suspension condition will therefore be used to determine the inherent dynamic properties of the tennis racquet.

Modal analysis of structures can be carried out in different ways. Appropriate experimental techniques need to be used in order to acquire valid data whereby test equipments should not interfere with the dynamic properties of the test structure (Dossing 1988; Gade *et al.* 2005; Ewins 1984). With lightweight structures such as the tennis racquet (~230g) sensing equipment and experimental techniques need to be chosen carefully. Mass loading of transducers is a potential source of error in the measurement of the structure's dynamic response. Therefore, transducers need to be lightweight together with none intrusive experimental techniques, in terms of effecting the dynamic response of the test structure. Attachments of transducers such as an accelerometer, along with the constraints of a shaker stinger rod introduce unwanted external force during the excitation of the structure. Therefore provide a potential source of error in the test results as these effects change parameters such as the structures natural frequency.

For lightweight structures such as a tennis racquet, transducers need to be lightweight to so it does not influence the dynamic response of the test structure. If transducers are too larger in comparison to the mass of the test structure, its attachment will cause shifts in natural frequencies, increase damping and in some cases introduce extra modes of oscillation (Ewins 1984). The mass of the transfer used should satisfy the relationship shown in equation(1.3), where  $M_A$  is the apparent mass of structure at the loading point and  $M$  is the mass of the transducer (in the case of impact hammer testing, an

accelerometer) (Dossing 1988). If the mass of the transducer exceeds the ratio of 1.03, the test results will have a significant shift in frequency as to make them invalid.

$$\frac{M_A + M}{M_A} < 1.03 \quad (1.3)$$

Experimental modal analysis is conducted used two methods of applying excitation to the test structure and they include shaker testing and impact hammer testing. Shaker tests are intrusive as they require the attachment of a stinger rod with a transducer to the test structure, which adds additional mass and may change its dynamic response. Force transducers are always attached to the structure in shaker excitation to measure the input force, while the response is measured using either a scanning laser vibrometer or an accelerometer (N.B. the accelerometer will add more mass to the test structure). Excitation of a structure using a shaker method can also limit the test structures movement in certain degrees of freedom (DOF) due to the constraints of the attached stringer rod. These potential sources of error with shaker testing are not of major concern with heavy test structures; however a lightweight structure will be affected. Application of excitation using an impact hammer can be carried out with the test structure in freely suspended condition so that all DOF can be assumed to be unrestricted as the structure's movement is not constrained in any direction.

As previously mentioned, the knowledge of the tennis racquets structural dynamic properties are required if the effect of additional parameters are to be investigated. An analysis of all parameters effecting the dynamic response of the tennis racquet must first be quantified if is optimisation is to be achieved with respect to vibration transfer to the

player. This chapter utilises experimental modal analysis techniques to determine the inherent structural properties of the tennis racquet to establish a point of reference for the analysis of external parameters such as the tennis grip and their effect on racquet dynamics. Furthermore, an investigation is conducted into the effect of tennis strings on the dynamic response of the racquet together with a comparison of the test racquets A and B. Establishing the natural frequencies, damping coefficients and modal shapes of the test racquets provides knowledge for the appropriate assessment of damping during ball impacts.

## **2.1 Methodology**

The main objective of the modal analysis was to ascertain the mode shapes, natural frequencies and damping coefficients of the two racquets in the frequency range 0-1200Hz. Previous research as shown that first three modes of the tennis racquet reside within this frequency ranges and are of most importance when investigating racquet vibration and the effect on upper extremity injuries (Brody *et al.* 2002; Reynolds *et al.* 1977). In addition to identifying these key modes of oscillation, the influence of the tennis strings on the dynamic response of the racquet was included in the modal analysis. The test racquets used (A & B) were analysed both with and without strings to identify mode which were inherent to the racquet frame and those that are a cause of string effects.

The testing factors regarding the choice of both the method of excitation and the use of transducers have been taken into consideration in the design of the test procedure for determining the inherent dynamic properties of the tennis racquet. It has been decided

that an impact hammer be used with a uniaxial lightweight accelerometer in conjunction with a freely suspended racquet to determine the inherent dynamic properties of the tennis racquet. The laser scanning vibrometer could not be utilised for measuring the response because rigid body motion of a freely suspended racquet (i.e. the racquet does not remain in a stationary enough position for the laser to measure the response). Impact tests reduce the magnitude of mass loading associated with the attachment of excitation shakers to the structure (Inman 1994). A roving impact hammer excitation/fixed response logic was also used in the modal analysis to avoid changes in mass distribution over the structure brought about by relocating the accelerometer for each measurement (Dossing 1988; Ewins 1984).

### ***2.1.1 Experimental set-up***

The data collection process was carried out on the two test racquets (racquet A and racquet B) in freely suspended condition. The following instrumentation was used to conduct the impact hammer modal analysis test:

- Miniature PCB (PCB Piezotronics, Inc.)352A25 accelerometer (mass – 0.48g)
- Impact Hammer PCB 086C03
- Brüel & Kjær LAN Interface module type 7535
- Brüel & Kjær PULSE Labshop v10.1 data acquisition software
- ME'scope (Vibrant Technology, Inc.) modal analysis software v4.0

Figure 8 shows the freely suspended racquet set-up for the modal test. The accelerometer was attached to an approximate location on the racquet that demonstrating the greatest magnitude of displacement for the first bending mode. Previous studies have shown this

location to be on the racquets shaft (aligning with the approximate base of the racquet head), and it was chosen so response measurements in the z-direction would be largest in amplitude (Brody *et al.* 2002; Kotze *et al.* 2000). This allows for enhanced post-data collection analysis, as excitation of the frequencies of interest will be measured at this location.

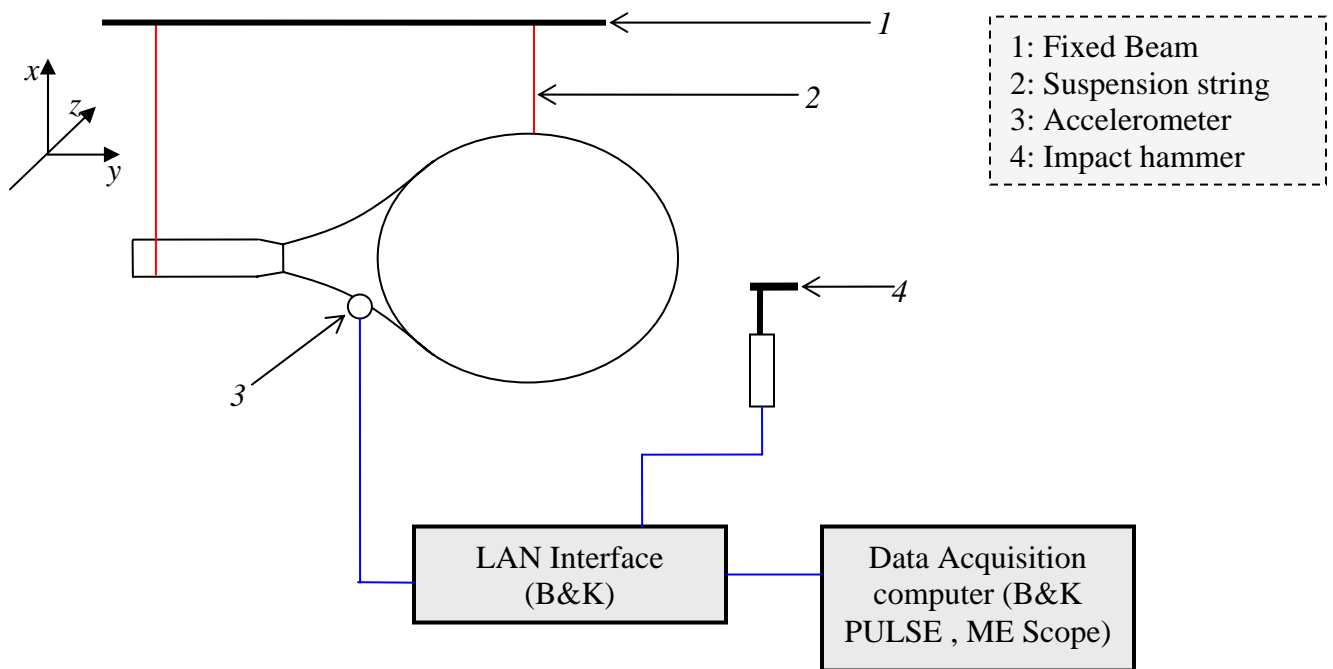


**Figure 8. Schematic of tennis racquet modal test set-up**

The force transducer and miniature accelerometer were connected to the Brüel & Kjær (Brüel & Kjær, Denmark) LAN interface module, using a light weight cable to limit its mass loading affects. The interface module provides internal amplification for the transducers so no external amplifiers were needed. The LAN interface module was connected to the PULSE Labshop (Brüel & Kjær, Denmark) data acquisition software. The software was configured to give an analysis frequency range of 0-1200Hz. This allowed for the identification of both bending and torsional modes of the tennis racquet.

In order to generate the required racquet excitation in the frequency range 0-1200Hz, a steel tip was used with the impact hammer to decrease the duration of the force impact. The excitation signal of the force transducer was filtered using a transient window, because of the short duration/impulse properties of the excitation impact. The transient window isolates the true impact signal (generated during the short impact time) and reduces the additional noise succeeding it by setting the signal to zero, allowing for clearer resolution of the frequency transfer function (Dossing 1988). The steel tip and transient filter condition the excitation signal from the force transducer, allowing for a large useful frequency range. In addition to the conditioning of the excitation signal, the response signal was also conditioned to reduce leakage effects brought about from the lightly damped structural response of the tennis racquet. The response signal of the accelerometer was filtered using an exponential window, because of the decay properties of the racquet when freely suspended. The lightly damped racquet structure produces a dynamic response with a slow decay. In order to avoid leakage effects when measuring the racquets dynamic response, an exponential window is implemented to force the response signal to zero within the data acquisition period.

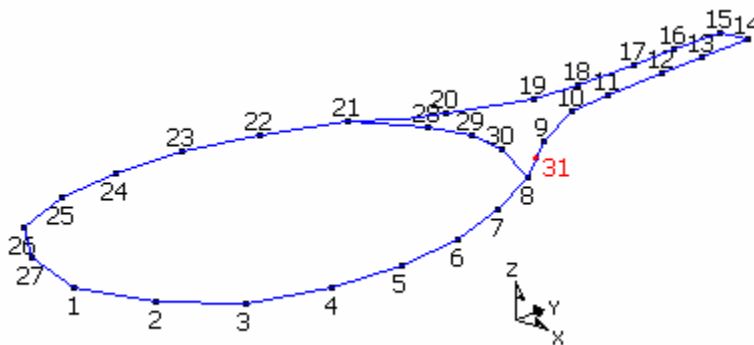


**Figure 9. Racquet geometry showing excitation points (response measured at point 31)**

To produce a resolution of the racquets structural dynamic response allowing for the modal shapes of interest to be calculated, 31 excitation points were identified as shown in figure 9. The racquet was excited at each of the 31 points using a hammer impact in the z direction, and the resulting dynamic response of the tennis racquet was measured using an accelerometer attached at point 31 (reference point for the response measurement), in the z axis.

Using hammer impacts, three responses were measured at point 31 for each of the excitation points. The three response measurements were then averaged to enable a H1 transfer function to be computed for the racquet. The estimated transfer function expresses the ratio between the output response (acceleration) and the input force (newtons). The resulting transfer function represents the response of the structure to the input excitation as a function of its inherent mass, stiffness and damping. The variations in these modal parameters can be estimated using the transfer function measurements as they allow for the estimation of the structures natural frequencies, damping coefficients and modal shapes.

The x,y,z coordinates for the impact locations and the H1 acceleration transfer functions for each impact point were imported to the modal analysis software ME Scope (Vibrant Technology, USA). Natural frequencies, mode shapes and modal damping were calculated using ME Scope software. Using the mode shapes, the racquet's node and anti-node locations were estimated.

### 2.1.2 Test racquets

Appropriate interpretation of modal analysis results requires structural properties of the tennis racquets (such as mass and racquet dimensions) to be determined. Properties such as mass define the dynamic response of a structure and therefore must be determined for an appropriate analysis of modal analysis results. Values for the parameters of racquet mass and centre of mass location were established and are shown in Table 2. The dimension parameters (including head size/area ( $\text{cm}^2$ ), string tension (N) and racquet length & width (mm)) for the test racquets were established and are shown figure 10. The dimensions of the racquets, in terms of racquet length and head area, were found to be identical; however the mass of the two racquets was different, as shown in Table 2.

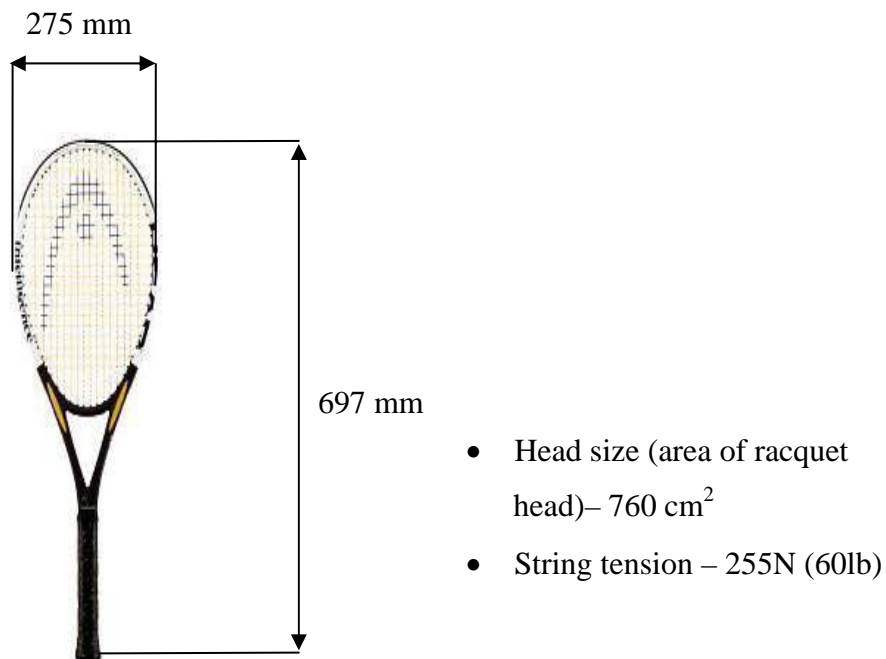


**Figure 10. Racquet dimensions**

<b>Racquet</b>	<b>Mass (grams)</b>	<b>Centre of mass/ Balance point (mm from tip)</b>
A	262	328
B	232	335

**Table 2. Racquet mass and centre of mass location**

The mass of racquet A is 30 grams heavier than that of racquet B. It was earlier stated that the racquets were given to the study with the understanding that they were identical, with the only different being the enable/disabled piezoelectric damping system. This is not the case as the racquets mass and centre of mass (balance points) are different (racquet A having a heavier head). The greater mass in racquet A means that the racquets are effectively two different racquets. This may mean that the effectiveness of the racquets piezoelectric damping system will be difficult to assess due to the racquets being too different. This will be taken into consideration throughout the thesis.

The additional mass of racquet A will lead to differences in the racquets inherent dynamic properties along with the player performance when using the racquet. Variations in mass distribution on the racquet structure will result in changes of swing weights leading to different levels of shock forces being transferred to the player's hand. Racquets with a heavier head (racquet A in this case) will generate a greater swing weight than a handle heavy racquet (racquet B in this case).

All difference between the two racquets, with respect to the racquets structure and its dynamic behaviour under various conditions, will be quantified during the research in-order to establish an appropriate conclusion regarding the effectiveness of the racquets

piezoelectric damping system. However, the interpretation of the racquets dynamic behaviour will be based on its inherent properties (i.e. mass, stiffness, etc.). For example the extra mass of racquet A (30 grams) may have an effect on its dynamic behaviour. The inherent mass of a structure is a property that defines its dynamic behaviour, along with its inherent stiffness and damping. Therefore additional mass will lead to changes in the dynamic behaviour of the structure with respect to natural frequencies, mode shapes and damping. Differences between the two racquets, such as this, will be considered during the analysis of their individual dynamic properties.

## **2.2 Experimental results**

The results of the modal analysis tests are presented for the two test racquets. The frequency response functions for each of the 31 response measurements for the racquets are presented, together with the identified natural frequencies, modal damping and mode shapes.

### 2.2.1 Racquet A

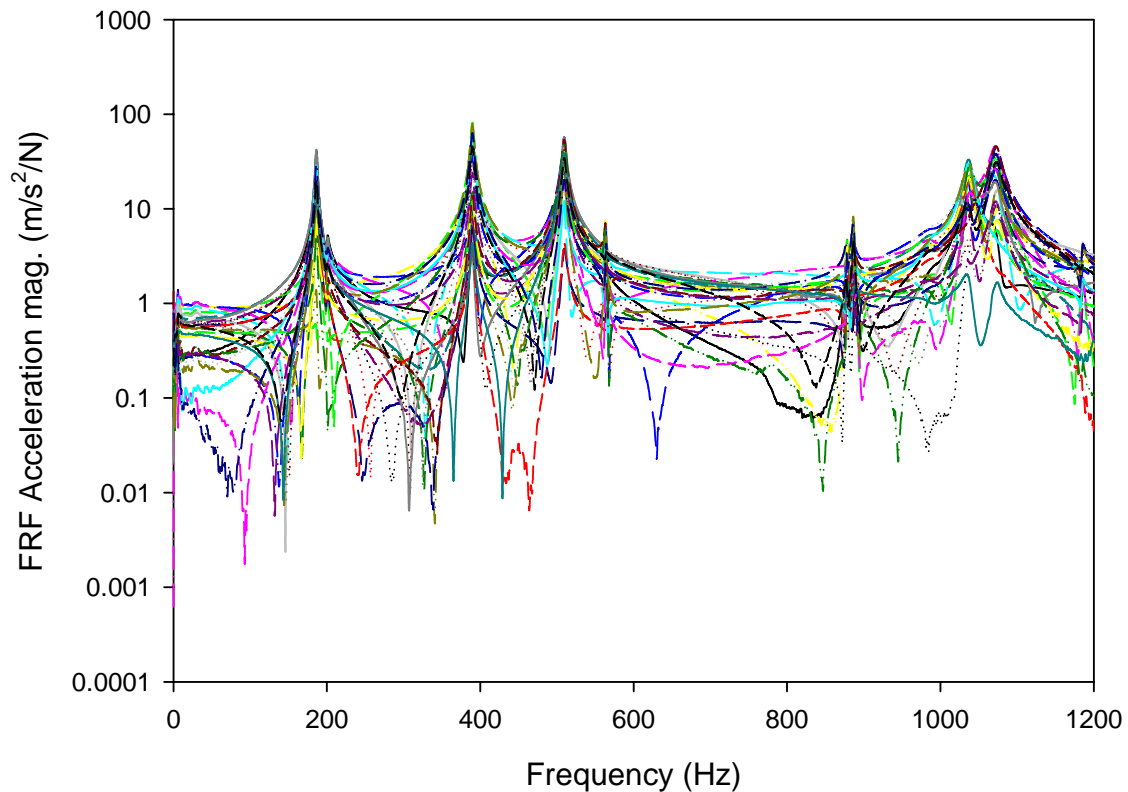


**Figure 11. Frequency response measurements for racquet A (with strings)**

Figure 11 shows the 31 individual FRF's (Frequency Response Functions) for racquet A using acceleration. The synthesised FRF for racquet A is shown in figure 14. Seven clearly identifiable resonance peaks can be seen in figure 11, indicating seven racquet modes. Table 3 shows the modal analysis results for racquet A, including natural frequencies, damping coefficients, mode shapes. Damping results indicate the percentage of the racquet's critical damping. (N.B. The critical damping of a structure can be defined as the degree of damping that separates non-oscillation from oscillation (Inman 1994). Effectively meaning if a system is critically damped there will be no oscillatory motion when excited (i.e. 100% damping). The damping coefficients in the modal analysis of this

thesis represent the percentage of a modes critical damping inherent to the racquet structure.) The mode shapes show the deflection of the racquet at the associated natural frequency. The shapes displayed in Table 3 contain arrows showing the direction of racquet deflection from its equilibrium state.

Mode	Natural Frequency (Hz)	Damping (%)	Mode Type	Mode Shape (x-axis view)	Mode Shape (y-axis view)
1	186	0.709	Bending		
2	390	0.563	Torsion		
3	509	0.515	Bending		
4	564	0.187	Rigid		
5	887	0.168	Torsion		
6	1040	0.502	Bending		
7	1070	0.631	Torsion		

Table 3. Modal analysis results for racquet A

Seven modes of oscillation have been identified for racquet A in the frequency range 0-1200Hz. The fundamental bending mode had an associated natural frequency of 186Hz. The racquets third mode was at a natural frequency of 509Hz, and had less inherent damping than the first mode. These values vary from previous research (Cross 2001), because the modal analysis has been carried out using different racquets. The higher natural frequencies shown in this research compared to previous studies are a result of the racquet being either lighter, stiffer or a combination of both. The racquets second mode of oscillation was identified as a torsional mode at a natural frequency of 387Hz, with the associated inherent damping less than the first modes. A sixth mode of oscillation was identified at a natural frequency of 1040Hz.

All bending shapes, natural frequencies and damping estimate trends given in this research support previous modal analysis of tennis racquets and simple beam structures (Brody et al. 2002; Vethecan and Subic 2002). Despite the absolute analysis values varying between different publications (e.g. higher/ lower natural frequencies, which depends on the structure under investigation), the frequency range where the mode of oscillation is identified remains constant, giving confidence in the results.

(N.B. The results presented on racquet A thus far were determined with the racquet strung. Additional modal analysis was carried out on the racquet in an un-strung condition, to establish genuine frame modes and those associated with the strings. These results are presented later in the chapter in the comparison between strung and un-strung racquets)

### 2.2.2 Racquet B

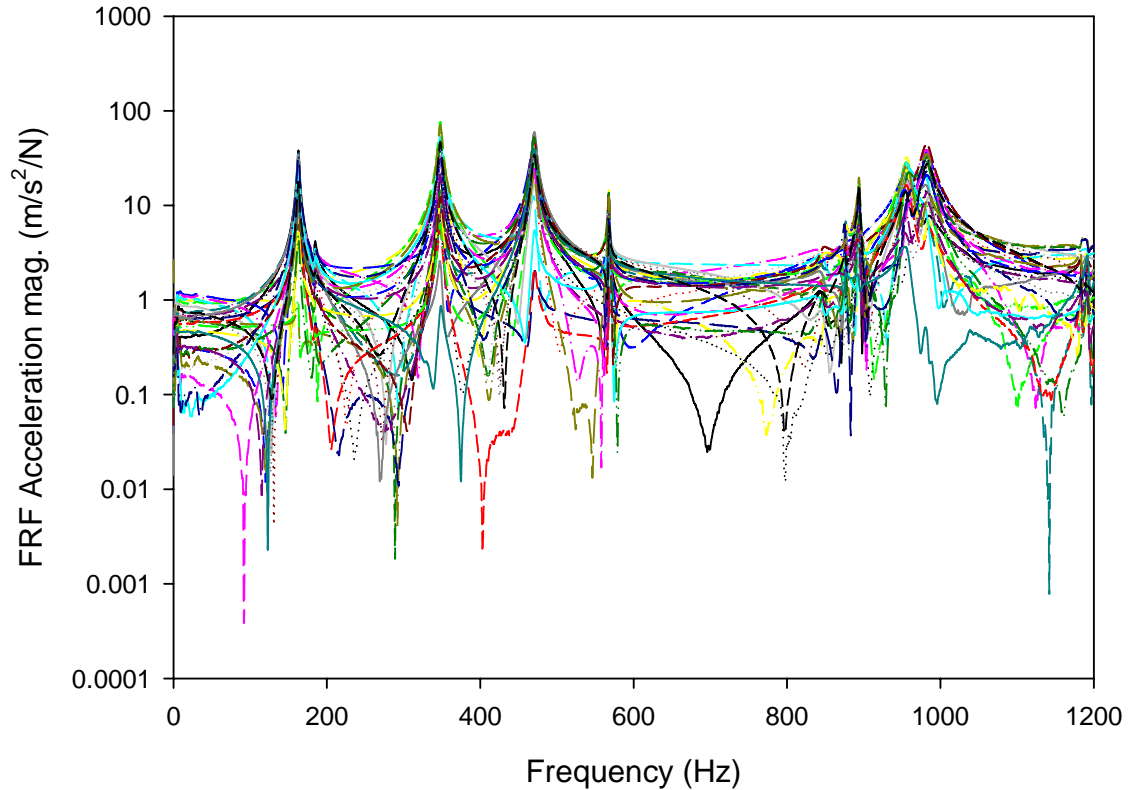


**Figure 12. Frequency response measurements for racquet B (with strings)**

Figure 12 shows the 31 individual FRF's for racquet B. Figure 14 shows the synthesised FRF for racquet B in comparison with racquet A. Figure 12 shows seven clearly identifiable resonance peaks for racquet B, similar to those of racquet A. Table 4 shows the modal analysis results for racquet B, including natural frequencies, damping coefficients and mode shapes. The mode shapes show the deflection of the racquet at the associated natural frequencies. The mode shapes contain arrows showing the direction of the racquet deflection from its equilibrium state. Damping results indicate the percentage of the racquets' critical damping.

Mode	Natural Frequency (Hz)	Damping (%)	Mode Type	Mode Shape (x-axis view)	Mode Shape (y-axis view)
1	163	0.894	Bending		
2	348	0.681	Torsion		
3	470	0.621	Bending		
4	568	0.141	Rigid		
5	894	0.161	Torsion		
6	955	0.629	Bending		
7	982	0.73	Torsion		

Table 4. Modal analysis results for racquet B

The modal analysis results shown in Table 4, have identified seven modes of oscillation in the frequency range 0-1200Hz. The fundamental bending mode of racquet B has a natural frequency of 163Hz with an associated damping coefficient 0.894%. The second mode is a torsional mode of oscillation with an associated natural frequency of 348Hz. The third is a bending mode of the racquet at a natural frequency of 470Hz and a damping coefficient 0.273% lower than that of the first bending mode. Once again, these natural frequencies of the identified modes support that of previous research regarding the modal analysis of tennis racquets, as they reside within the same frequency ranges.

Node locations for the first bending mode were found to be the same for both racquets. The determined distances between nodes and the racquet tip are shown in figure 13. The quoted distances for the node location on the tennis racquet are based on the node of the racquet frame. Previous research has shown the node line between the nodes of the racquet head to be curved (Cross 2001). The modal analysis conducted in this thesis was only based on the excitation and response of the racquet frame and therefore only frame nodes are shown.

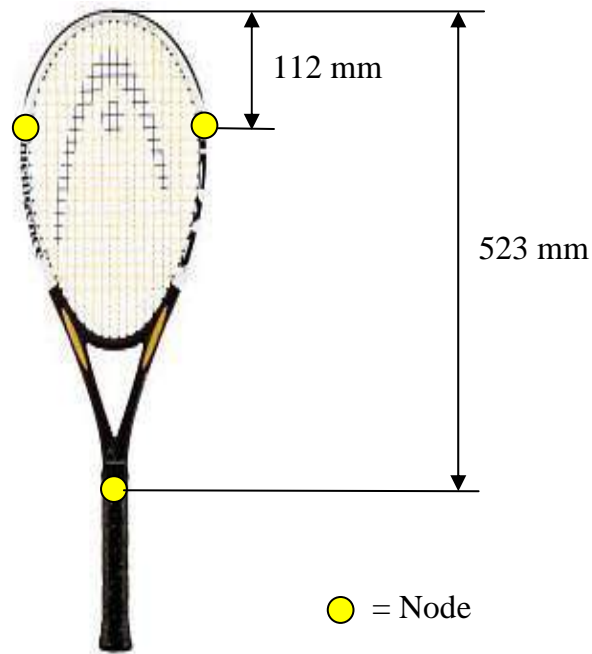


**Figure 13. Node location associated with the first bending mode for racquets A and B**

### **2.3 Discussion of results**

Both test racquets displayed seven modes of oscillation in the frequency range 0-1200Hz. However it is the fundamental mode of oscillation that is thought to be of most concern to injuries such as tennis elbow, and this mode has been measured below 200Hz for both racquets. The additional modes (i.e. those resonating at a higher frequency) provide knowledge of the racquets inherent structure. These higher frequency modes have been measured due a metal tipped hammer being used as excitation. These higher frequency modes may not be seen when the racquet is excited using a tennis ball. This is because during excitation, the impact duration of a metal tipped hammer is much shorter than that of a tennis ball. Therefore damping of vibrations by the method of excitation will be greater when using a tennis ball. It is still important to know the inherent behaviour of the racquet so the effect of the tennis grip and the ball on the dynamic response of the racquet can be quantified in later chapters.

Determining the first bending mode of the two tennis racquets has allowed for the identification of the racquets nodal sweet spot. However, all of the modes of oscillation identified in the analysis are important for the “feel” of the tennis racquet as they affect the response of the racquet’s handle (Vethecan and Subic 2002). The magnitude of the racquet handles oscillatory response determined by the impact location of the ball and its proximity to the racquet’s node. The further from the node the ball impact is, the larger the oscillatory response of the tennis grip. However, previous research regarding vibration and human discomfort has shown it is the modes of oscillation at the lower frequencies that are believed to cause the pain and discomfort of tennis elbow (Brody 1981). For this reason, the analysis of the lower frequency bending modes is of up most importance if the mechanics of grip damping are to be understood.

The natural frequency of this first bending mode was identified as 186Hz for racquet A and 163Hz for racquet B. The difference of 23Hz for the first mode of oscillation is shown visually in figure 14. By superimposing the average FRF’s for the two test racquets differences in inherent dynamics properties can be seen.

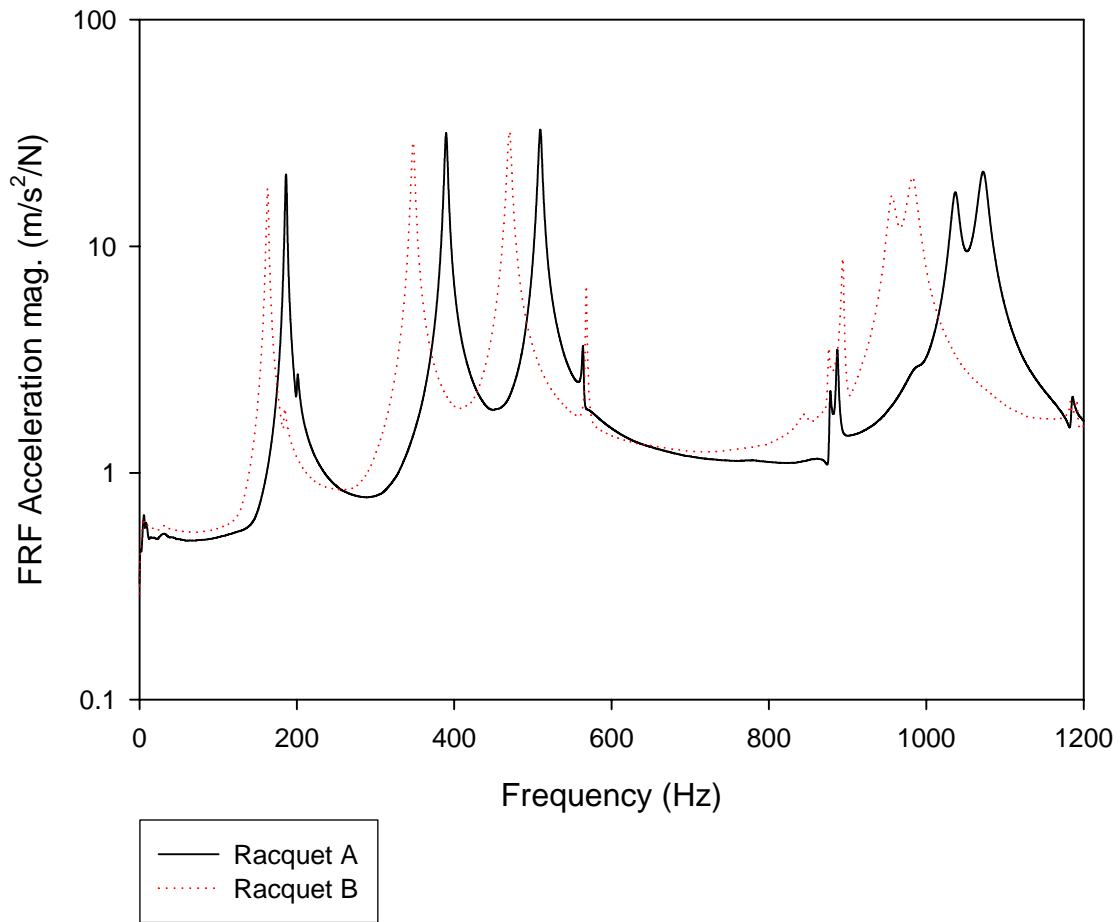


**Figure 14. Comparison of average FRF's for racquets A and B**

All modes of oscillation for racquet B are lower in their natural frequency than the associated modes for racquet A. As previously stated the first mode of oscillation is 23Hz lower for racquet B than for racquet A, with a similar trend for the higher modes identified. Racquet B has a torsional mode of oscillation 44Hz lower than the corresponding torsional mode of racquet A. The third mode of oscillation (second bending mode) for racquet B is 34Hz lower than that of racquet A. The natural frequency is described using equation (1.4); where  $(\omega_n)$  represents the natural frequency,  $(k)$  represents modal stiffness and  $(m)$  represents modal mass:

$$\omega_n = \sqrt{\frac{k}{m}} \quad (1.4)$$

With a greater modal mass there will be a reduction in the structure's natural frequency (Inman 1994). However, a greater modal stiffness will lead to an increased natural frequency. If we consider the results obtained through modal analysis, the differences in natural frequencies are attributed to either the modal mass or the stiffness of the racquet. The mass of racquet A is 12% heavier (30g) than racquet B. This would indicate a lower natural frequency in racquet A due to the extra mass; however this is not the case. Racquet A has a natural frequency 13% higher than that of racquet B. The differences in natural frequencies between the two racquets have determined that racquet A has a greater stiffness than racquet B. The magnitude of stiffness in racquet A is great enough to compensate for the larger mass, attributing natural frequencies of oscillation higher than that of racquet B, which is a lighter, more flexible structure.

### ***2.3.1 Effect of racquet strings***

In addition to modal analysis of the two strung test racquets structures, additional analysis was carried out to establish the effect of the strings on the structural dynamic response of the racquet frame. Additional modal analysis provided measurements to establish genuine frame modes and those which are brought about by the inclusion of strings to the system. Modal analysis of both racquets was carried out and the effect of strings on racquet frame dynamics was consistent in both racquets. Measurements of racquet B are presented and discussed in this section.

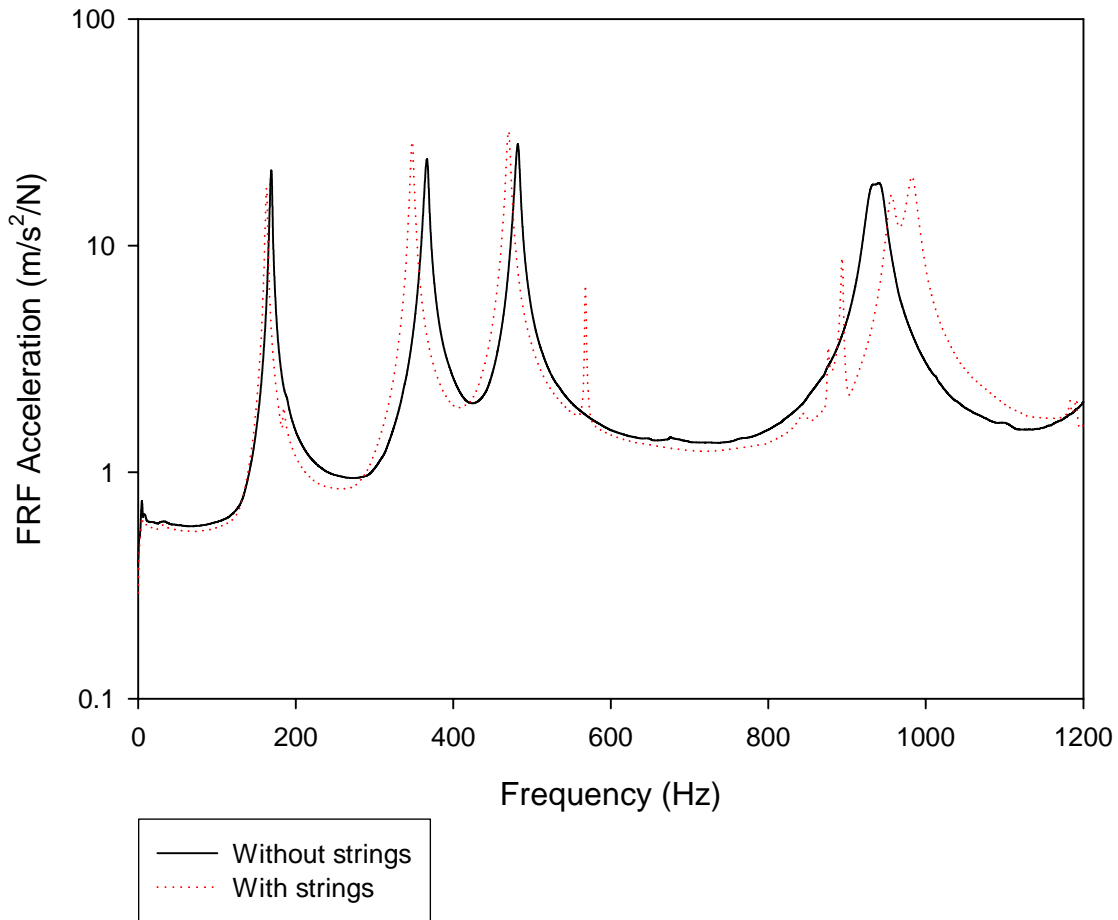


**Figure 15. Comparison of average FRF's for racquet B with and without strings**

Figure 15 shows the average FRF for racquet B both with and without strings present. The presence of strings in the racquet system has brought about the reduction in natural frequencies for the mode of oscillation. The first bending mode decreased from 169Hz to without strings to 163Hz with strings. Reasons for this can once again be derived from equation(1.4). The addition of the strings to the racquet will bring about an increase in stiffness, and theoretically an increase in natural frequencies. However, it is the additional mass of the strings that brings about the decrease of the racquet's natural frequencies. The effect of the additional stiffness generated by the strings can be thought of as negligible in comparison to the effect of the additional string mass and its effects.

The extra mass of the tennis strings has a greater effect on the racquet in terms of natural frequencies than the extra stiffness they provide.

Similar to the first mode, the second and third modes decrease in frequency by 18Hz and 11Hz respectively. It can also be seen from the frequency response of the racquet that there are more identifiable modal peaks in the frequency response of the tennis racquet when strung as opposed to un-strung. The 4<sup>th</sup> (568Hz) and 5<sup>th</sup> (894Hz) modes are only present with the strung racquet. These additional modes seen in strung tennis racquets are not genuine frame vibrations. Tennis strings can be considered a sub-structure of the racquet system that will have inherent dynamic properties. The vibrations of the tennis strings have an effect on the racquet frame and introduce additional modes of oscillation.

### **2.3.2 *Vibration excitation***

An impact hammer generating an impulse excitation on the racquet frame has excited the modes of oscillation identified in modal analysis. However, when the racquet is used during a tennis match, the frame vibrations are excited by the ball impact on the racquet string bed. The location of the ball impact on the string bed will define the level and frequency of frame vibrations felt by the player. The racquet's fundamental mode of oscillation has a node that has been identified near the centre of the racquet head. If the ball impact location resides at this location the vibrations associated with the node will not be excited and will not produce a dynamic reaction in the racquet handle. This applies to all the racquet's modes of oscillation. The identified torsional mode of oscillation will be excited by off-centre impacts (Iwatsubo *et al.* 2000). Modes of oscillation with a dynamic reaction in the racquet handle will be felt by the player and it is known that

vibrations felt by humans are in the range  $<1$  kHz. However, not all vibrations excited below 1 kHz will be felt by the player due to the damping properties of the ball during impact, as previously discussed in chapter 1.

Chapter 1 discussed the effects of ball damping. The tennis ball actively damps string vibrations during its dwell time (Brody *et al.* 2002). The ball dwell time on the string bed is approximately 5ms (Brody 1979; Hatze 1976). Vibrations exceeding approximately 200Hz will be damped by the ball during its dwell time, as a result of their waveform characteristics. Excited vibrations travel to the perimeter of the racquet's structure where they are reflected back towards the impact location. Reflected vibrations reaching the impact location before the ball has left the string bed will be damped by the ball itself.

The expression  $\frac{1}{t}$  was used in chapter 1 to determine the frequencies damped by the ball and those that will continue to vibrate after the ball has left the string bed. If the approximate dwell time of the ball is 0.005s,  $\frac{1}{t}$  equates to 200Hz. Vibrations exceeding 200Hz will be dramatically damped by the ball during its dwell time on the string bed. This is an important phenomenon for analysing racquet vibrations during game type situations. The modes of oscillation identified in this chapter will aid in analysis of racquet frame vibrations during game situations. However, ball damping must also be considered in the analysis of racquet frame vibrations.

## **2.4 Conclusions and significance**

The modal analysis has identified the inherent structural dynamic properties of the tennis racquet. Natural frequencies of the test racquets have been identified together with

associated damping coefficients and mode shapes. This information will aid the analysis of racquet dynamics during play. Inherent structural dynamic properties obtained through modal analysis will be used to assess the effect of parameters (such as the tennis grip) contributing to the racquet's dynamics response during play. Previous research has shown that the tennis grip is a strong racquet vibration attenuator and its effectiveness is dependant upon gripping pressure (Brody 1987; Elliot 1982); however this thesis builds on this knowledge by conducting experimental tests to quantify not only the magnitude but also the mechanics of grip damping.

Modal shapes identified by modal analysis can be associated to the resonances of the racquets frequency response. This information can be utilised for the interpretation of the grip damping mechanisms. Gripping pressure distribution with respect to the mode shapes of the tennis racquet will influence the effectiveness of grip damping. Previous research has shown that the effectiveness of vibration attenuators is determined by their location on the structure with respect to the anti-nodal positions of the mode shape of interest (Vethecan and Subic 2002). As the tennis grip is itself a vibration attenuator similar principles apply to its effectiveness, and this is one of the objectives focused on in the thesis.

Analysis of racquet vibrations under game conditions must take into consideration not only the inherent structural dynamic properties of the tennis racquet but also the dynamics involved in the excitation of frame vibrations. Impact parameters (i.e. ball location and racquet interaction) determine the level of frame vibrations felt by the player at the handle. Ball impact dynamics also contribute to the damping of higher frequency

vibrations. If these higher frequency vibrations are damped by the ball the magnitude of their response in the racquet handle will be reduced and not felt by the player. This brings about rationale for investigating the transfer of vibration to the player via the tennis grip.

Investigation of tennis racquet vibration proposed in this research will focus on the mechanics of vibration transfer to the player's upper extremities. The analysis of vibration transfer to the player must identify relevant vibrations that are thought to cause player discomfort and aggravate injuries such as lateral epicondylitis. It has been reported that vibrations below 180Hz cause the human discomfort (Reynolds *et al.* 1977). Therefore, the rationale is to analyse the generation and transfer of racquet vibrations to the player in this frequency range. Moreover, vibrations exceeding 200Hz are damped during the ball's dwell time on the string bed and are not felt by the player at all. The transfer of these lower frequency vibrations is of major focus in this research.

## **Chapter 3**

# **Characterisation of tennis grip pressure distributions**

Characterisation of the tennis grip is of paramount importance for establishing the dynamics of gripping pressure during impact. Gripping dynamics establish not only the variation in magnitudes of pressure distribution, but also the relationship between these variations and the ball impact in the time domain. It is important to quantify and characterise these grip pressure distribution variations before correlations are established with the structural dynamic response of the tennis racquet.

The tennis grip pressure affects the magnitude of frame vibration by providing additional damping via the player's hand (Hatze 1976; Elliot 1982). Previous research has shown that when comparing the response of freely suspended and hand-held racquets, frame vibrations are damped far quicker in hand-held condition (Brody 1987). This indicates that the tennis grip, with respect to the player's hand, has a profound effect on the damping of racquet frame vibrations. Previous investigations that subjectively compared gripping tightness to racquet vibration levels, have revealed that the degree to which the tennis grip dampens racquet vibrations is associated with the tightness of the tennis grip itself (Hatze 1976). Research has shown that a tighter tennis grip generates an increase in the damping of the racquet structure and moreover, an increase in the magnitude of shock and vibrations transmitted to the player's hand and forearm. However the relationship between the gripping tightness and vibration damping need to be quantified if grip damping characteristics are to be fully understood. By quantifying grip pressure distribution characteristics it is possible to establish correlations with the dynamic response of the tennis racquet with regards to vibration damping.

It is important to determine grip pressure distributions for different tennis stroke types, as this information will help establish relationship between not only the tennis grip and the dynamic response of the racquet, but also with the estimations concerning the mechanics of vibration absorption with respect to muscle contractions. By experimentally determining grip profiles it is possible to depict the distribution of gripping pressure across the racquet handle in terms of both magnitudes of pressure and variations of this distribution in the time domain. Gripping profiles need to be determined to establish locations of the greatest magnitudes of pressure in relation to both the racquet handle and the player's hand. Determination of grip pressure profiles needs to therefore be conducted using real time data acquisition in order to show the variations in the distribution of pressure during the tennis stroke. Determining magnitudes of gripping pressures with respect to locations on the racquet handle will provide knowledge to enable the damping mechanics of the tennis grip to be deciphered.

Knowledge regarding the contributing factors of the transfer of racquet vibration was required in order to correlate their effects. Factors such as gripping pressure and locations of gripping pressure on the tennis racquet determine the magnitude of vibration damping and the effect of their variability need to be quantified in order to optimise vibration attenuation. The parameters needing to therefore be investigated to allow for grip damping to be quantified are the magnitudes of pressure and the distribution of pressure within the tennis grip.

Research to date has attempted to quantify the tennis grip, by using measurements of force at single locations in the tennis grip. The research used force transducers to measure

gripping forces, and was done primarily to investigate the effects of grip tightness on ball velocities and examine the forces imparted on the players hand during impact (Hatze 1998; Knudson and White 1989; Knudson 1991). All studies investigating the tennis grip have show the forces involved to be dynamic in nature (i.e. not constant), with significant reaction forces of the tennis racquet acting on the hand (Brody *et al.* 2002; Kotze *et al.* 2000). This chapter involves a comprehensive investigation into gripping characteristics, with an aim to determine real time pressure distributions before, during and after the ball impact. A range of experimental techniques have been developed to acquire data to enable the grip characteristics to be determined. These characteristics include magnitudes of pressure distribution and their variation during impact with respect to both locations on the racquet handle and the player's hand.

This research focuses on an experimental investigation of multiple contact locations in the tennis grip to determine pressure distributions, rather than on single point force measurements as reported in literature to date. Experimental measurements of multiple points allows for more comprehensive analysis of gripping pressures across the racquet handle , which is essential for detailed descriptions of vibration transfer from the racquet to the hand.

Table 5 depicts the individual objectives of this chapter together with the experimental methods used to investigate them. The results and analysis from the experimental testing and the significance of the findings are described. The table provides an outline of the methodology and rationale in this chapter.

Objective	Experimental method	Results & analysis	Significance
Establish locations in the tennis grip demonstrating the greatest magnitudes of pressure	Pressure sensitive film	<ul style="list-style-type: none"> <li>▪ Qualitative grip pressure distribution profiles</li> <li>▪ Qualitative magnitude of pressure (Maximum values over time)</li> </ul>	Identifying areas in the tennis grip exhibiting the greatest magnitudes of pressure provides the knowledge required to acquire real time measurements of gripping pressure.
Quantify real time gripping dynamics during impact	Strain gauge cantilever system	<ul style="list-style-type: none"> <li>▪ Quantitative magnitudes in terms of gripping force during impact</li> <li>▪ Develop of grip pressure models in relation to the ball impact, with respect to gripping times</li> </ul>	Allows for both influences of both the players hand and the racquet reaction forces to be analysis in relation to impact in the time domain. The behaviour of the player with respect to their grip preparation before impact and response to impact are also described.
Quantify the real time distribution of pressure in the tennis grip during impact	Hydrocell pressure sensors	<ul style="list-style-type: none"> <li>▪ Real time measurements of gripping pressures in the tennis grip</li> <li>▪ Develop of grip pressure models during impact with respect to stroke type</li> </ul>	<ul style="list-style-type: none"> <li>▪ Measurements provide knowledge which can be utilised to estimate the pressure acting on both the racquet handle and the player's hand.</li> <li>▪ Provides measurements essential for the description of vibration damping by the hand.</li> </ul>

**Table 5. Outline of experimental investigation of tennis gripping pressure**

### **3.1 Identification of locations in the tennis grip with the greatest contact pressure**

The locations of the greatest magnitudes of grip pressure on the racquet handle have been identified using a pressure sensitive film (Pressurex). In addition to qualitatively analysing these locations, it is essential that the locations are determined accurately to ensure correct positioning of those pressure sensors capable of real time data acquisition. The pressure sensitive film enables a descriptive overview of the pressure distribution in the tennis grip together with an approximation of the maximum gripping pressures reached during the stroke.

### 3.1.1 Instrumentation

The following instrumentation was used to acquire measurements for data showing locations with the greatest magnitudes of contact pressure in the tennis grip:

- Ultra Low pressure film (Sensor Products, USA) ( $19 - 58 \text{ N/cm}^2$ )
- Topaq<sup>®</sup> pressure analysis system
- Head<sup>©</sup> i.X16 Chipsystem racquet

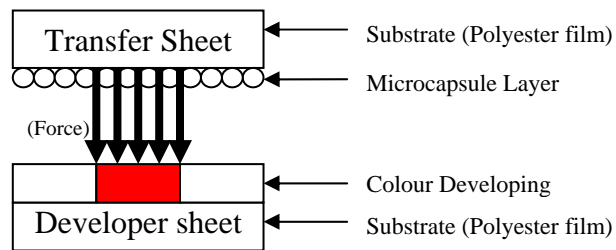


Figure 16. Pressure film layout

The pressure indicating film used in this experimental investigation is a specialist product able to qualitatively display pressure distribution loads. The film is based on a transfer sheet and a developing sheet system. The transfer sheet holds substrate microcapsules of polyethylene terephthalate (PET) with the developer sheet containing a colour-developing layer. The sheets are placed between two contacting surfaces (the player's hand and the tennis handle surface in this case). When the pressure between the two surfaces is applied the microcapsules are ruptured and the developer sheet permanently changes colour (see figure 16). The colour intensity of the developer sheet is directly proportional to the pressure applied. The analysis of the developed film shows pressure ( $\text{N/cm}^2$ ) distribution across the film.

The pressure film is analysed using the Topaq<sup>®</sup> pressure analysis system. Developed pressure sheets are imported to the Topaq<sup>®</sup> computer analysis software using a densitometric scanner. The pressure sheet is then analysed using the Topaq<sup>®</sup> software based on the colour intensity. This Windows<sup>®</sup> based analysis software produces a high resolution image that displays the colour intensity of the developed film and uses this to give a quantitative analysis of the applied pressure (N/cm<sup>2</sup>). The qualitative pressure analysis uses the scanned images to produce pseudo and 3D imaging of the pressure distribution profiles.

### ***3.1.2 Testing protocol***

The tennis racquet grip fabric is removed and the developer sheet (cut to the length and diameter of the racquet handle) is attached around the tennis racquet grip. The transfer sheet (cut to the same dimensions as the developer sheet) is then attached over the developer sheet. Both sheets are attached to the racquet handle using either double or single sided adhesive tape.



**Figure 17. Continental gripping technique**

An ATP (Association of Tennis Professionals) male tennis player was used in all hand held racquet tests to ensure consistent ball impact locations together with the correct gripping and stroke technique. The same player will be used for all hand-held racquet experiments in this research to ensure consistent data collection. (N.B. Use of only 1 test subject will limit the validity of test results regarding the grip pressure distribution profiles. Multiple subjects are usually used for experiments involving humans, and it should be noted that the grip pressure profiles given in this are subjective to the individual player. The values may vary from player to player and this aspect requires further investigation to this thesis. The gripping techniques used in this thesis are accepted by the tennis community and the grip pressure profiles are based on these techniques (e.g. continental forehand.). However, the absolute values and distribution profiles may still vary from player to player, which limits the applicability of the results in this research. It is also understood that the use of only right handed strokes may limit the grip profiles validity. However, the main objective of this research is to identify the mechanics of vibration absorption by the player's hand, therefore the main focus is on the tennis racquet behaviour. The dynamic behaviour of the racquet will not vary as its structure will not change. The racquet's response will vary depending on the grip pressure distribution and this is the main objective of this research.)

The test subject was told to use a continental forehand gripping technique (figure 17) to hold the racquet. A single forehand stroke from a ball drop was carried out and the pressure indicating film was removed and analysed using the Topaq<sup>®</sup> system. Figure 18 shows the developed pressure indicating film attached to the racquet handle prior to its removal and analysis. Eight trials were carried out in order to identify characteristic

pressure distribution patterns. Each pressure distribution was subject to varied gripping tightness' because of swing speeds and gripping techniques of the test subject. Consequently, results showed different magnitudes of pressure. However, the results showed clearly the gripping locations with the greatest magnitude of contact pressure.



**Figure 18. Developed pressure film attached to racquet handle**

### ***3.1.3 Results and discussion***

The results from the Topaq<sup>®</sup> analysis of the pressure film showed the distribution of pressure within the tennis grip. The pressure distribution results identified contact locations in the tennis grip with the greatest magnitude of contact pressure ( $\text{N}/\text{cm}^2$ ). Figure 19 shows the results of the pressure film tests for the palm and figure 20 shows the results for the phalanges. A colour pressure scale is included in both figures to show the approximate pressure values in each distribution respectively. Both figures have anatomical clarification of the bones in the hand to show the relationship between the pressure distributions and the specific locations on the hand.

The pressure distribution has been analysed in relation to the anatomical orientation of the hand. Figure 19 shows the pressure distributions for the metacarpals and thumb and figure 20 shows the pressure distributions for the MP joints and phalanges. The areas

displaying the greatest magnitude of pressure are highlighted (circled) in both figures. Highlighted areas are labelled alphabetically to allow for accurate interpretation in the text. Both figures include an anatomical diagram depicting the bones in the human hand to aid in the interpretation of pressure analysis results.

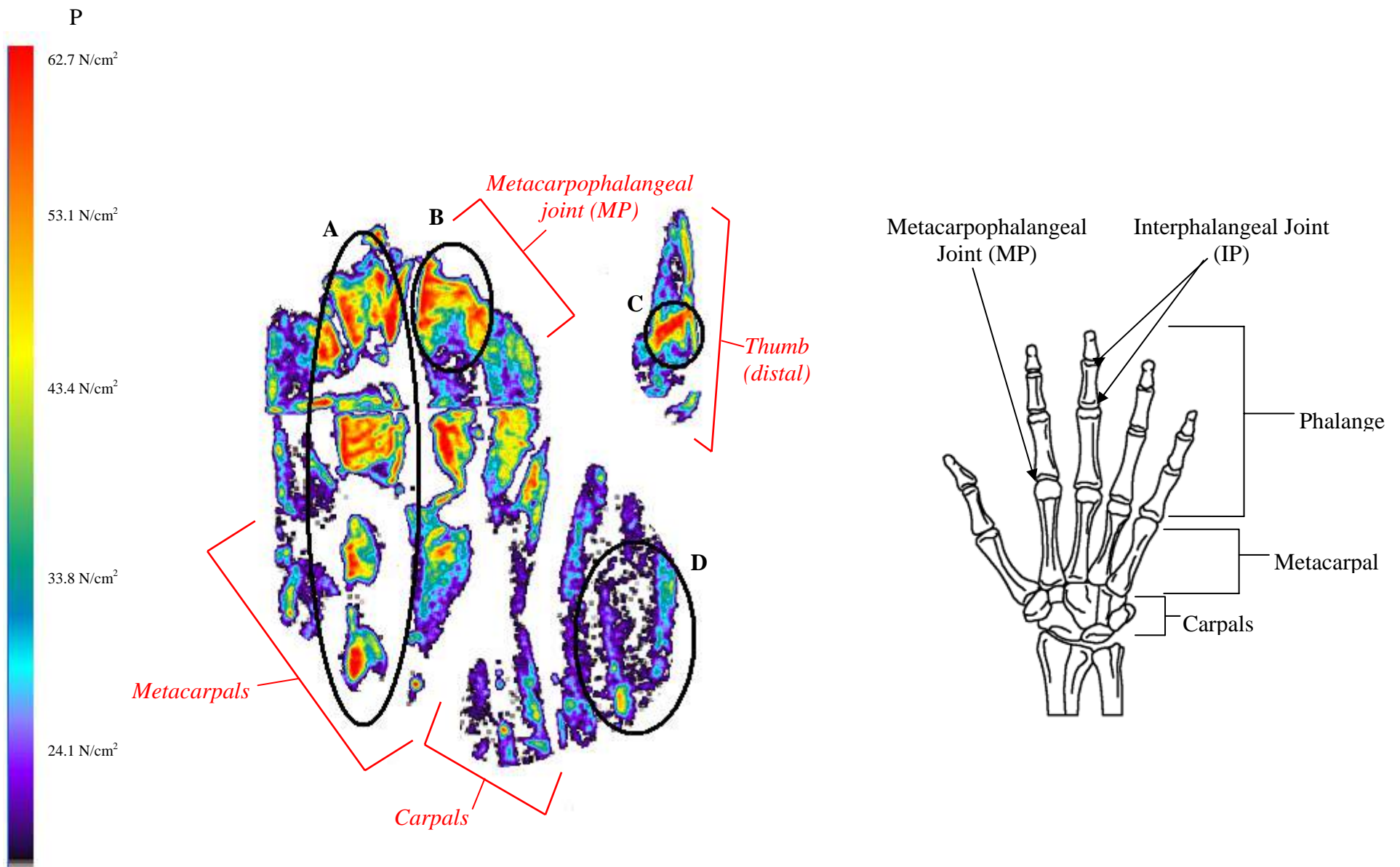


Figure 19. Pressure film results for a forehand stroke for the metacarpals and thumb

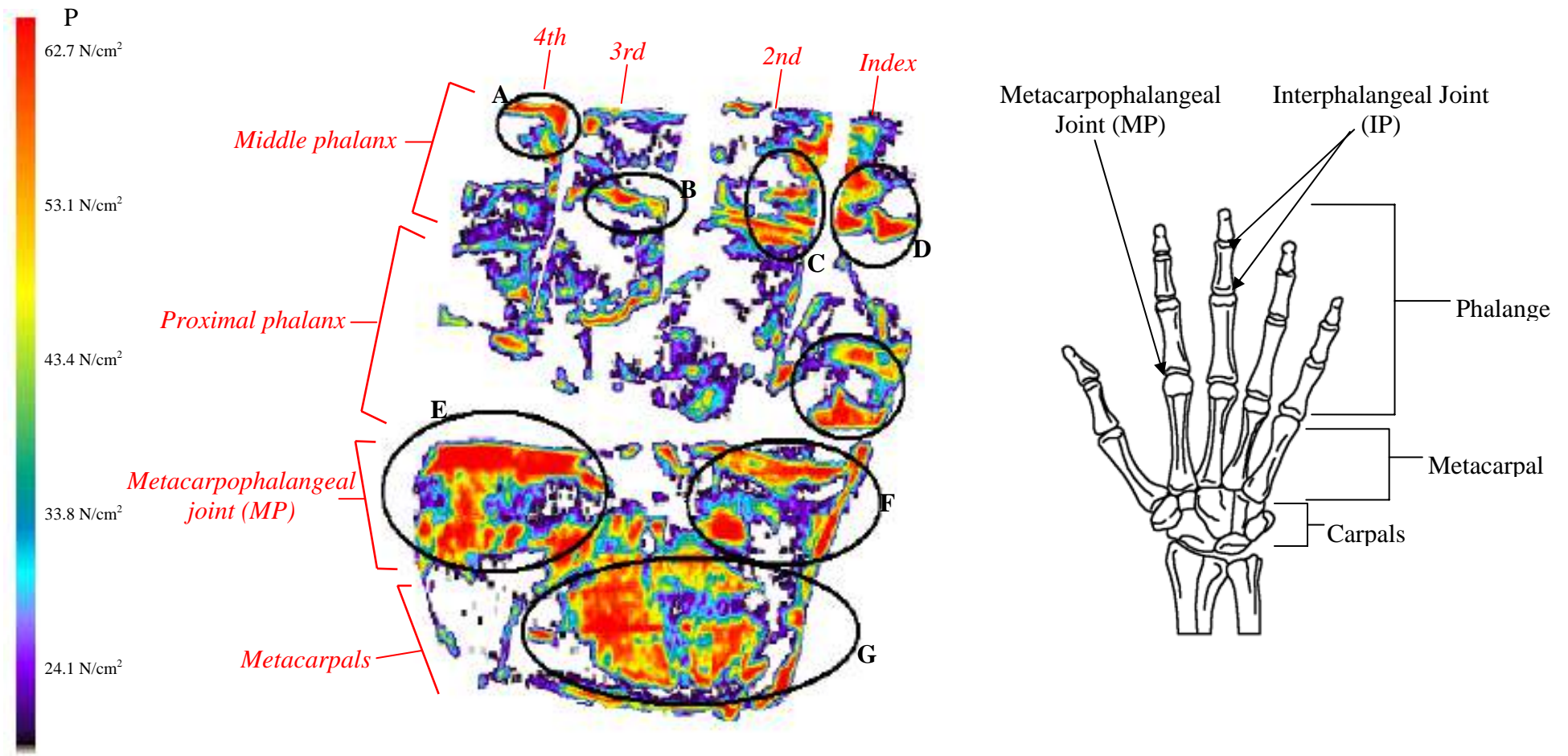


Figure 20. Pressure film results for a forehand stroke for the MP joint and phalanges

It has been found that the contact locations in the grip with the greatest pressure values are at the metacarpophalangeal joint (MP) of the index finger (figure 19 A) and the third and fourth fingers (figure 20 E). The distal phalanx of the thumb shows a concentration of pressure larger  $60 \text{ N/cm}^2$  (figure 19 C). The middle phalanxes of all phalanges show a similar concentration of pressure. The concentrations of pressure on all phalanges around the middle interphalangeal (IP) joint cover a smaller area than the concentrations in the palm. The contact locations of the palm displaying pressures greater than  $60 \text{ N/cm}^2$  (figure 19 A) are larger in area than those on the phalanges. The phalanges display pressures larger than  $60 \text{ N/cm}^2$  but only over the small areas of the IP joint (figure 20 A, B, C and D). The pressure distributions on the phalanges display magnitudes between  $20 \text{ N/cm}^2$  and  $40 \text{ N/cm}^2$ .

Pressure distributions in the palm of the hand are concentrated on the lower 4<sup>th</sup>, mid 3<sup>rd</sup> and upper index metacarpals, giving a diagonal line of pressure through the palm (figure 19 A). This distribution of pressure across the centre of the palm coincides with the racquet handle having a diagonal orientation through the tennis grip (figure 17).

Pressure distribution across the 3<sup>rd</sup> and 4<sup>th</sup> phalanges ranges between  $20 \text{ N/cm}^2$  and  $30 \text{ N/cm}^2$  with small areas displaying pressures greater than  $60 \text{ N/cm}^2$ . Pressure distributions across the 2nd and index phalanges (figure 20 C and D) display pressures between  $40 \text{ N/cm}^2$  and  $60 \text{ N/cm}^2$ . The MP joint of the 3<sup>rd</sup> and 4<sup>th</sup> phalanges display concentrations of pressure more than  $50 \text{ N/cm}^2$ .

The experimental investigation of pressure distribution in the tennis grip using the pressure sensitive film represents a qualitative method of data collection. Pressure sensitive film has provided a measure of pressure distributions in the tennis grip for the continental forehand stroke. Contact locations with the greatest magnitudes of pressure have been identified. The pressure distributions have not been analysed using real time data acquisition at this stage. The pressure distributions obtained in this analysis depict magnitudes that represent the total pressure applied throughout the forehand stroke. Hence the pressure film analysis can only be used as a qualitative data collection method because it is not a time dependant analysis. A data collection method capable of acquiring real time gripping data is needed to determine accurate pressure distribution variations with respect to the ball impact in the time domain.

### **3.2 Use of strain gauge cantilever system grip characterisation**

The pressure film analysis showed only single pressure distribution values in the tennis grip for the forehand stroke as the method did not use real time data acquisition. The results represent the maximum of all gripping pressures generated during the tennis stroke. Gripping dynamics in terms of pressure distribution variations need to be experimentally determined using a real time data analysis technique. The real time analysis of tennis gripping dynamics to date has involved force measurements at single or multiple points in the grip (Hatze 1976, 1998; Knudson and White 1989; Knudson 1991; Li *et al* 2004). As a result, such investigations have been unable to display the pressure distribution variations across the entire tennis grip. Therefore, multiple point pressure measurements using real time data acquisition is required in this research to model the complete pressure distributions in the tennis grip.

The application of strain gauges in conjunction with cantilever beams has been used in previous investigations to quantify gripping forces and their distributions for everyday hand actions (Chadwick and Nicol 2001) (such as handle gripping and jar gripping in stationary state). The gripping device used by Chadwick and Nicol (2001) to analyse the grip involved four cantilevers beams, each with a two full Wheatstone bridge strain gauge configuration attached. A number of gripping techniques were used to assess the magnitudes of force when the device was gripped. This experimental methodology has been further developed and applied in this research to measure gripping characteristics under dynamic conditions involving ball impacts; similar to the experiments conducted by Li *et al* 2004 (i.e. the data acquired by Chadwick and Nicol 2001 is representative of a stationary gripping device. The application of this system to the racquet scenario introduces the reaction forces of the racquet into the gripping measurements. The forces measured by the system become dynamic in nature as a consequence of the racquet being in motion). This methodology has been used to assess the variations in gripping forces during ball impact. The relationship between the tennis gripping tightness and ball impact in terms of racquet reaction forces and gripping variations can be analysed using the strain gauged cantilever system.

The principles of the developed cantilever force transducer system used in this investigation of gripping pressures (Chadwick and Nicol 2001), are governed by the relationship between the magnitudes to strain imparted on the beam with respect to the distance from the applied load. This importance of this relationship for quantifying gripping tightness is now described. Figure 21 shows the relationship between strain and

distance from the applied load, and its application to the strain gauge on the cantilever beam.

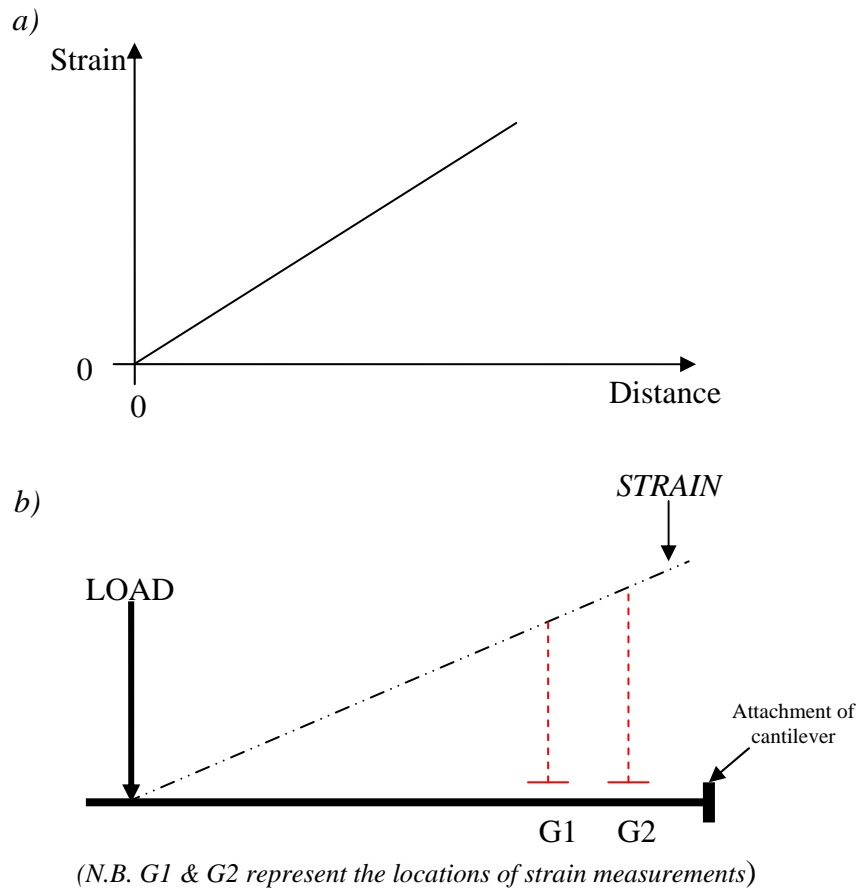


**Figure 21. Strain gradient: a) relationship between strain and distance from load applied to the beam; b) measurement locations on the cantilever beam**

The linear relationship means that the greater the bridge's distance from the applied load, the greater the measured strain. If we apply this principle to the cantilever beam attached to the end of the tennis racquet, shown in figure 21. b), two strain measurements (G1 and G2) can be used to determine the gradient of the strain between the two locations. The linear relationship between strain and distance on a cantilever beam allows for the difference between the two measurements to be used in determining the applied load. The

objective of the cantilever system is to determine the magnitude of the applied load. Therefore, the voltage changes measured from the strain gauges can be directly calibrated to a force unit (N). The measurement of the strain gradient results in a calibrated measurement of the applied load irrespective of loading location on the beam. Multiple loading locations will result in the load measurement representing the cumulative force at all locations.

### ***3.2.1 Experimental set-up***

A strain gauge cantilever system was developed for the measurement of tennis gripping forces. The development of the system is shown in Appendix 1. This system utilises four cantilevers with strain gauges in two full Wheatstone bridge configurations to estimate the force of the tennis grip. The system was calibrated to measure the total grip force (N) on four surfaces of the tennis racquet handle (see Appendix 1).

### ***3.2.2 Testing protocol***

The strain gauge test handle system enabled the measurement of gripping tightness, in terms of force in real-time. This is required in order to assess the gripping tightness change in time during ball impact. The strain gauge cantilever system was used to investigate the relationship between the ball impact and the gripping dynamics, under laboratory conditions. The gripping dynamics include magnitudes of force and their variations during impact. Additional measurements of gripping dynamics included the times at which certain gripping characteristics occurred. These “gripping times” included both the time of the maximum and the initial increase of gripping force during impact.

A stationary racquet- moving ball experiment was conducted to determine the grip force variations in the time domain with respect to ball impact. The player's arm was strapped to a table allowing for the racquet to be both hand-held and stationary (i.e. no racquet swing generated and the player can only control the racquet during impact). A stationary hand-held racquet test acquires measurements based only on grip force variation and their relationship with the ball impact. The measurements acquired from the stationary racquet experiments are not influenced by racquet swing speeds as it is considered stationary at the time of impact. Stationary tests enable an analysis of the gripping force without any effects of racquet swing of variable ball speeds. Once the gripping dynamics (i.e. the variations in grip forces during impact) are described in this context, more comprehensive data acquisition can be used to analyse the tennis grip during moving racquet- moving ball environment.

The test subject was requested to grip the test racquet using a continental forehand grip. The four cantilever beams of the test racquet were located at the following hand locations in the continental forehand gripping technique:

1. The distal phalanx
2. The proximal phalanx
3. The MP joints and distal metacarpals
4. The metacarpals

Figure 22 shows the locations of the cantilever beams with respect to the bones of the gripping hand. The cantilever beam set-up is used to measure the total force imparted on

the beam (i.e. the cumulative force applied to the entire surface of the beam). The measured force (N) represents the sum of the force imparted on the racquet handle by both the hand and the reaction force of the racquet due to the rotation of the handle in the tennis grip after impact. The rotation of the racquet about an axis in the tennis grip is determined by the ball impact location and its proximity to the racquets COP, as described in chapter 1.

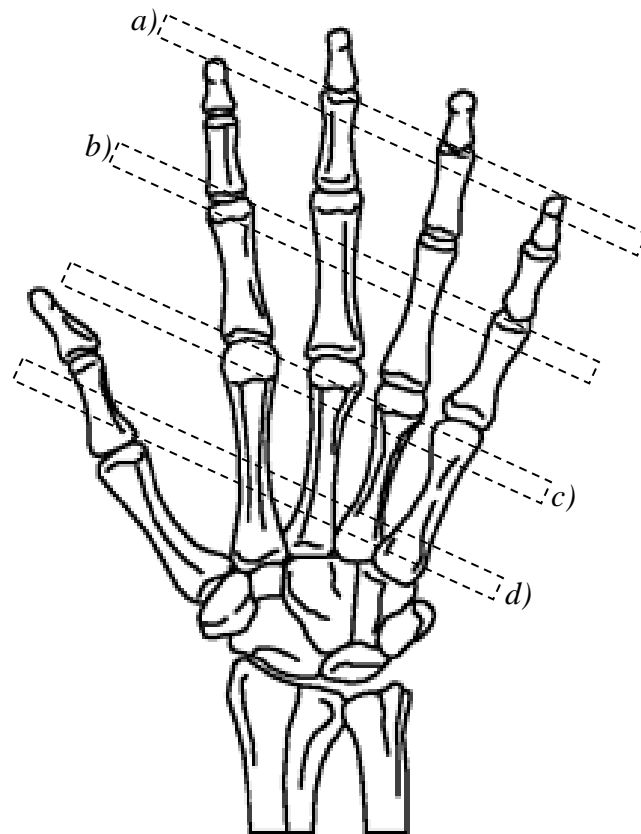


**Figure 22. Location of cantilever beams with respect to the gripping hand for a)distal phalanx; b) proximal phalanx; c) MP joints and distal metacarpals; d) metacarpals**

The experimental set-up for the ball drop test is shown in figure 23. Two Velcro straps were used to clamp the subject's forearm to the mounting desk to minimise the movement of the arm during impact (i.e. stationary racquet conditions). A tennis ball is

dropped, from rest, from an approximate height of 2m. The ball impact was aligned with the approximate centre of the racquet head and was allowed to impact the string bed once. Aligning the ball impact with the approximate centre of the racquet head will generate an impact allowing for the measurement of both racquet vibrations and the movement of the racquet in the tennis grip. A single PCB lightweight accelerometer was attached to the tip of the racquet frame to measure the impact of the ball. The PCB accelerometer and the eight full bridge strain gauge configuration attached to the handle were connected to a National Instruments DAQ. The National Instrument DAQ card was set-up to acquire data at a sampling frequency of 1000Hz with the total number of scans set to 4000. The data acquisition was triggered by ball impact measured by the accelerometer signal, with 2000 pre-trigger and 2000 post-trigger scans. This set-up configuration of the DAQ card was used to record the variation of the gripping forces both pre and post-impact.

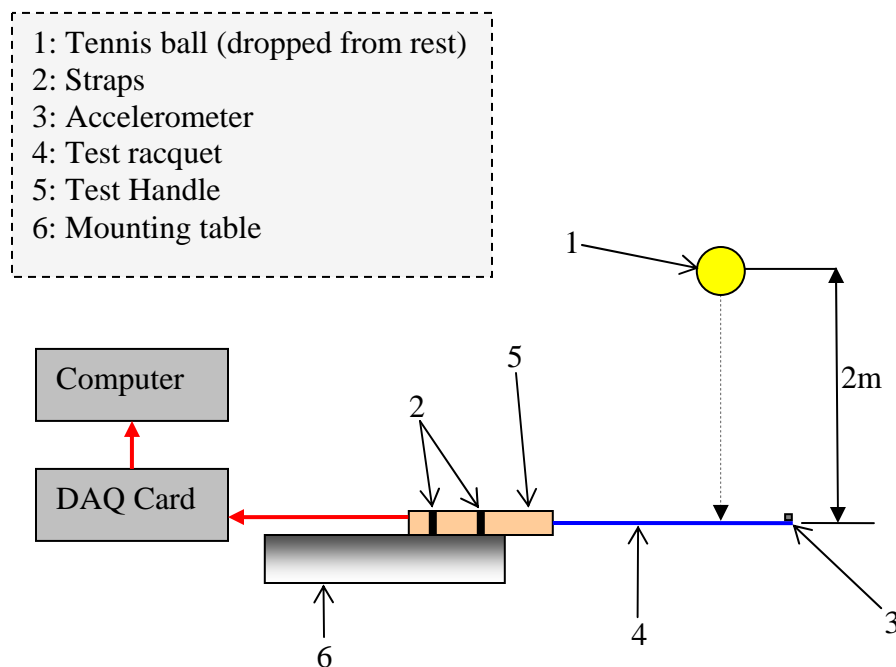


Figure 23. Diagram of drop test set-up

The handle test system enables the magnitude of the gripping forces to be quantified in real time. Not only was the system used to quantify the magnitudes of grip force, but also to describe the times at which significant gripping events/ gripping times occur with respect to impact. These gripping times are firstly analysed in terms of the test subject's anticipation of ball impact by initially increasing the gripping force. Secondly, the time of the maximum gripping force is also estimated to show how the player reacts to impact in terms of grip force variations. For this analysis of player anticipation and grip reaction, two types of ball drop tests were conducted, "visual" and "blind" tests. This was done to describe the player's perception of the ball impact and their changes in gripping force after impact. Both tests were identical in set-up but with the test subject's sight of the ball impact varied. "Visual" drop tests permitted the test subject to observe the ball travel from rest to impact on the racquet string bed. In the "blind" drop tests the sight perception of the ball was changed by requesting them to look at the mounting table and not the ball release. As the ball dropped from rest, ear guards were used to eliminate any noise generated by the test procedure in order to ensure the test subject could not use hearing to detect and anticipate the impact event. Twenty ball drop trials were conducted in total, 10 "visual" and 10 "blind", to allow for comparisons between the gripping characteristics, in terms of initial increase in gripping force and maximum force times.

### ***3.2.3 Results and discussion***

The results obtained from the drop tests using the strain gauge cantilever system contained noise on the measured signals. The noise present in the measurements creates difficulties when attempting to establish magnitudes of force and gripping times in

relation to the ball-racquet impact. Noise present in the measurements can produce errors and therefore needs to be removed before parameter estimations of could be made. Frequency analysing software (Sigview v.1.9.5) was utilized to reduce the noise present in the strain gauge and accelerometer measurements. This was done using a Hanning window with a scan length of 50. The de-noised measurements were then calibrated using the gradient equations taken from the calibration charts in Appendix 1. Following the calibration of the raw voltage signal measurements into force units (N), the data was analysed and interpreted with respect to magnitudes and gripping times.

The measured data was used to analyse the gripping times with respect to the “visual” and “blind” drop tests. Gripping times describe the behaviour of the gripping force during by indicating when both maximum and initial increases in grip forces occur during ball-racquet impact. Two gripping times were calculated for each trail to show, a) the time of the maximum observed gripping force with respect to ball impact; and b) the time of the initial increase of gripping force with respect to ball impact. The time of the initial increase of gripping force from the stationary state is termed here the threshold time.

The threshold time is calculated by establishing the time at which the gripping force exceeds 10% of its maximum. A level of 10% was set due to the remaining noise present in the measurements. Any peaks in the noise present would result in incorrect estimations of the initial grip force increase time, as they would indicate an increase in grip force despite the tennis grip remaining at a constant tightness. Figure 24 shows an example of a single beam measurement together with the accelerometer signal to illustrate the

relationship between the gripping force and the ball impact. The figure shows the calculation of the 10% threshold level.

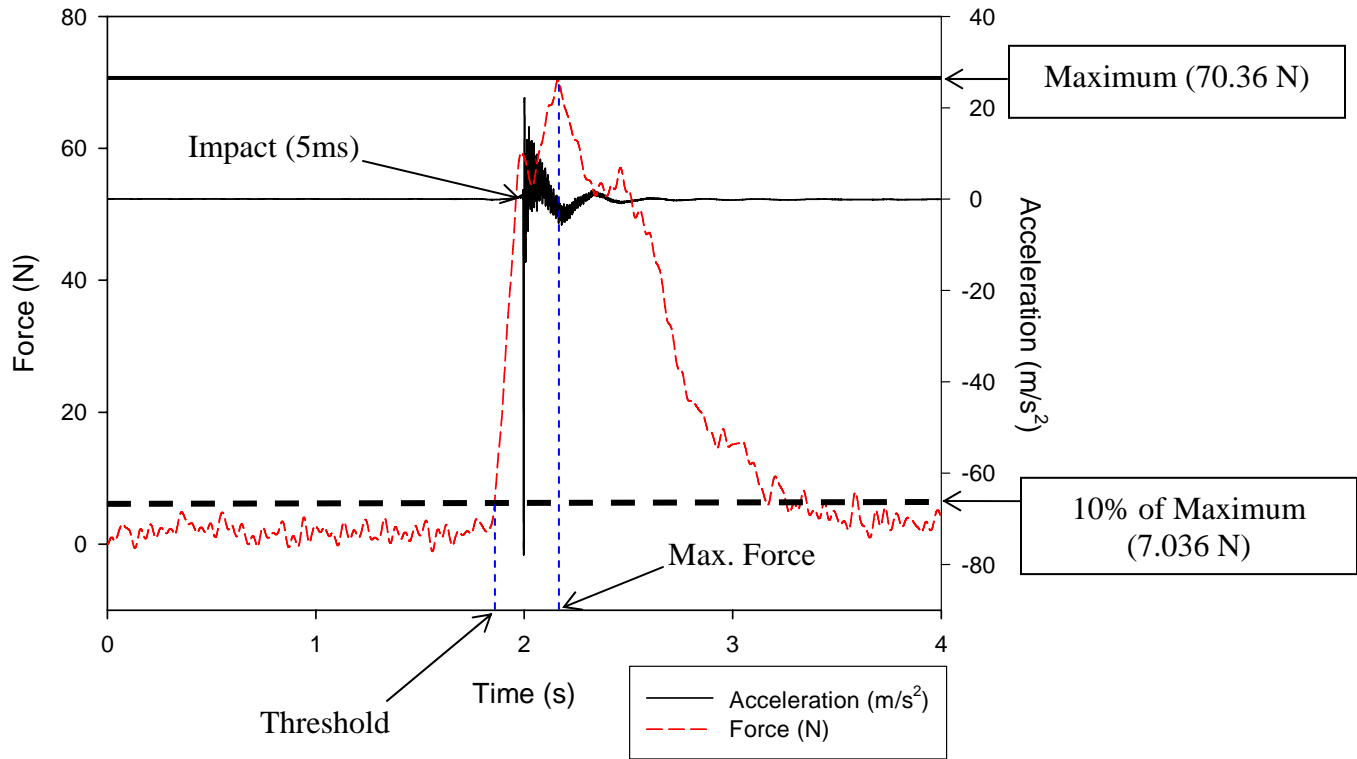


**Figure 24. Threshold calculation**

All gripping times are calculated in relation to the ball impact time (i.e. a negative value represents a post-impact time and positive represents a pre-impact time). Table 6 and table 7 show the grip time results for the “seen” and “blind” drop tests respectively. The gripping times shown in table 6 (“visual” tests) and table 7 (“blind” tests) are calculated averages of the four individual cantilever beams. The average times for the ten trials carried out for each category of drop test are given together with an overall average.

<b>Trial</b>	<b>Average Max Force time (s)</b>	<b>Average Threshold time (s)</b>
1	-0.109	0.083
2	-0.091	0.124
3	-0.051	0.640
4	-0.092	0.862
5	-0.111	0.071
6	-0.041	0.098
7	-0.099	0.435
8	-0.072	0.496
9	-0.126	1.032
10	-0.083	0.143
<i>Average</i>	<i>-0.087</i>	<i>0.398</i>
<i>St Dev.</i>	<i>0.026701</i>	<i>0.353246</i>

**Table 6. “Visual” drop test gripping time results**

<b>Trail</b>	<b>Average Max Force time (s)</b>	<b>Average Threshold time (s)</b>
1	-0.246	-0.068
2	-0.233	-0.027
3	-0.234	-0.055
4	-0.174	-0.009
5	-0.144	-0.017
6	-0.241	-0.038
7	-0.192	-0.044
8	-0.142	0.000
9	-0.294	-0.024
10	0.403	-0.037
<i>Average</i>	<i>-0.150</i>	<i>-0.032</i>
<i>St Dev.</i>	<i>0.200118</i>	<i>0.020808</i>

**Table 7. “Blind” drop test gripping time results**

The gripping times show that under “blind” conditions, the threshold gripping time is 0.43 seconds longer than in the “visual” tests. If the subject is permitted to observe the ball drop they will begin to increase the gripping force approximately 0.398 seconds before the ball impacts the string bed. With the subject’s anticipation of the ball drop affected they will not begin to increase the gripping force until approximately 0.032

seconds after the ball impact. The test subject needs to see the incoming ball in order to prepare the tennis racquet for the impact and produce a more controlled rebound ball. The increase in the gripping force will generate a stiffer racquet-hand interface. A stiffer racquet-hand grip will produce a better controlled ball impact by the player as the recoil of the racquet will be reduced. An increase in gripping force was observed approximately 0.389s before impact in the “visual” tests, indicating the subject’s preparation of the racquet with respect to racquet-hand stiffness. The “blind” test results yields different threshold times as the subject is not permitted to observe the ball drop. A reduced anticipation of the ball drop results in a delayed increase of gripping force until after the ball impact. With the reduced anticipation of the incoming ball, the increase in gripping tightness can only be initiated by the subject’s feel of the ball impact. The “blind” test threshold gripping times obtained using the strain gauged cantilever system show that if the subject’s knowledge of the incoming ball is reduced, the stiffness of the racquet-hand grip does not increase until after the ball impact. The time delay between ball impact and the increase in gripping force indicates the reaction time of the player.

Visual stimulated hand-eye reaction times are in the order of 0.19s, while audio stimulated reaction times are approximately 0.16s (Brebner and Welford 1980; Welford 1980). The threshold time in the “blind” test is 0.032s which is faster than the visual and audio stimulated reaction. The present investigation is based on a touch stimulus which is the movement of the racquet in the subject’s hand, and the response time to a touch stimulus has been proven to be immediate (Robinson 1934). However, the threshold time of 0.032s is the reaction time it takes the subject to begin to increase the gripping force.

The time observed for the maximum gripping force is greater than the threshold time as the maximum gripping force will not be reached instantaneously but over a period time.

Maximum gripping force time observed in both the “visual” and “blind” tests have been reached post-impact. Maximum gripping force has been reached approximately 0.15s post-impact in the “blind” test conditions and 0.087s post-impact in the “visual” tests. The longer period of time required to reach the maximum gripping force under “blind” conditions is primarily due to the increase in the “tightening” of the grip being initiated post impact. Under “visual” conditions, the maximum gripping force has been reached approximately 0.087s post-impact. The earlier threshold time achieved in the “visual” drop test shows that the maximum gripping force is reached much earlier after the ball impact than in the “blind” conditions. Tennis gripping conditions prepare the racquet in terms of racquet-hand stiffness and needs to remain stiff throughout the impact phase to ensure ball control. Previous investigations have shown that the rebound velocity of the ball is independent of the gripping tightness because the ball will have left the string bed before the gripping force can be increased to produce a stiffer racquet-hand system (Baker and Putman 1979; Grabiner 1983). The kinetic energy of the deformed racquet will not return energy to the rebound ball as it will have left the string bed before the racquet returns to equilibrium (Brody 1979). However, other research has stated that a looser tennis grip will results in reductions in the ball rebound velocities (Hatze 1976). The tennis grip pre-conditions the racquet in terms of the racquet-hand interface stiffness. Changes in this interface stiffness during impact will have little effect on the ball rebound velocity, as shown in previous investigations (Baker and Putman 1979; Grabiner 1983). This research shows that the test subject continues to increase the gripping force

throughout the impact phase even though this will have no effect on the ball rebound velocity. Increases in gripping force post-impact are required regardless of the subjects' perception of the incoming ball, as the player needs to maintain/regain control of the racquet. The changes/ increases in gripping force post-impact have been observed in previous research (Hatze 1998) and are attributed to the player's desire to maintain/regain control of the racquet. An increase in the gripping force generates a resistance to the movement of the racquet within the tennis grip by clamping the handle. This results in the player being able to control/ the movement of the racquet in their hand. This post-impact increase of gripping force is illustrated in figure 25 and is now discussed further.

Following the estimations of the gripping times using data acquired in the stationary racquet tests using the strain gauge cantilever system, gripping force measurements were analysed in relation to the ball impact in the time domain. Figure 25 shows a sample of the gripping force traces obtained from tests using the strain gauge cantilever system. The figure shows the four traces for the cumulative force across the: *a)* distal phalanx; *b)* proximal phalanx; *c)* MP joints and distal metacarpals; and *d)* the metacarpals. The four gripping force traces are shown in relation to the acceleration measured at the tip of the racquet head.

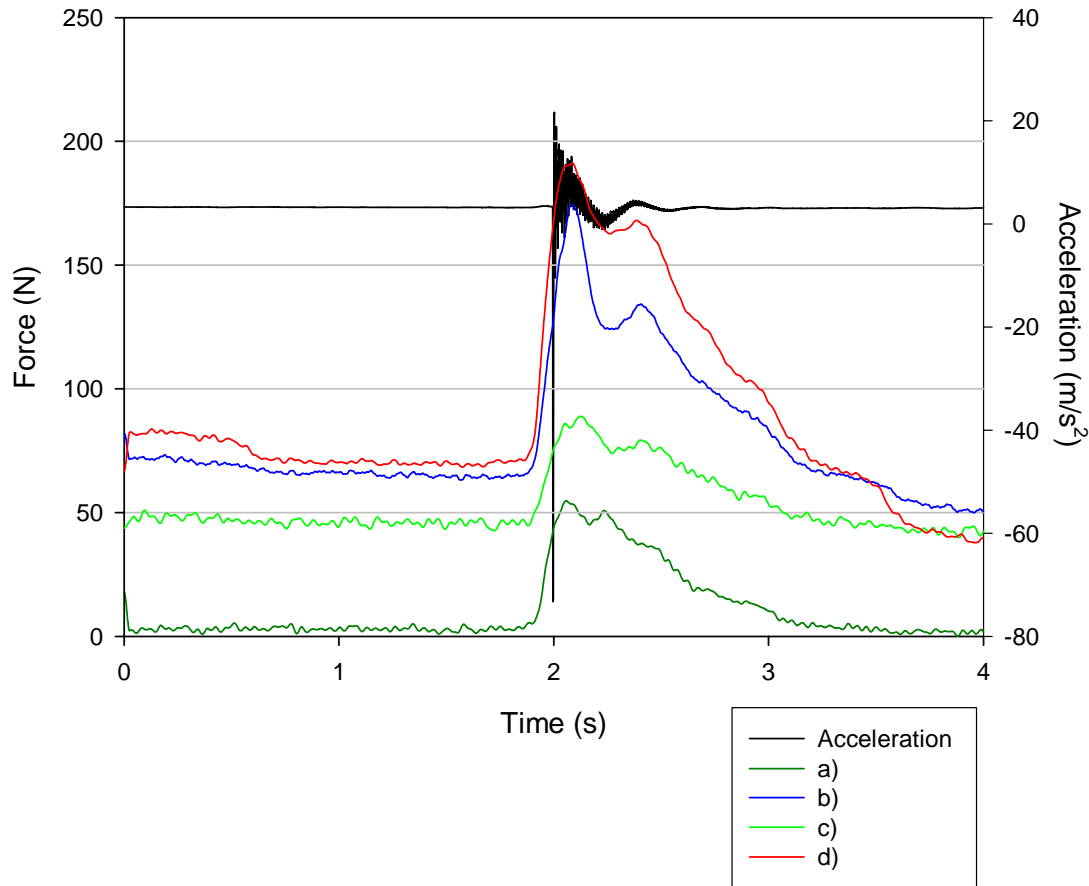


**Figure 25. Sample of measured strain gauge for a visual test at: a) distal phalanx; b) proximal phalanx; c) MP joints and distal metacarpals; d) metacarpals.**

Figure 25 shows that the gripping forces are dynamic in nature (i.e. do not remain constant throughout impact) and follow a general increase and decrease in magnitude with respect to the ball impact. The gripping forces do not have a single peak magnitude but two peaks before returning to a resting state. Gripping forces rise to an initial peak approximately 0.087s post impact when the subject is permitted to observe the incoming ball. A decrease in gripping force precedes the initial peak, after which a second peak is observed. This second peak in gripping force is common in all four measurements and can be attributed to two factors. Previous research has suggested that the second force peak can be attributed to the subjects attempt to regain control of the racquet after the ball

impact (Hatze 1998; Knudson and White 1989). Another cause of the second force peak is the movement of the racquet within the tennis grip. The racquet rotates about an axis in the tennis grip. The axis in the tennis grip about which the racquet will rotate is directly related to the impact location (Brody *et al.* 2002). Rotation of the racquet within the tennis grip generates reaction forces which are imparted on the subjects' hand. Therefore measurements obtained using the strain gauge cantilever handle test system, show a cumulative result of both gripping and racquet reaction forces. The second peak observed in the results can be attributed to both the movement of the racquet and the second increase in gripping force to regain control of the racquet by the test subject after impact.

The movement of the racquet within the tennis grip can often be shown by measuring the opposing increase and decrease in gripping force at opposing locations on the handle. The strain gauge system cannot be used to describe this more comprehensively because the data acquired represents a cumulative force obtained across an area of the racquet handle. The strain gauge test racquet is unable to distinguish force with respect to location and therefore the rotation of the racquet is difficult to determine. Therefore, the rationale for subsequent tests focuses on the development of a data collection method based on the real time quantification of tennis grip characteristics such as the variation of pressure distribution across both the racquet handle and the player's hand. Individual pressure sensors will be used to obtain results in the next section of this chapter to quantify the variations in the distribution of pressure across both the racquet handle and the player's hand. The methodology of this will be fully explained in the next section.

It can be concluded that the measurements acquired from the strain gauge test support previous research findings that give explanation for the gripping dynamics (Brody et al. 2002; Hatze 1998; Knudson and White 1989; Knudson 1991). The second force peak identified by in this research is generated by a second increase in gripping force by the subject attempting to maintain/ regain control of the racquet due to its rotation in the tennis grip. In addition to this, the results obtained have shown that the player requires a period of approximately 0.398s to prepare the tennis racquet for impact. This approximation of racquet preparation time has been obtained using a hand-held racquet that is not swung before impact by the player. It is likely that this time may increase when the racquet is swung before impact as the player will require additional gripping force to swing the racquet. As the player usually swings the racquet well before impact, the initial increase in gripping tightness should occur even earlier.

### **3.3 Real time analysis of tennis grip pressure distribution characteristics**

The developed strain gauge cantilever system was used to acquire real time data in order to determine gripping times and variations in the magnitudes of force during impact. However, as previously stated the system had limitations in terms of the quantification of the tennis grip with respect to the location of force and the distribution across the racquet handle. Therefore a new system was developed taking into consideration the locations of gripping force on the racquet, to allow an analysis of the variations in distribution. It is necessary to acquire data with respect to the distribution of gripping force, because it is essential that a comprehensive understanding of grip pressure distribution is formed if correlations are to be established with the structural behaviour of the tennis racquet. As discussed in chapter 1, the damping of racquet frame vibrations by the tennis grip is

defined by the gripping tightness. If a quantification of this relationship is to be established then the distribution of gripping pressure must first be measured. The strain gauge cantilever system used previously measured the application of force (N) on the racquet handle at four locations. The method developed in this chapter measures multiple locations within the tennis grip and thus measures the distribution of grip pressure ( $\text{N}/\text{cm}^2$ ).

Previous investigations based on the analysis of the tennis grip have used experimental techniques focusing on single or multiple point force measurements of the tennis grip (Knudson and white 1989; Knudson 1991; Elliot 1982; Li *et al* 2004). The number of measurement points was inadequate to model the distribution of pressure in the tennis grip. The effect of the tennis grip on vibration absorption by the hand can only be analysed if the distribution of gripping pressure is known and understood, as the gripping tightness defines vibration absorption. Multiple contact locations within the tennis grip need to be measured (i.e. those of greatest importance shown in the section 3.1) simultaneously using real time data acquisition, to allow for correlations to be established between the distribution of grip pressure and the damping of racquet vibrations.

The analysis of pressure distribution within the tennis grip will describe not only the magnitudes of pressure across the racquet handle, but also at the contact locations of the player's hand. When discussing the injuries caused by the transfer of racquet vibration to the players arm, these contact points are an important issue as they provide the locations for this transfer to the player. Section 3.1 identified these contact locations within the tennis grip, and it is these that will now be quantified to show the variations in gripping

pressure. Understanding the pressure variations at these contact locations within the tennis grip will provide measurements to describe the transfer of racquet vibrations to the player's arm. In addition to this, the measurements of grip pressure distribution can also be used to estimate the biomechanical relationship between the tennis grip and upper extremity injuries. This is done by establishing sources generating the measured pressure within the tennis grip in order to hypothesize the hand movements of the player (i.e. pronation, flexion etc.).

### ***3.3.1 Experimental set-up***

An experimental technique has been developed to assess the grip pressure distribution across the racquet handle. Up to 21 hydrocell pressure sensors are required to measure variations in the distribution of pressure at the important contact locations identified in section 3.1. The following instrumentation was used for real time data acquisition of the tennis grip pressure at up to 21 locations:

- 21 x hydrocell pressure sensors
- Paromed Datalogger – (hardware) v2.1
- External power cell (NiCd 9.6V/ 0.8A max)
- 2 megabyte PCMCIA memory card
- HF remote control (range 200metres; frequency: 433.920MHz  $\pm$  150KHz)
- 2 x Miniature PCB 352A25 accelerometer (mass – 0.48g)
- 2 x PCB ICP signal conditioner (model 480C02)

### 3.3.1.1 Hydrocell pressure sensors

Hydrocell pressure sensors have been originally used for the analysis of plantar pressure distributions of human gait. The hydrocell sensors have been embedded in a shoe insole and pressure distribution data was acquired to assist physical therapy treatment techniques and human movement studies (Orlin and Mcpoil 2000; Zequera *et al.* 2003; Perttunen and Komi 2001). This research uses the hydrocell technology to measure and describe the tennis grip pressure distributions in a real time analysis.

Paromed hydrocell (Paromed Medizintechnik, Germany) pressure sensors are based on a piezoresistive bridge configuration, embedded in a silicon filled bladder. The piezoresistive bridge sensor generates an electrical voltage when a load is applied to the surface of the sensor and deformation of the silicon bladder occurs. The hydrocell contains a Wheatstone bridge circuit fixed within the silicon bladder. The deformation of the bladder caused by the applied load generating a gradual decrease in bridge resistance within the silicon cell. This change in bridge resistance generates a voltage signal that couples both shear and vertical loading, due to the piezoresistive nature of the sensor (Scahff 1993; Rosenbaum and Pecker 1997; Cavanagh 1992). The generated voltage is calibrated to show the total pressure applied to the surface of the sensors. The design of the hydrocell, with respect to the variations of the bridge resistance due to pressure changes, allows for the quantification of pressure irrespective of the loading location. This is a requirement of the data collection method in the present investigation as the application of the load to the sensor's surface does not have stationary properties. Lateral movement of the player's hand across the racquet handle will occur during the tennis stroke. The design of hydrocell pressure sensors enables acquisition of the data

irrespective of the loading location, limiting the error in pressure measurements generated by the player's hand movement across the racquet handle. The hydrocells were attached to the racquet handle at the locations that provided measurements of pressure distribution over the contact points in the tennis grip. Appendix 2 outlines the precise locations on the racquet handle where the 21 hydrocells were attached.

A Paromed datalogger was used to measure the variations in voltage of the 21 hydrocell sensors. Two miniature PCB accelerometers were connected to additional channels of the data logger, via signal conditioners, to measure the vibration response of the racquet during the tennis stroke. The accelerometers were attached to the tip of the racquet head and approximately 263 mm up from the racquet butt. The locations of the accelerometer attachment were chosen based on the modal analysis carried out in chapter 2. They are the locations which display the greatest racquet displacement at the natural frequencies of interest at 183Hz and 163Hz for the two test racquets A and B (i.e. the first mode of oscillation as this is thought to be the natural frequency that instigates and aggravates injuries such as tennis elbow). Figure 26 shows a schematic of the data collection set-up using the hydrocell sensors and the accelerometers. Due to the datalogger measuring and recording data independently of external computer, the data acquisition system was mounted onto the test subject's belt allowing them to move freely.

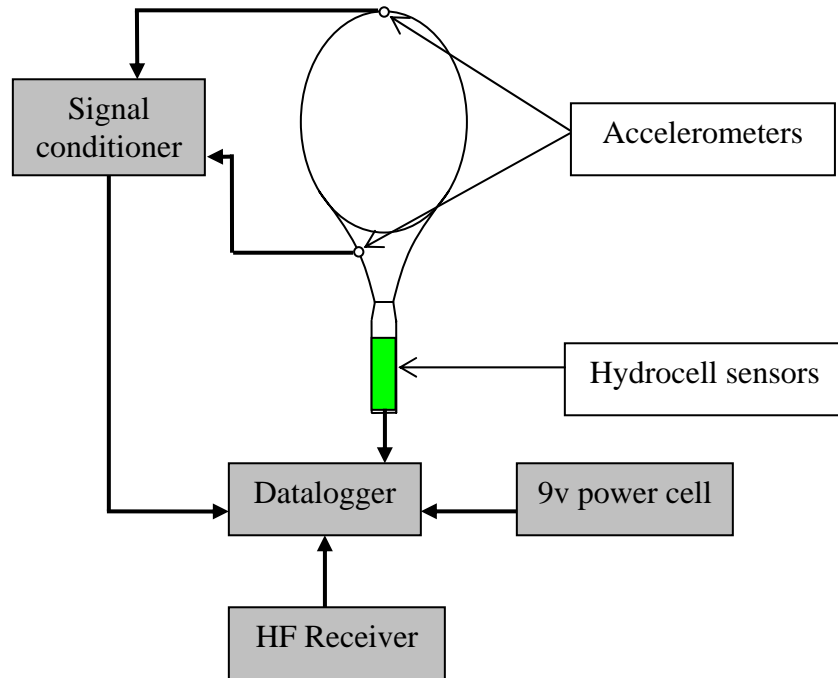


**Figure 26. Schematic of hydrocell sensor data collection set-up**

The 21 hydrocell channels, together with the additional accelerometer channels were scanned by the data logger at specific sampling frequencies. The datalogger was configured to acquire data at sampling frequencies of 200Hz for the hydrocell channels and 800Hz for the accelerometers. It was determined from the inherent structural dynamic properties of the racquet (Chapter 2) that these sampling rates would allow for an analysis of the gripping pressure variations and their effect on the response of the racquet with respect to the first mode of oscillation at 163Hz and 183Hz for the two test racquets A and B. Figure 27 shows the attachment locations of the two PCB miniature accelerometers. Using a manual trigger to initiate the data acquisition, the datalogger was configured to acquire measurements for a five second period. The system was triggered using a high frequency remote control with the receiver connected to the data logger.

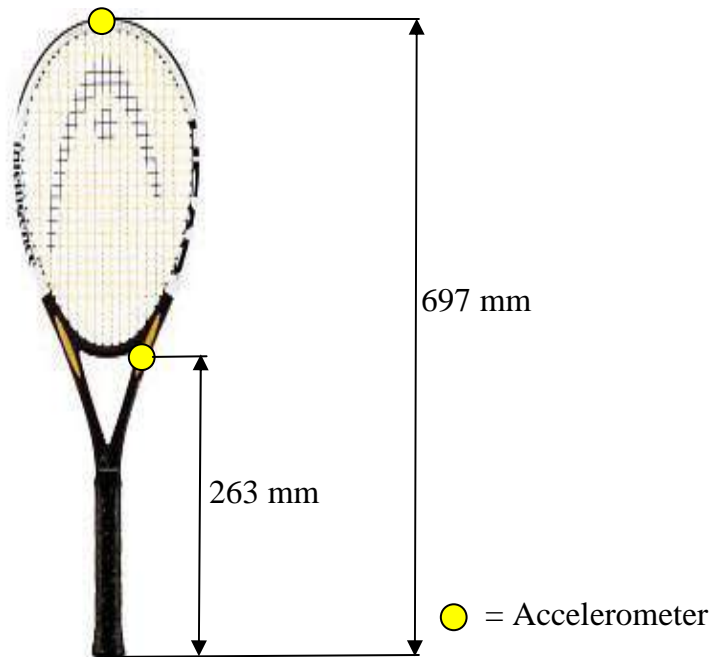


**Figure 27. Accelerometer locations**

### ***3.3.2 Testing protocol***

Three stroke types were investigated including a continental forehand, a service and a back hand slice. The tests were conducted on a tennis court using the baselines as the landmark positions for a ball cannon and the test subject. Figure 28 shows the complete ball cannon experimental set-up.

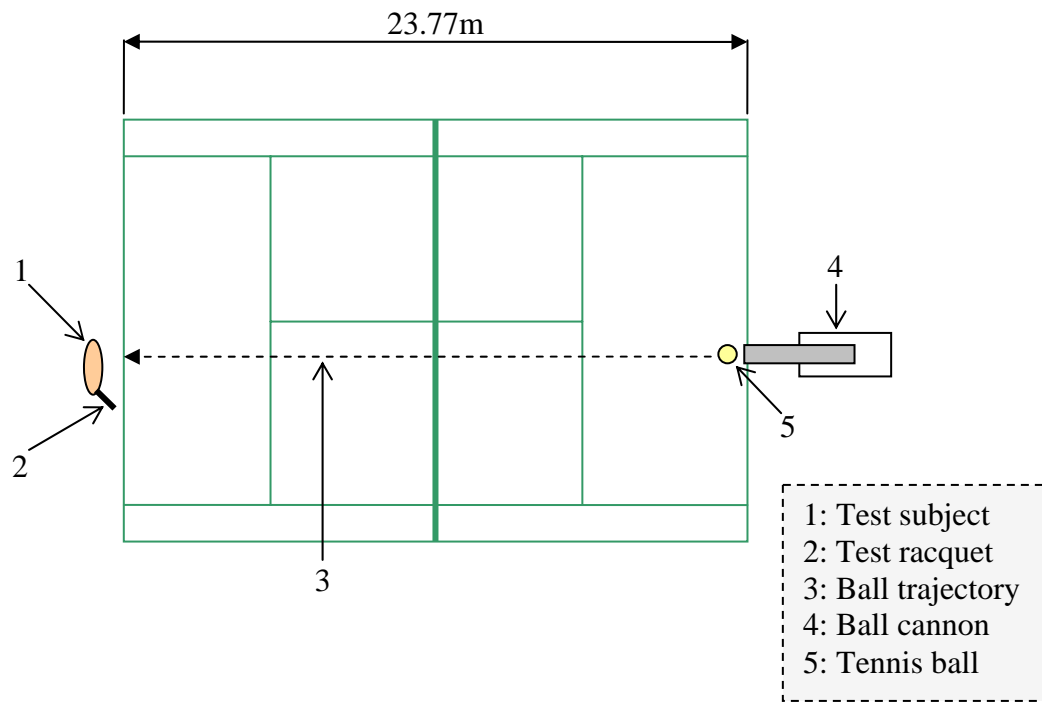


**Figure 28. Experimental set-up on a tennis court**

A ball cannon was used to project a tennis ball towards the test subject at an approximate velocity of 13.8 m/s (50 kph). The ball cannon was only needed for the forehand and back hand slice strokes as the service is performed using a ball toss by the player. 78 trials were carried out to produce adequate data for modelling of the gripping characteristics (29 forehand; 27 service; 22 backhand slice).

Triggering of the data acquisition was accomplished by connecting the HF remote control to the datalogger. The HF remote control allowed for the system to be triggered manually when the ball left the cannon. Once the tennis ball entered the cannon, the datalogger was triggered using the remote control. The data acquisition time was set to five seconds, allowing for a single ball impact to be measured by the system.

### ***3.3.3 Results and discussion***

The measurements obtained from the tests using hydrocell sensors, were analysed in the time domain to show the relationship between the variations in the distribution of gripping pressure and the time of impact. This investigation needed to establish the grip pressure distributions across the racquet handle so that correlations could be established with the damping of frame vibrations. The correlations between gripping pressure and racquet vibration damping need to be established to analysis the transfer of vibrations to the player's hand via the tennis grip.

The racquet was divided into "gripping sections" (A: H) to enable the pressure distributions to be analysed with respect to the specific zones of the handle and contacts points with the hand. Figure 29 shows the handle gripping sections A: H, with the distance each cover from the handle butt. Sections E: H covered the lower handle and reach from the end of the racquet (0cm) to 6.25cm up the handle from the butt. Sections A: D covered the upper handle area, 6.25cm – 12.5cm from the racquet butt. The side of the racquet where the ball impact occurs is also indicated in figure 29. It is important to note the handle orientation in order to allow for the interpretation of the pressure data, in terms of the direction of the measured pressure and contact points where it is generated. It has been shown earlier in this chapter that the racquet rotates about an axis within the tennis grip determined by the location of the ball impact and its proximity to the racquet COP (N.B the location of the racquets COP depends on the forces acting on the structure. The COP for a freely suspended racquet will be quite different from that in hand-held conditions. Therefore the precise location of the axis about which the racquet rotates

within the tennis grip is difficult to estimate). The orientation of the handle sections in relation to the side of the ball impact is therefore needed to understand the pressure distribution analysis, with respect to both the movement of the racquet handle and the applied pressure of the player's hand.

Each hydrocell sensor is assigned to one of the eight handle sections. The total pressure measured by the hydrocells across each handle section is then used to analyse the gripping dynamics in the time domain.

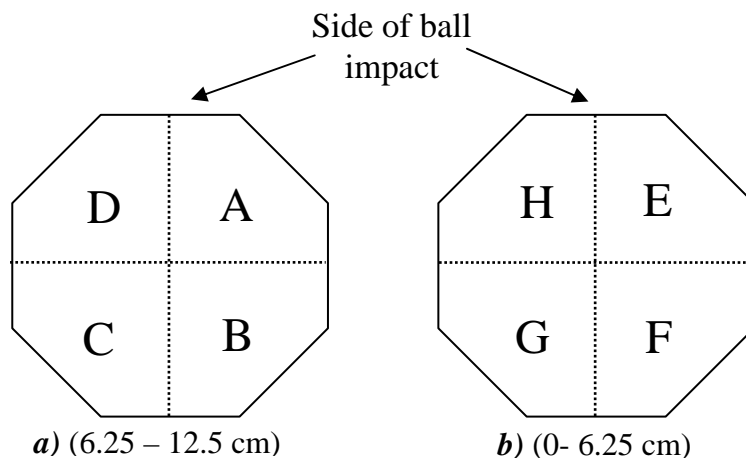


**Figure 29. Racquet handle: a) upper and b) lower gripping sections**

The five second data collection period is analysed for each trail using the pressure measurements obtained on the eight handle gripping sections (A: H) together with the acceleration measurements. The time plots presented in this analysis use a reduced time scale instead of the complete five second data collection period. This is to focus the analysis on the ball impact and enable the relationship with the variations in the distribution of pressure to be established.

Pressure distribution analysis has been conducted using the eight handle gripping sections. The upper and lower gripping sections, shown in figure 29, have been used to show the distribution of pressure over the designated areas of the racquet handle. Time plots are used to show the variations in the section pressures in relation to the ball impact. In addition to this, radar plots are used to display the variations the distribution of pressure across the racquet handle both pre and post-impact.

Magnitudes of pressure during impact were calculated at time increments of 0.02s. The pressure magnitudes are calculated for a total time period of 0.1 seconds pre and post-impact. Pre and post-impact radar plots are then used to show the variation in grip pressure distribution over the racquet handle, both before and after the impact. Radar plots for the upper and lower gripping sections have been calculated to show the variations in total pressure across the racquet handle at each of the time intervals.

Both time and radar plots have been calculated for all stroke trails; however the modelling of the grip characteristics was achieved by using the radar plot data. The time plots did not have a consistent ball impact time and therefore average variations in grip pressure distribution are difficult to calculate from this data source. The calculated radar plots are based on the same time periods in relation to the ball impact and can therefore be averaged to model the variations in pressure distributions of the tennis grip.

The pressure distributions of the tennis grip have been analysed initially in order to determine the magnitude of contact pressure and their locations on the racquet handle.

The analysis of the pressure distributions in terms of the racquet handle and the anatomical locations on the subject's hand, allows for the implications the distribution of pressure has on injuries such as lateral and medial epicondylitis to be estimated. The estimations are based on the biomechanical relationship between the tennis gripping pressure distributions and the upper extremity injuries experienced by tennis players, and are described by examining the sources generating the measured pressure. Both racquet and player generate pressure in the tennis grip, and this is taken into consideration during the interpretation of the following results. In addition to this the grip pressure measurements given in the analysis are based on the distribution of pressure across the specified handle section. Due to single point measurements not being shown, identification of shock forces becomes difficult as the pressures shown are calculated from the summation of the individual hydrocell measurements. In addition to this the sensitivity of the hydrocells was such that the small displacements of the post-impact racquet vibrations were not able to be measured by the pressure sensing equipment.

Figure 30 shows a sample time plot of the section pressure variations for the forehand tennis stroke. The figure includes an example of the pressure measurements of the eight handle gripping sections with the acceleration measurement, using the same time scale. From this, the relationship between variations in gripping pressure and the ball impact can be seen. Figure 31 shows the radar plots of the average pressure distribution of the pre-impact upper and lower handle section. Figure 32 shows average pressure plots of the post-impact variations for the forehand stroke, based on the 29 trials.

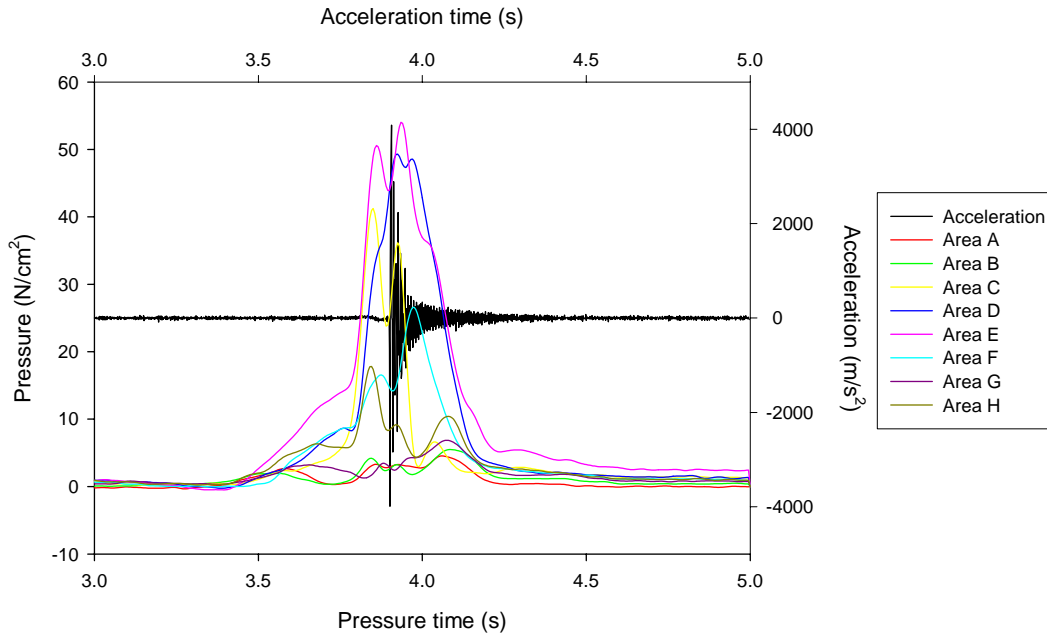


**Figure 30. Sample of right-handed forehand stroke handle section pressure variation measurements during impact**

The absolute pressure values measured for the different stroke types in this investigation are not relevant to the results as the grip tightness levels will vary with the individual player, incoming ball speed and racquet swing speeds. Therefore the profiling of grip pressure distribution will be based on the averages taken from the data of all trials.

The pressure variations shown in figure 30 display multiple peaks during impact, similar to those observed in the strain gauge cantilever handle system experiments (see section 3.2). The two peaks observed in the previous test are also detected using hydrocell sensors, indicating the movement of the racquet in the tennis grip during impact, and the players attempt to regain/ maintain control of this movement post-impact (Knudson and White 1989). The cantilever system showed an increase in gripping tightness approximately 0.398 seconds pre-impact. Similar trends are seen in the hydrocell test

with respect to a pre-impact increase in gripping tightness and a post-impact decrease in gripping tightness. The threshold and maximum tightness times for the hydrocell tests vary as a result of the racquet being in motion pre-impact rather than in a static state. The differences between static and non-static racquet tests will now be analysed.

The forehand pressure distribution measurements reveal that the pressure across the upper handle section of the tennis grip is concentrated in sections C and D. The pressure is primarily distributed at the distal thumb and across the 1<sup>st</sup> and 2<sup>nd</sup> fingers stretching from the metacarpophelangeal (MP) joint to the proximal phalanx bones. The opposite is true of the lower handle sections with the gripping pressure concentrated largely in areas E and F. Pressure distribution across these sections is concentrated across the base of the metacarpal bone system and through the middle and proximal bones of the 3<sup>rd</sup> and 4<sup>th</sup> fingers.

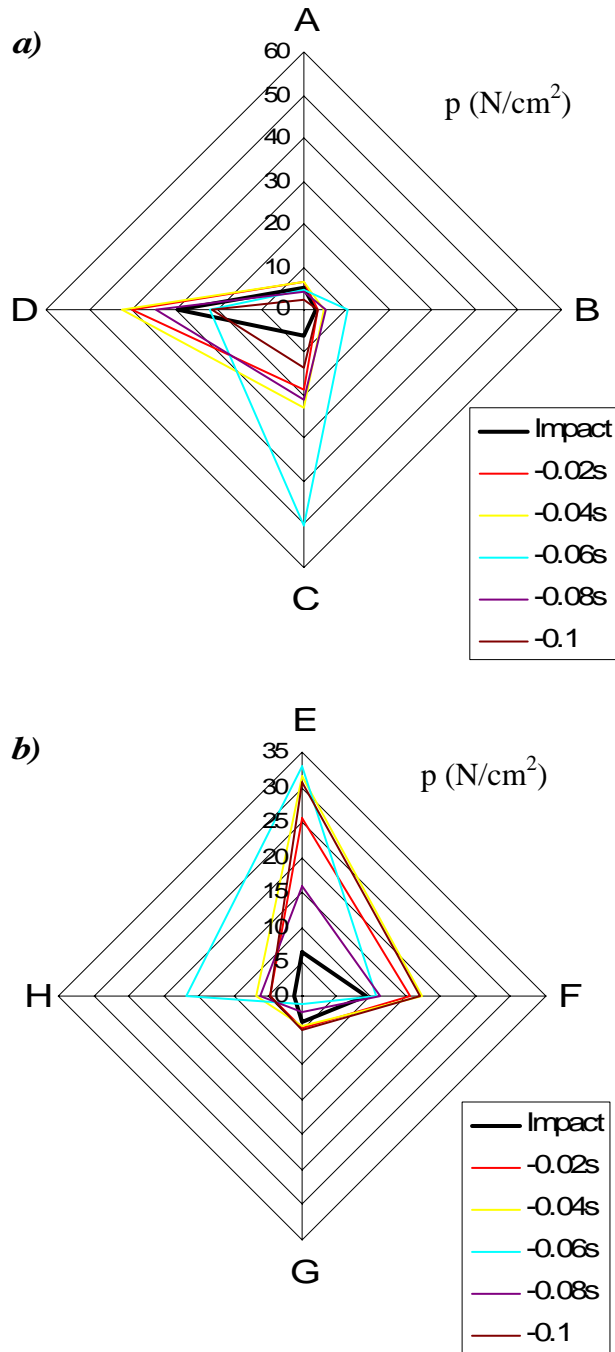


**Figure 31. Pre-impact pressure distribution in a forehand stroke for: a) upper handle and b) lower handle**

Figure 31 shows the pre-impact pressure distributions across handle sections, and figure 32 shows the post-impact distributions, for the 29 forehand stroke trials. The plots represent a calculated average based on the total pressure measured over the handle

surface from the 29 forehand trials. The origins of the gripping pressures measured in this research have previously been discussed earlier in the thesis (see section 3.2). All pressure measurements are representative of the combined gripping tightness of the player and the reaction forces of the tennis racquet over the hand area. Therefore the analysis of the pressure distributions here is based on both the reaction forces of the racquet across the hand, and the gripping tightness applied by the player. The reaction forces acting on the hand have been observed in the pressure distributions shown in figure 31 and figure 32.

The opposing distributions between the upper and lower handle sections indicate that there is movement of the racquet in the tennis grip. The opposing pressure distributions between the upper and lower handle section are governed by the racquet as it rotates about an axis located within the tennis grip. The direction of rotation is determined by the ball impact location on the racquet face (Brody et al. 2002; Elliot 1982). Off-centre ball impacts will create both linear and transverse rotation of the racquet. The measured pressure is due to the movement of the racquet within the tennis grip and the resistance to this movement by the tennis player. The movement of the racquet in the tennis grip imparts pressure on the player's hand which will generate a counter increase in gripping tightness. This counter increase in grip tightness by the player is required to generate the necessary racquet-hand stiffness to produce the desired racquet speed throughout the stroke.

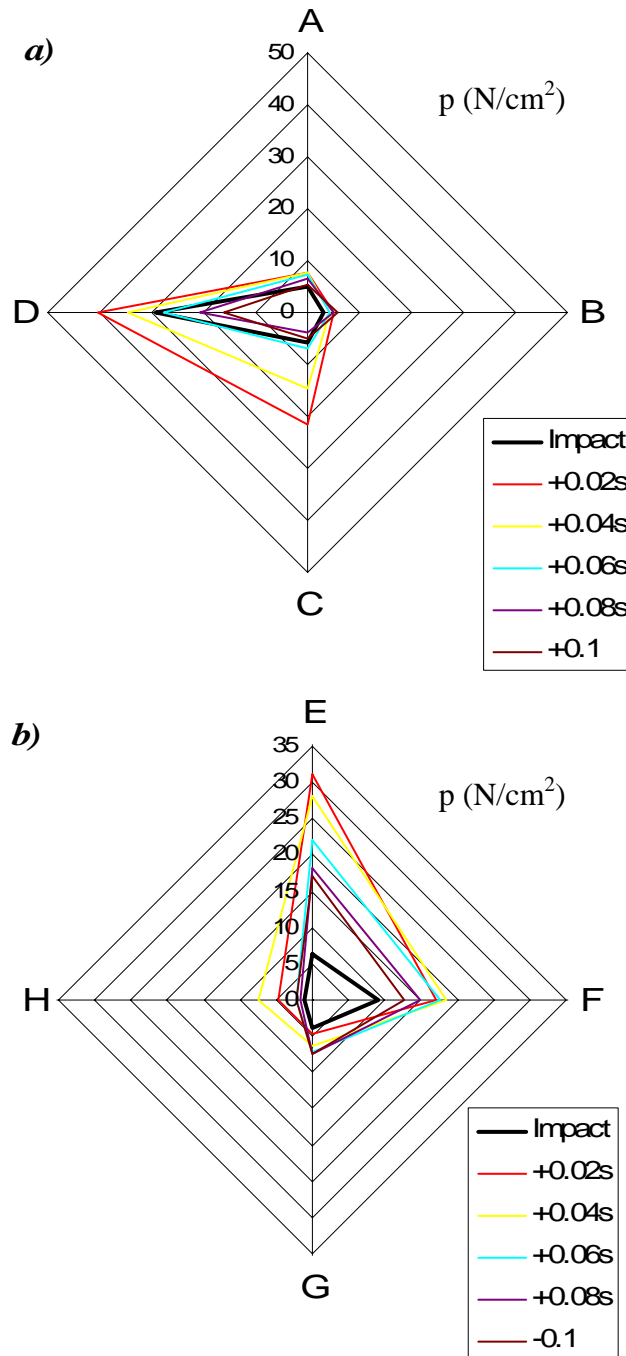


**Figure 32. Post-impact pressure distribution in a forehand stroke for: a) upper handle and b) lower handle**

The pressure distribution plots obtained for the forehand stroke displayed in figure 31 and figure 32 show a general increase in pre-impact gripping pressure. A maximum pressure of approximately  $50N/cm^2$  (on upper handle section C) and  $35N/cm^2$  (on lower handle

section E) is reached 0.06s before impact. Following this pre-impact peak there is a relaxation in the grip, indicated by the decrease in pressure to an approximately 30N/cm<sup>2</sup> (on upper handle section D) and 10N/cm<sup>2</sup> (on lower handle section F) at the moment of impact. However immediately after the impact there is a second increase in the grip pressure across the racquet handle. The maximum pressure of approximately 40N/cm<sup>2</sup> (on upper handle section D) and 30N/cm<sup>2</sup> (on lower handle section E) is reached 0.02s after impact for the forehand stroke.

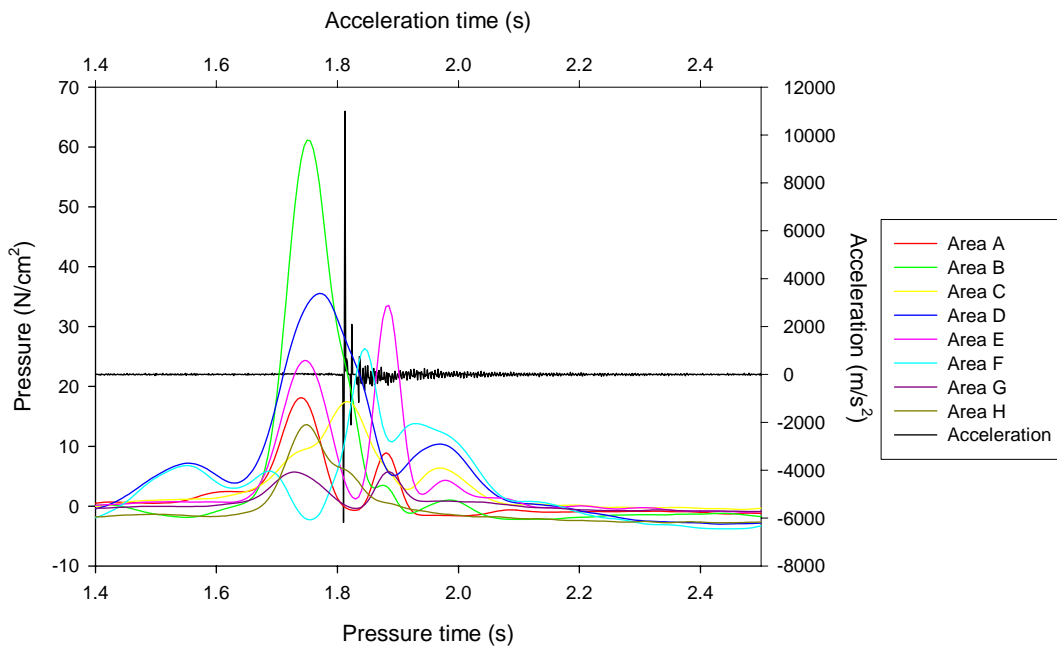


**Figure 33. Sample of service stroke handle section pressure variation measurements during impact**

Figure 33 shows a sample time plot of section pressure variations for the service tennis stroke. Based on the 27 trials, the time plots showed increases in sections A, B, D, E and H before impact. This represents a concentration of pressure across the index MP joint (section B), together with pressure across the 4<sup>th</sup> proximal and middle phalanx (section H). There is also a concentration of pressure across the 3<sup>rd</sup> IP joint (section H). Contrary

to this there is a decrease in the pressure over the 2<sup>nd</sup>, 3<sup>rd</sup> and 4<sup>th</sup> middle metacarpals (Section F). These opposing pressure variations on the hand follow the movement of the racquet as the tennis subject swings before ball impact. There is a relaxation of the tennis grip for the tennis stroke before the ball impact, indicated by the decrease in pressure measurements over sections A, B, D, E and H. This is also indicated by the pressure distribution plots shown in figure 34a) and b), with maximum pre-impact pressures larger than 50 N/cm<sup>2</sup> (in section B) and larger 20 N/cm<sup>2</sup> (in sections E and H)) at approximately 0.08-0.06s before the impact.



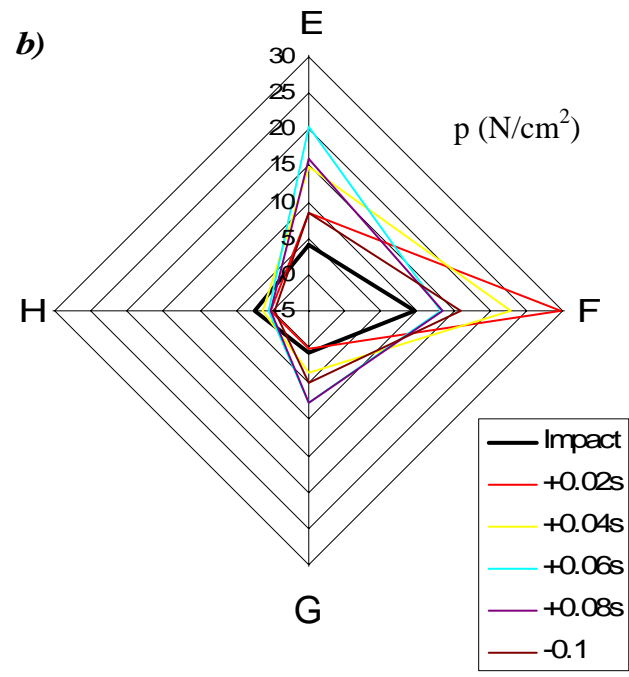
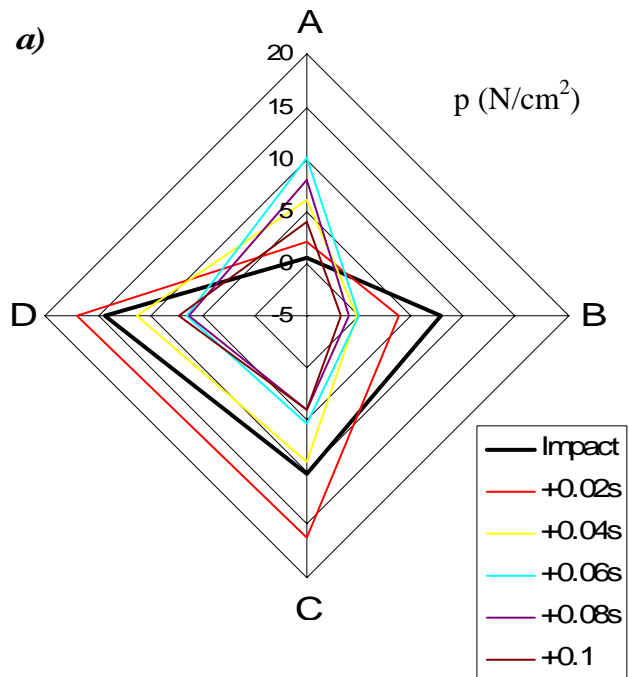


**Figure 35. Post-impact pressure distribution for the service stroke at: a) upper handle and b) lower handle**

Post-impact pressure distribution in the upper handle section is concentrated over sections C and D (figure 35.a)). This indicates a pressure distribution across the index middle IP joint and distal phalanx. Pressure is also concentrated across the MP joint, proximal phalanx, middle IP joint and distal phalanx of the 2<sup>nd</sup> finger. The maximum post-impact pressures for upper handle across sections C and D (approximately 16.2N/cm<sup>2</sup> and 16.9N/cm<sup>2</sup> respectively) are reached 0.02s after impact.

The maximum pressures across the lower handle sections E (20N/cm<sup>2</sup>) and F (29.5N/cm<sup>2</sup>) are reached approximately 0.06s and 0.02s respectively. This pressure is focused around the distal phalanx of the 2<sup>nd</sup> and 3<sup>rd</sup> fingers (section E), together with the middle of the 2<sup>nd</sup>, 3<sup>rd</sup> and 4<sup>th</sup> metacarpals. There is also a concentration of pressure around the 4th carpometacarpal (CM) joint.

If we compare the service and the forehand strokes, the distribution of pressure is concentrated around the centre of the palm and the index and 2<sup>nd</sup> fingers for the service stroke. The forehand stroke has a greater concentration of pressure around the base of the 2<sup>nd</sup> 3<sup>rd</sup> and 4<sup>th</sup> bones of the metacarpal systems (the palm) and the distal bones of the 3<sup>rd</sup> and 4<sup>th</sup> fingers. With respect to the maximum pressures measured in the experiments, the service stroke required a similar pressure to that of the forehand (approximately 50N/cm<sup>2</sup>). However, the time at which the maximum pressure is reached is faster in the service stroke (0.08s pre impact) than in the forehand (0.06s pre-impact).

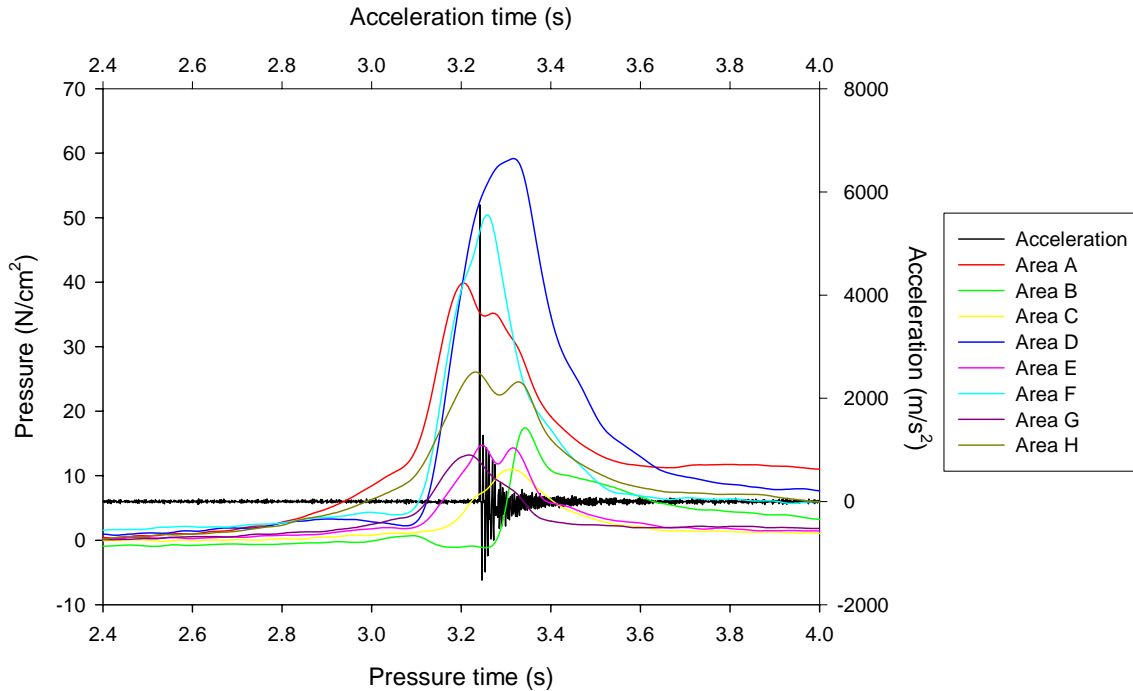


**Figure 36. Sample of backhand slice stroke handle section pressure variation measurements during impact**

Figure 36 shows a sample time plot for a single backhand slice stroke. The analysis of pressure distribution is carried out using the averages from the 22 backhand trials. It was concluded from these trials that there is a distribution of pressure over handle sections A, D, F and H, which involves an increase before impact. Distribution of pressure across these sections is confirmed by the average gripping characteristics of the backhand slice stroke, shown in figure 37 and figure 38. The distribution of pressure is primarily across the distal and proximal IP joints of the thumb (section A); the middle IP joint and proximal phalanx of the 2<sup>nd</sup> finger together with the distal phalanx of the index finger (section D); the middle of the 2<sup>nd</sup>, 3<sup>rd</sup> and 4<sup>th</sup> metacarpals, and the CM joint of the 4<sup>th</sup> metacarpal (section F); and the IP joints of the 3<sup>rd</sup> and 4<sup>th</sup> fingers together with the proximal phalanx of the 4<sup>th</sup> finger (section H).

The pre-impact pressure distributions shown in figure 37.a) indicate that grip pressure rises to an estimated maximum of  $49.5\text{N/cm}^2$  (section D) at approximately 0.04s before impact. The lower handle section F rises to an estimated maximum pressure of  $50.8\text{N/cm}^2$  approximately 0.08s before impact. Compared to the forehand stroke, and similar to the service, the pre-impact maximum pressure is reached approximately 0.02 seconds faster in the backhand slide. The gripping tightness across the racquet handle sections falls to a pressure of approximately  $23.3\text{N/cm}^2$  at impact (section D).

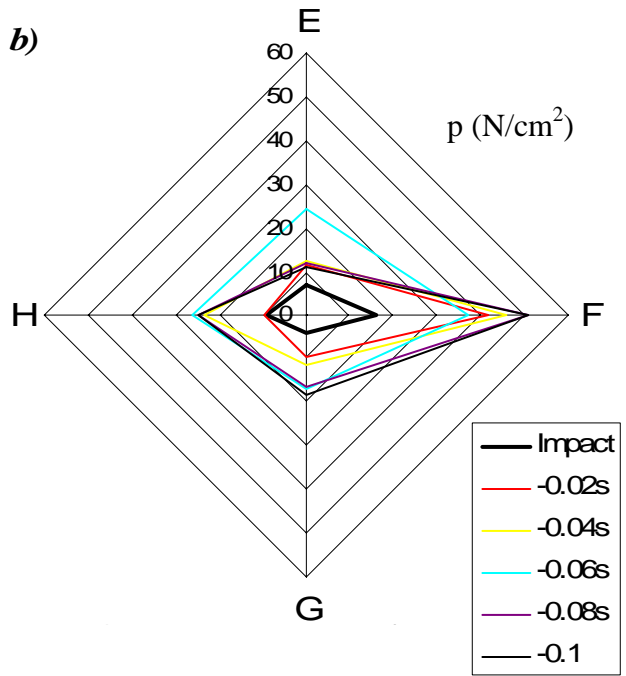
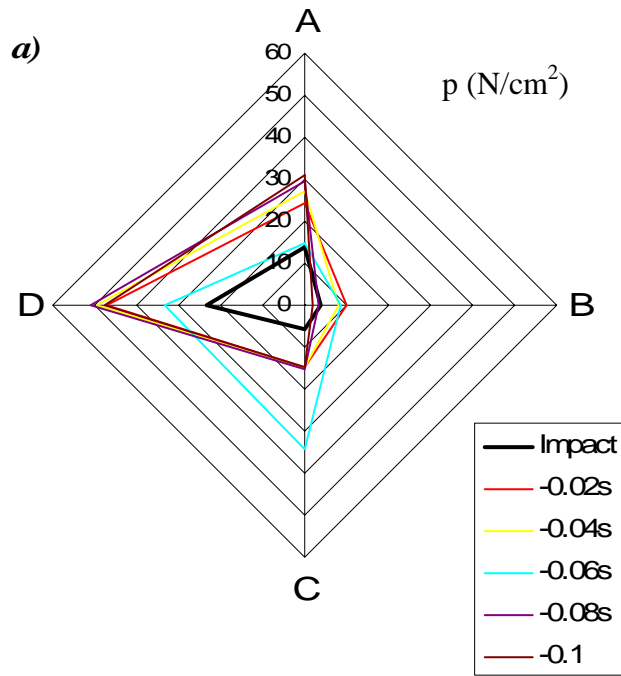
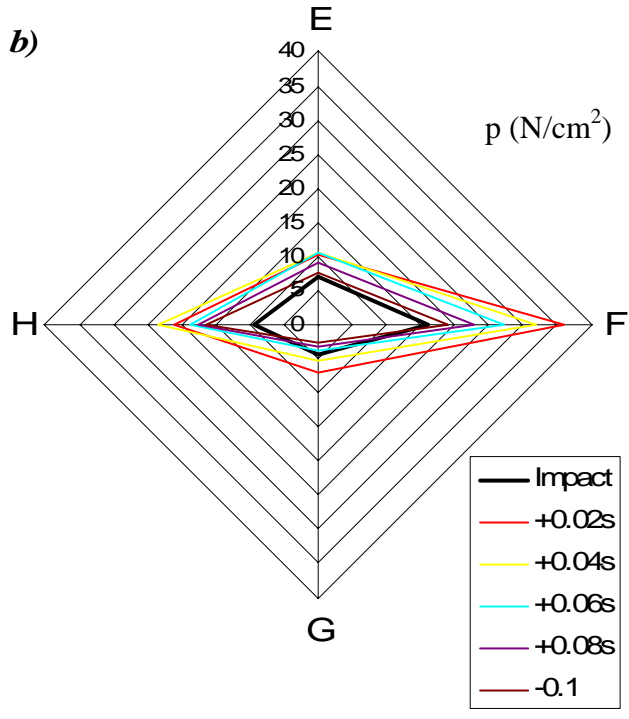
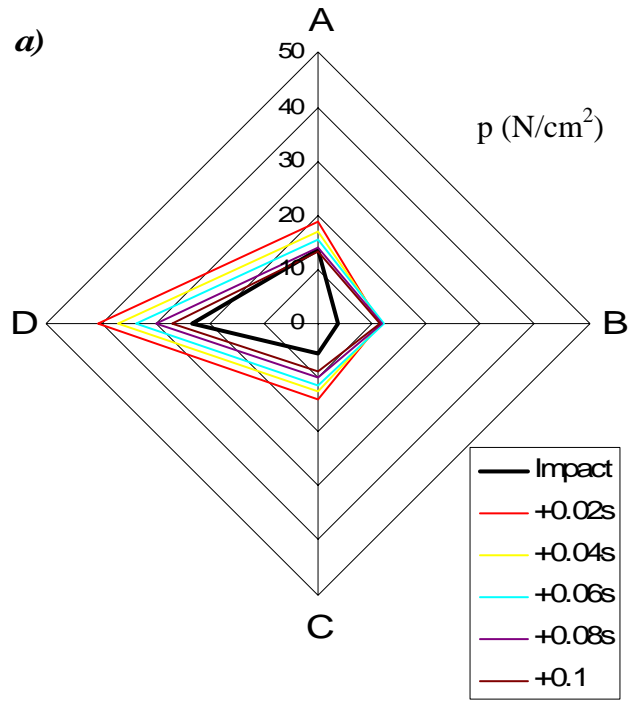


Figure 37. Pre-impact pressure distribution for the backhand slice stroke at: a) upper handle and b) lower handle



**Figure 38. Post-impact pressure distribution for the backhand slice stroke at: a) upper handle and b) lower handle**

The distribution of grip pressure post-impact, remains concentrated on the same areas as the pre-impact distribution, however there is a slight increase in pressure across the proximal phalanx of the 4<sup>th</sup> finger and the middle IP joints of the 3<sup>rd</sup> and 4<sup>th</sup> fingers (section H). The pressure rises to 40.3N/cm<sup>2</sup> in the upper handle and 35.7N/cm<sup>2</sup> in the lower handle sections approximately 0.02s post-impact.

The backhand slice pressure distribution profile has similar attributes to the service stroke. The pressure is distributed across the middle of the metacarpal systems (the palm) and the proximal phalanx of the fingers, with a concentration around the 4<sup>th</sup> finger. The backhand slice shows additional concentrations of pressure over the thumb, which is not so in the service stroke. All three strokes have unique pressure distribution attributes which can be used to hypothesis relative muscle contractions in the forearm and ultimately aid in the understanding of vibration transfer to the player via the tennis grip.

The observed pressure distributions for the analysed stroke types are not only attributed to the gripping tightness of the player, but also the racquet reaction forces acting on the player's hand. The racquet structure displays rigid body motion throughout the tennis stroke. The rigid body motion is generated by the forces imparted on the structure to generate racquet swing. The racquet will subject forces across the player's hand as a consequence of the player increasing the gripping tightness in order to swing the racquet. The results of this investigation show that the application of pressure in the tennis grip is greater in magnitude at the point of impact and after the ball has left the string bed, than before impact. An increase in gripping pressure after the impact has been observed,

which have been attributed, in previous research, to the player's attempts to regain/maintain control of the racquet (Hatze 1998; Knudson and White 1989; Knudson 1991).

In order to analyse the pressure distribution data in relation to hypothetical muscle contractions on in the player's forearm, a simple free-body diagram of the hand-racquet force/pressure interaction is shown in figure 39. The diagram represents the player's hand in contact with the racquet handle during impact and the forces/ pressures within this interaction. The player applies a variable pressure to the racquet handle to control the racquet forces. The racquet forces are the natural reaction force combined with the rotation forces of the racquet handle to produce an overall reaction force. These are the 'horizontal' forces in the tennis grip. In addition to this there are 'vertical' forces acting on the player's hand. In order for the player to maintain control of the racquet, the grip pressure must provide a frictional resistance greater than that of the 'vertical' forces.

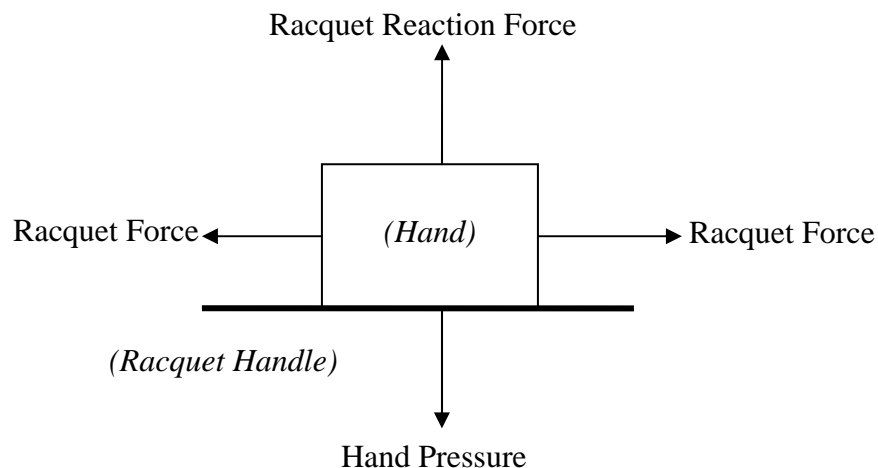


**Figure 39. Simple free-body diagram of hand-racquet interaction**

Figure 39 displays the force/ pressure interaction of the tennis grip. The pressure distribution data measured in this chapter can be thought of as a combination of all the forces/ pressure outlined in the free-body diagram. However, in order to hypothesis muscle contractions in the forearm, the pressure measurements are thought of as a representation of the player's resistance to the racquet forces. If the player was in-capable of resisting the 'vertical' racquet forces the racquet would slide and leave the grip position in the hand and the player would have limited control of the racquet. When hypothesising muscle contractions the racquet can therefore be considered to remain in the same position in relation to the hand locations in the tennis grip.

For the purpose of this research, the pressure distribution measurements are considered to represent the player's resistance to racquet movement at the specified locations in the tennis grip. Additional forces may have contributed to the measured grip pressures, but this requires further investigation which is outside the scope of this thesis. However, for the purpose of hypothetical estimations of forearm muscle contractions, it is feasible to consider the measured pressure distributions as the player's resistance to racquet movement at specific locations in the grip and therefore the required hand motions in order to produce this resistance can be hypothesised. (N.B. The estimated muscle contractions discussed in this thesis are hypothetical based on the pressure distribution measurements. Further research using EMG technology is required to confirm the hypothetical analysis given here.)

The concentration of pressure in the continental forehand gripping technique has been identified at the MP joint of the index and 2<sup>nd</sup> fingers, along with the associated proximal

phalanx bones. Distribution of pressure over these areas in the tennis grip indicates pronation and flexion of the hand in order to both generate racquet speed and resist the racquet's reaction forces during impact. The muscles required to generate pronation and flexion of the hand are the wrist flexors and pronator teres (Grollman 1969; Sinclair 1975). Contraction of these wrist flexors in order to generate the racquet swing, leave their tendon origins at the elbow susceptible to injury. The contracted forearm muscles are stiff and, as previously discussed in the thesis, allow for the transfer of shock and vibrations to the tendon origin of the muscle, via the muscle itself (Roberts *et al.* 1995). The greater the stiffness of the contracted forearm muscle, the greater the transfer of racquet vibrations to the tendon origin and muscle itself. Attempts to maintain control of the racquet after impact bring about further contractions of the muscles to produce the required resistive pressures in the tennis grip. The opposing reaction forces of the tennis racquet are transferred to the already contracted forearm muscles, which place large strains on the tendon origins causing discomfort to the player.

Similarly, the service stroke has post-impact pressure concentrations over the distal phalanx of the 2<sup>nd</sup> and 3<sup>rd</sup> fingers, together with the middle of the 2<sup>nd</sup>, 3<sup>rd</sup> and 4<sup>th</sup> metacarpals. This pressure is coupled with a concentration of pressure around the 4<sup>th</sup> carpometacarpal (CM) joint indicating similar pronation and flexion hand movements for the forehand stroke. Therefore, strain will be placed on similar muscle and tendon groups to those of the forehand stroke. Results presented in this thesis have shown the forehand and service strokes to place pressure on specific areas on the hand which require pronation and flexion of the hand, placing strain on the medial forearm muscles. The

contractions of the lateral muscles of the forearm (wrist flexors) are also required to resist the racquet movement in the backhand stroke.

The grip pressure distribution post-impact in the backhand slice stroke is concentrated on the proximal phalanx of the 4<sup>th</sup> finger and the middle IP joints of the 3<sup>rd</sup> and 4<sup>th</sup> fingers. The backhand slice grip pressure distribution characteristics indicate a supination and extension of the hand. The muscles required for these movements are the wrist extensors, bicep brachii and supinator (Grollman 1969; Sinclair 1975). As previously stated in the discussion of the forehand stroke, the contracted muscles of the forearm will allow for the transfer and absorption of racquet shock and vibration energy (Roberts *et al.* 1995). The backhand strokes involve the contraction of the wrist extensors resulting in the absorption of racquet frame energy by the lateral forearm muscles and their associated tendon origins. Previous research has described the use of these wrist extensor muscles in the backhand stroke using electromyographic techniques (Giangarra *et al.* 1993; Morris *et al.* 1989); however, this investigation has hypothesised the hand movements using pressure distribution profiles of the tennis grip. By describing hand movements using grip pressure profiles contact locations within the tennis grip are quantified and can be hypothetically related to the absorption of racquet vibration by the hand and forearm muscles. The quantification of the gripping pressure during impact will allow for the grip damping phenomena to be quantified in subsequent chapters, by analysing the magnitude of racquet vibration damping by the hand at the contact points measured here. (N.B. The estimations of muscle contractions in this research are hypothetical and not conclusive. Future research should focus on identifying muscle behaviour using EMG technology to

establish specific muscle contractions during the tennis stroke in order to analyse precise locations of racquet energy absorption by the player's forearm muscles.)

The upper extremity injuries suffered by tennis players, such as lateral epicondylitis, are thought to be a result of the strain imparted on the tendon origin at the lateral epicondyle. It is believed that the injury does not develop instantly during a single impact, moreover prolonged exposure to racquet energy, in the form of shock and vibration (with the greatest magnitude of energy associated with racquet shock). Prolonged absorption of racquet energy results in overuse of the muscles and tendon origins. Repeated absorption of racquet energy by the forearm muscles and tendons is believed to contribute to the development of injuries such as lateral epicondylitis (Nirschl 1986; Kamien 1990; Cassel and McGrath 1999).

### **3.4 Conclusions and significance**

This chapter presented experimental determination of tennis grip pressure distribution characteristics. This included pressure magnitudes and associated locations of peak pressure, together with the variation in pressure distribution during impact. Particular experimental techniques have been developed to acquire data allowing for the characteristics of the tennis grip to be quantified with respect to pressure distribution. Pressure film has been used along with the application of strain gauge techniques to quantify gripping characteristics in terms of variations in grip tightness during impact under laboratory conditions. A real time data acquisition system was developed, using hydrocell and accelerometer sensors, to measure both pressure variations and racquet vibrations during various tennis strokes. This allowed for the variation in pressure

distribution in the tennis grip to be quantitatively described. Variations in pressure across the racquet handle with respect to the time of impact were described and hypothetically related to potential upper extremity injuries sustained by the tennis players. Using the pressure distribution profiles, it was possible to hypothesise the player's hand movements and their relationship with the injuries sustained by tennis players. This was achieved by relating the pressure distribution of the tennis grip to both the racquet handle and in anatomical terms to the player's hand. This showed the distribution of reaction forces across the hand together with the direction of their application, from which particular hand movements could be hypothesised. Identifying these particular hand movements allowed for the identification of the contracted forearm muscles for stroke types. Using this information the locations at the elbow absorbing the racquet energy (in the form of shock and vibration) were ascertained.

When a tennis player grips a tennis racquet the muscles of the forearm will become somewhat contracted both laterally and medially (Mogk and Keir 2003). The experimental pressure distribution analysis undertaken in this thesis has identified where the concentrations of pressure are in the tennis grip (i.e. contact points). By establishing locations of pressure concentration it is possible to hypothesise the movements of both the hand and racquet pre and post-impact. As a result, estimation of the involved muscles during hand movement was possible to show the region of the forearm where shock and vibration is transferred from the racquet frame and absorbed.

Grip pressure distribution profiling undertaken in this chapter has provided essential information for determining the magnitude of damping of racquet frame vibrations in the

tennis grip. Previous research regarding gripping tightness has established the opposing pressures over the racquet handle (Hatze 1998; Knudson and White 1989; Knudson 1991), which is supported by the experimental measurements obtained in this investigation. The behaviour of the tennis grip in terms of pressure distribution during the ball impact has been shown to be variable (i.e. no constant throughout) as a result of the generation of action and reaction forces by the hand and racquet. With the hand generating gripping forces in order to swing the racquet and strike the ball, the racquet in-turn produces reaction forces on the player's hand during the racquet swing and impact. These are the action and reaction forces that have been observed in this investigation.

This research has described the grip tightness variability over the entire racquet handle in the tennis grip using pressure distribution profiles. This has been hypothetically related to the hand and racquet movements both pre, during and post-impact. The following chapter now establishes the relationship between the developed grip pressure distribution profiles and the magnitude of racquet vibration damping by the tennis grip during impact. The quantification of the pressure distribution also describes the contact locations in the tennis grip at which the transfer of racquet shock and vibration occurs. Relating these contact locations (in terms of magnitudes of pressure) to the magnitude of vibrations damping will allow for the mechanics of vibrations absorption by the tennis player at these transfer points to be understood.

## **Chapter 4**

# **Experimental investigation of damping in tennis racquets**

The inherent structural dynamic properties of the tennis racquet and gripping characteristics have been determined in previous chapters. Previous research has shown the structural response of the tennis racquet to be defined by the tennis gripping conditions and the ball-racquet interface (Brody *et al.* 2002). For example, the tighter the tennis grip, the greater the damping of racquet vibrations, and in addition to this, the ball will also have a damping effect on the response of the tennis racquet. Parameters, such as ball damping and grip damping, which define the structural response of the racquet during the impact need to be quantified in order for their mechanics to be described.

It has previously been discussed in chapter 1, that the interaction of the ball with the racquet string bed defines the level of the racquet frequencies excited. Ball interaction with the racquet string bed has a dwell time of approximately 0.005s (Brody 1979; Hatze 1976), and this defines the level of the excited racquet vibrations with a combination of its incoming speed, impact location on the racquet and dwell time on the string bed. Wave propagation from the impact location on the string bed is reflected from the racquet boundaries at different time intervals depending on their frequency. If the reflected waves return to the impact location before the ball has left the string bed, damping of the wave by the ball will occur. It has been established in previous research that vibrations with a frequency greater than 200Hz are drastically damped by the tennis ball before it leaves the string bed (Brody *et al.* 2002). The main objective of this chapter is to describe the mechanics of ball and grip damping to determine the effect on the level of vibrational response of the tennis racquet. The effects of ball and grip damping phenomena on the vibrational response of the racquet need to be understood in greater detail in order for their damping mechanics to be described.

The tennis grip has previously been investigated (Brody, 1987, 1987; Elliot 1982) whereby its effect on the damping of racquet vibrations has been described in a subjective manner. The decay of racquet oscillations has been found to be far greater in hand-held racquets than those that are freely suspended, but also increase with greater grip tightness. This relationship between the tennis grip and the damping of racquet vibrations (i.e. grip damping) has not been quantified in previous studies in terms of the magnitude of damping with respect to grip tightness. The following chapter will present experimental measurements of the racquet vibrational response during impact acquired from both hand-held and freely suspended states, to examine the effect of the hand grip on vibration damping. The variability of the tennis grip will be related to the change in the damping of racquet vibrations. For this purpose two methods will be used to determine the damping of tennis racquet vibrations in both the time and frequency domains. A comparison of the results obtained using the two methods will enable the variability of grip damping to be identified. Also, it will enable correlations with the gripping pressures (characterised in chapter 3), in order to describe the transfer of racquet vibration to the player's hand.

The levels of vibration damping will be compared for racquets A and B (which were analysed in chapter 2), in order to analyse the effectiveness of the built in piezoelectric damping system. The effectiveness of the racquet's piezoelectric damping system is assessed using the logarithmic decrement method, which describes the magnitude of decay of vibration over time. The rate of vibration decay is directly related to the damping ratio of the racquet and therefore can be used to rate the effectiveness of the

piezoelectric damping system, by comparing the response of a racquet with the piezoelectric element and a racquet without one.

A number of simple ball impact laboratory tests were conducted to acquire the relevant measurements of racquet oscillations with hand-held and freely suspended conditions. A comparison of the racquets vibrational response during tennis and golf ball impacts was also measured, to investigate the effect of ball dwell time. The measurements of the racquet's dynamic response during these impacts were required for the analysis of racquet vibration damping.

#### **4.1 Experimental set-up**

Racquet B, used for modal analysis in chapter 2, is used here to analyse the damping involved in the racquet-ball impact. Two ball types were used in ball impact tests (tennis and golf balls) to show the effect of their dwell time on the damping of racquet vibrations. A golf ball is used for comparison as it has a harder surface than the tennis ball and will deform less on the racquet string bed. The golf ball will therefore have a shorter dwell time on the racquet string bed and not dampen the same vibrations as the tennis ball.

The following instrumentation is used here to determine the vibrational response of the tennis racquet and allow for ball and grip damping to be analysed:

- 1 x PCB 352A25 accelerometer (mass, 0.48g)
- Polytec PSV-400 Junction box

- Polytec PSV modal analysis software (v8.3)
- Suspension string
- 1 x tennis ball (53.5grams)
- 1 x golf ball (45.9grams)

Both hand-held and freely suspended racquet set-ups were used experiments for the comparison of vibration responses. Figure 40 shows the complete set-up of the freely suspended racquet-ball impact experiment.

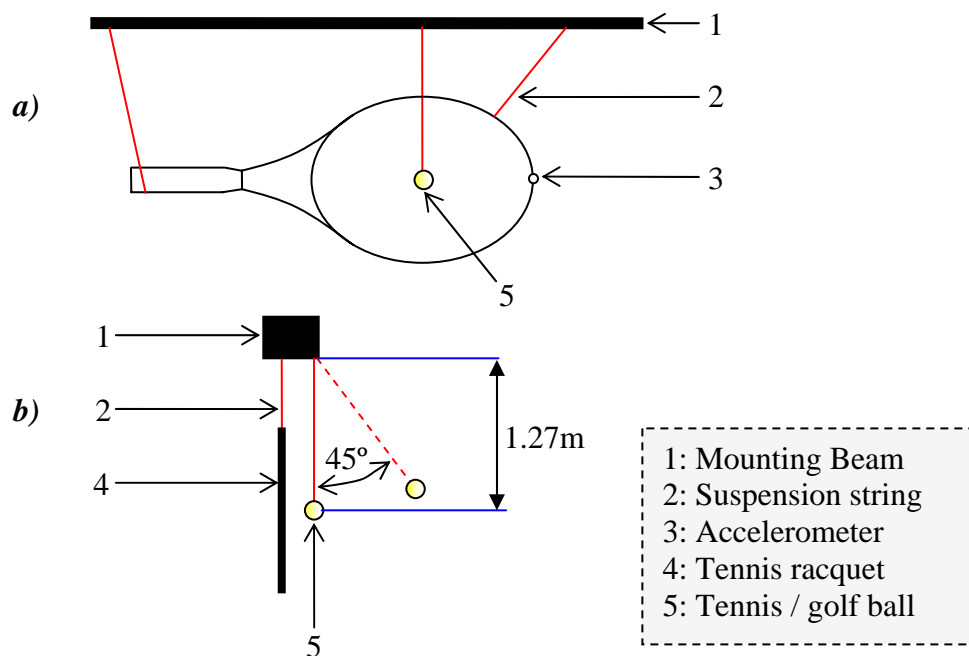


**Figure 40. Free suspension racquet-ball impact experiment: a) front view; b) side view**

Strings were used to suspend the racquet from a mounting beam to achieve the freely suspended condition (see figure 40). A miniature PCB accelerometer was attached to the racquet tip to measure the racquet's vibration response during impact. The accelerometer

is connected to a Polytec (Polytec, Germany) PSV-400 junction box, which is used as a signal amplifier and to also measure the accelerometer signal during impact. Polytec PSV modal analysis software was used to record the accelerometer signal. The PSV system is predominately used for modal analysis testing, however for this experiment it was utilised as a data acquisition system to record the vibrational response of the tennis racquet during impact. The data acquisition system was configured to a sample frequency of 2560Hz to allow for the first three bending modes (experimentally determined in chapter 2) to be analysed. The trigger function of the PSV data acquisition software was utilised and set to acquire data when the accelerometer signal reached 5% of its range (1V maximum). The sample time of the data acquisition was set to 0.8s.

In freely suspended tests, the tennis ball and golf ball were individually suspended using strings so that the impact of the ball is approximately at the centre of the racquet head. The ball was released approximately 45° from its vertical equilibrium and allowed to impact the racquet once. The hand-held racquet tests are based on the ball drop set-up devised in chapter 3, with the test subject's hand strapped to a mounting desk, as shown in figure 41. The tennis/golf ball was released from a resting state (using a vacuum to form a suction cup), to drop at the approximately the centre of the racquet head from a height of 0.5m. Again, the tennis/golf ball was allowed to impact the string bed only once.

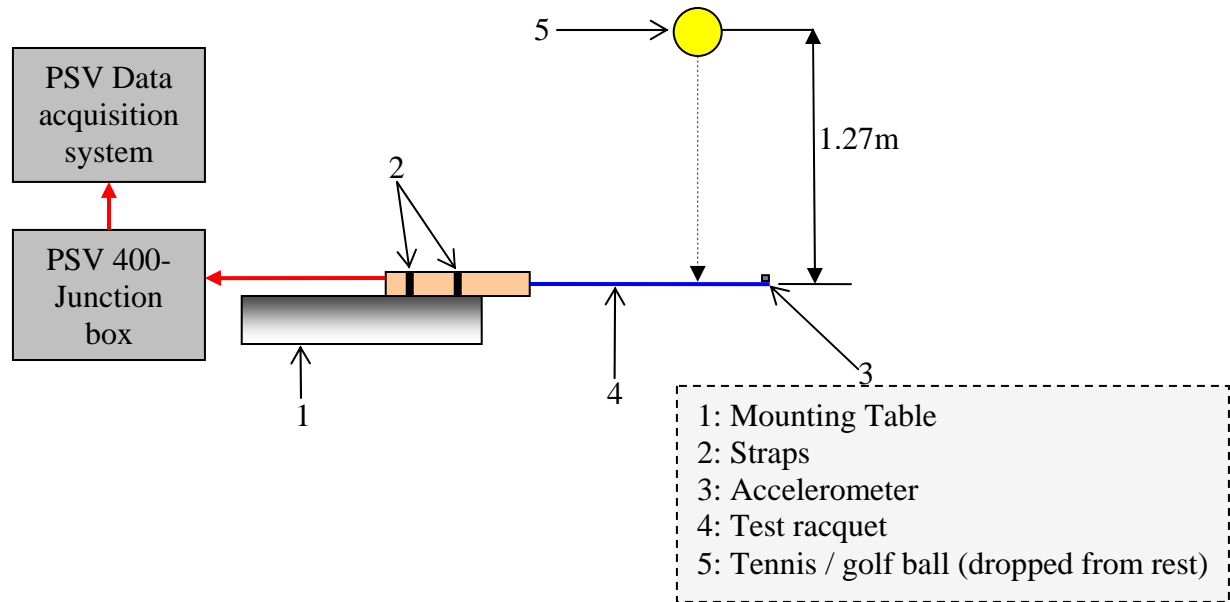


**Figure 41. Schematic diagram of hand-held ball drop test**

The aim of the experimental investigation was to determine the effect of both the ball and the tennis grip on the damping of racquet vibrations and to distinguish between the two effects. Five trials were carried out with the racquet in both freely suspended and hand-held conditions using the tennis and golf ball, using 1 test subject. (N.B. only one test subject was used to ensure a consistent grip for all trials. This would normally limit the results if the main objective was to investigate the gripping pressures. However, the main objective in this research is to investigate the dynamics of the tennis racquet and related them to the variations in tennis grip.) The tennis ball impact tests were then expanded to show the effect of subjective variable gripping tightness' on the damping of racquet vibrations. Five trials were conducted with the variable subjective gripping tightness' (ranked as light, medium and very tight gripping condition). In addition to this, the effectiveness of the piezoelectric damping system was evaluated by using the two racquets A and B in the free suspension racquet-ball impact tests.

## **4.2 Results and discussion**

The measurements obtained from the racquet-ball impact tests were firstly analysed in the frequency domain, by producing FFT spectrums, to show the effect of both the ball and tennis grip on the frequency response of the tennis racquet. The Fast Fourier Transform (FFT) was used to obtain a frequency spectrum (using acceleration response) for the tennis racquet with a resolution of 800 FFT lines. This was done for each of the measurements from the five trials and for each of the racquet conditions (golf and tennis ball impacts freely suspended racquet; golf ball impacts with hand held racquet; tennis racquet with light, medium and very tight ranked gripping tightness). The five obtained frequency responses were then averaged to give a single frequency response representative of the racquet's dynamic behaviour under the different gripping conditions. Figure 42 shows the frequency response of the freely suspended racquet for impacts with the golf and tennis balls.

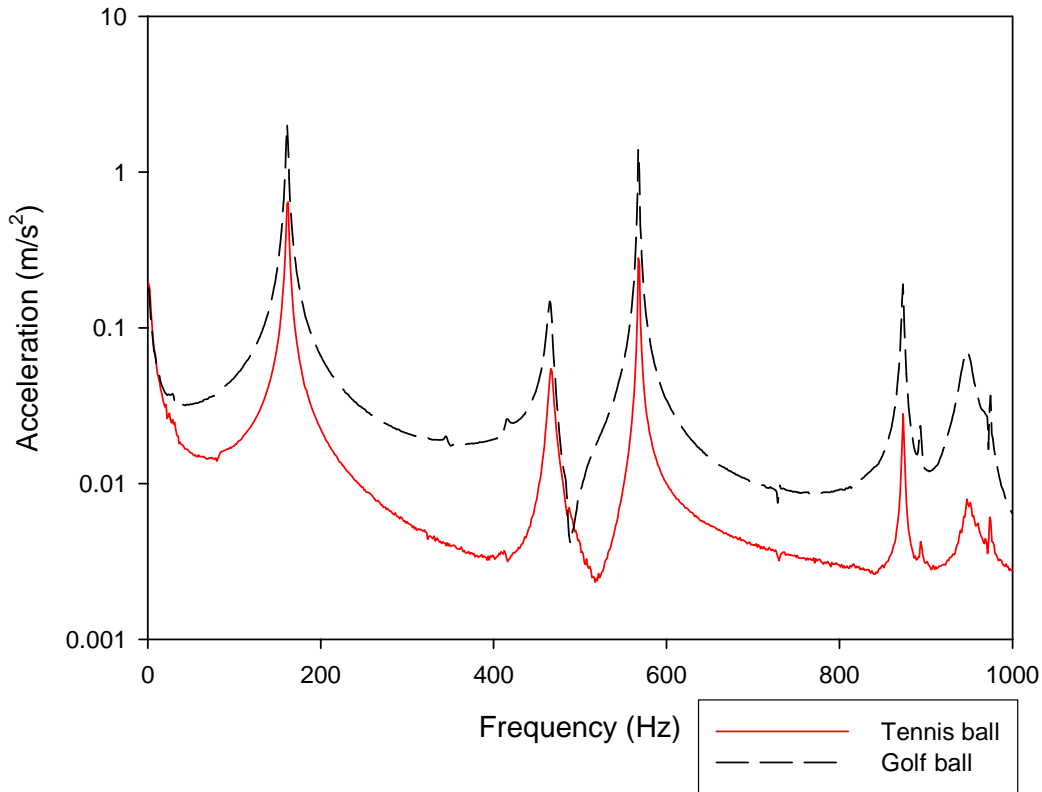
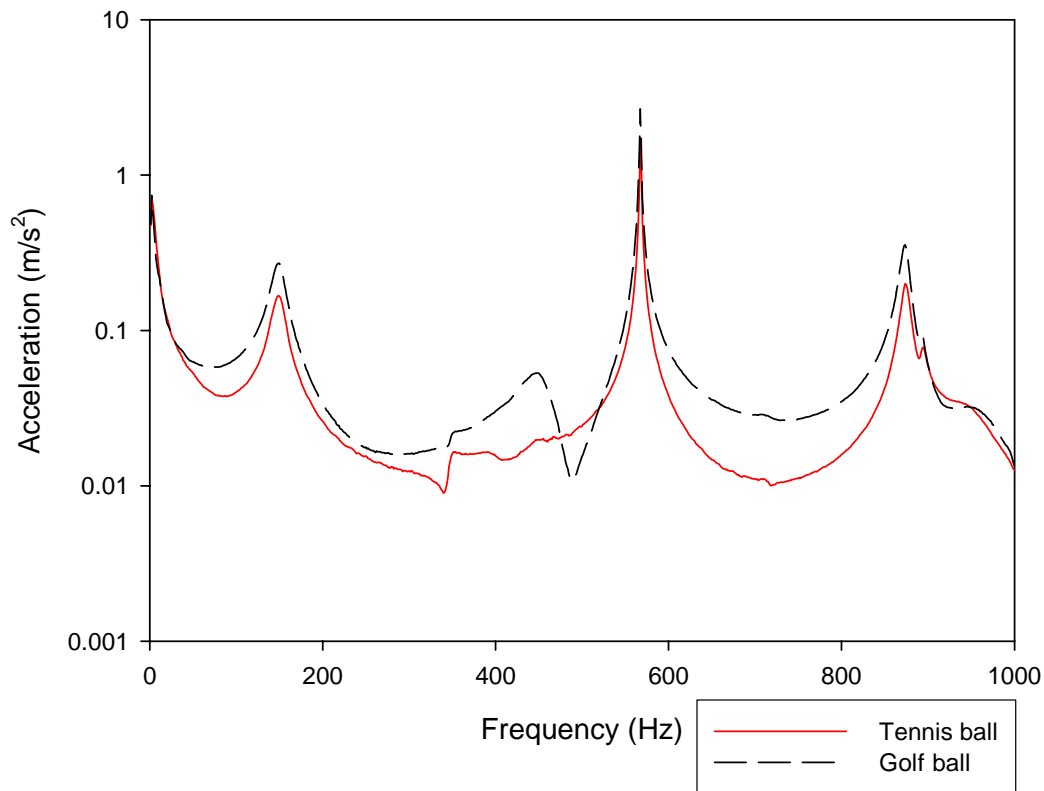


**Figure 42. Average frequency response of freely suspended tennis racquet (B) for tennis and golf ball impacts**

The frequency response results shown in figure 42 represent a calculated average from the FFT data involving each of the five trails for racquet B. Resonant peaks are clearly identifiable at approximately 161Hz, 466Hz, 576Hz, 875Hz for both the golf and tennis ball impacts. The resonant frequencies relate well to the modes of oscillation identified in chapter 2. The first (161Hz) and second (466Hz) bending modes identified in chapter 2 for racquet B are excited by both the golf and tennis ball impacts under freely suspended condition. However, there is a slight decrease in the natural frequencies measured in chapter two, 2 Hz decrease for the 1<sup>st</sup> mode and 4 Hz decrease for the second mode. This decrease has been brought about by the different excitation methods used for the two experiments. The modal analysis was carried out using an impact hammer to excite the frame. This method has a much shorter impact time than the tennis ball excitation used in

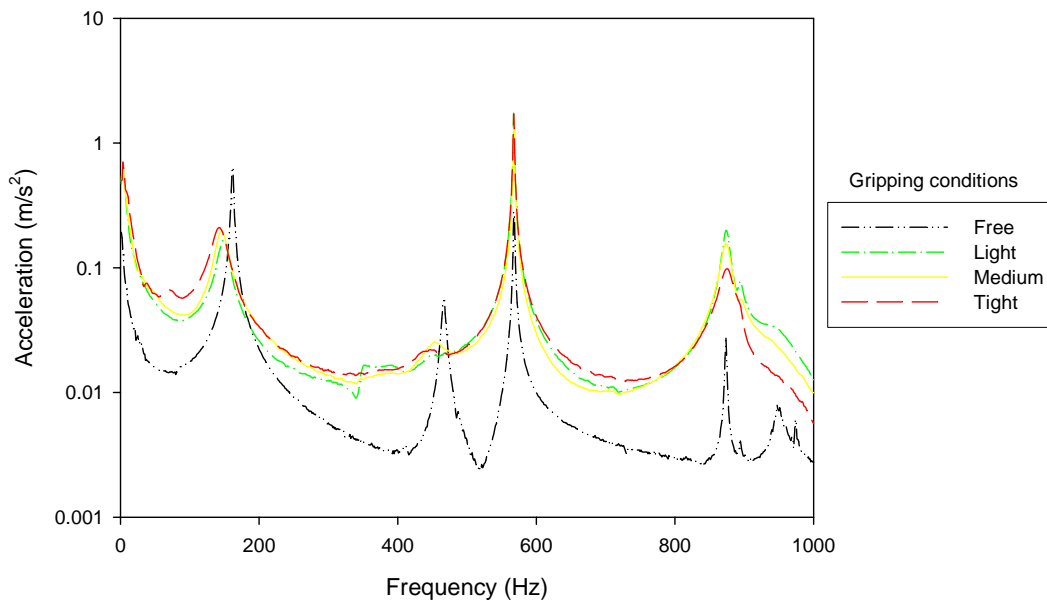
this experiment. The decrease in natural frequencies measured in this chapter can be associated with the additional damping (see equation (1.5)) brought about by the increased dwell time of the ball impact, as discussed in chapter 1 and will be discussed later in this chapter. It is also noticeable that the torsional mode identified in chapter 2 at approximately 348Hz is not excited in this experiment. The probable reason for this is that the ball impact location aligns with the centre line of the tennis racquet. An impact at this impact location will not excite the torsional mode measured in chapter 2 as the node line associated with this mode is at the same location.

Figure 43 shows the average frequency response of racquet B under hand held condition for golf and tennis ball impacts.



**Figure 43. Average frequency response of hand-held tennis racquet (B) for tennis and golf ball impacts**

The resonance frequencies identified for the freely suspended racquet are also excited under the hand held condition by golf ball impacts, but at slightly lower frequencies (157Hz, 453Hz, 576Hz and 873Hz). However, under hand-held condition involving tennis ball impacts, the second mode of oscillation identified in chapter 2 (453Hz) has been dampened to the extent that there is no identifiable resonance peak. This ball damping effect is also evident in figure 44.



**Figure 44. Comparison of racquet frequency responses for different gripping conditions**

Figure 44 shows the average frequency responses of racquet B with varying levels of grip tightness (ranked as freely suspended, light, medium and very tight grip). For these tests a tennis ball was used to impact the racquet. Two noticeable differences are shown between the freely suspended and hand-held racquets. Firstly the racquet's second mode is

drastically dampened in the hand-held racquet, and secondly the resonance frequency of the first mode decreases with increasing gripping tightness.

The second mode of oscillation (approximately 466Hz) is clearly identifiable in case of impact with the tennis racquet in a freely suspended condition. However, there is no corresponding resonance peak in case of impact with the racquet involving a light gripping condition. The second bending mode has been drastically dampened in case of impact with the hand-held racquet. A possible reason for this damping effect could stem from the reduction in racquet recoil generated by the introduction of the hand to the racquet system. With the racquet in freely suspended condition, the ball impact will generate racquet recoil (movement away from the ball). This reduces the dwell time of the ball as a consequence of the reduction in ball-string deformation during impact. A dwell time of approximately 0.005 seconds will damp the second bending mode of the racquet (Brody *et al.* 2002), but a shorter dwell time will excite this mode without such drastic damping. This effect of ball damping has not been observed in case of the freely suspended racquet, but in the case of the hand-held racquet the second mode is dampened because of an increased ball dwell time resulting primarily from a reduction in racquet recoil.

The investigation into the gripping characteristics during ball impact presented in chapter 3, described the dynamic interaction and pressure distribution between the racquet handle and the players hand. The measurements obtained were used to model the pressure profiles in the tennis grip, which demonstrated the direction of both the player's gripping forces and the distribution of racquet reaction forces across the handle. The results

showed that the player produces resistive forces across the racquet handle to maintain the required tightness of the grip in order to produce the desired rebound ball. The tightness of the grip determines the degree of racquet recoil and therefore the dwell time of the tennis ball on the string bed. The hand-held racquet has greater grip tightness than under freely suspended condition, and therefore there will be a greater magnitude of ball and string bed deformation. Analysis of the frequency responses of both hand-held and freely suspended gripping conditions has revealed that damping by the ball (ball damping) of the racquets second mode of oscillation, only occurs under hand-held conditions. Ball damping only occurs in hand-held racquets due to the reduction in racquet recoil.

The propagation of vibration waves from the ball impact location to the racquet boundaries takes place irrespective of the gripping conditions. The degree to which the modes of oscillation are excited depends on the gripping conditions and their effect on the racquet recoil. If the racquet is allowed to recoil, the dwell time of the ball on the racquet string bed will not be sufficient to dampen the racquet's second bending mode of oscillation due to wave propagation properties. The introduction of the hand to the racquet system, in the form of the tennis grip, provides resistance to racquet recoil and therefore increases ball dwell time. The increase in ball dwell time results in the damping of the racquet's second mode as the vibrations at the associated frequency will be reflected back to the impact location before the ball has left the string bed. Estimations for the damping of all vibrations are calculated later in the chapter.

The results of the ball impact tests have also shown that there are resonant peaks present in the racquet's frequency response, which are higher than the damped second mode of

oscillation. These modes can be attributed to either torsional modes of oscillation or the vibrations of the strings themselves (Brody *et al.* 2002). The ball does not cover all stings on the racquet head and therefore their individual modes of oscillation will not be dampened by the mass of the ball. Most research to date has shown that frequencies less than 200Hz are thought to be the most influential in the instigation of upper extremity discomfort (Reynolds *et al.* 1977). Therefore, this research will focus on the behaviour of the 1<sup>st</sup> mode of oscillation (which is excited regardless of the gripping conditions), and the level to which it is dampened by the player's hand with respect to grip tightness. Figure 44 showed there to be a noticeable decrease of the racquets first resonance peak (approximately 162Hz) generated by the tennis grip tightness. This decrease in resonance frequency can be used to estimate the level of damping inflicted by the grip.

The major difference between the freely suspended and hand-held racquets, with respect to the first mode of oscillation, is in the peak frequency and width of the resonant peak. The peak resonant frequency for the racquet hand system decreases from 162.5Hz in the freely suspended condition to 148.75Hz for the lightly gripped racquet.

Equation (1.5) is used to calculate the damped natural frequency ( $\omega_d$ ). If we consider the first natural frequency of the tennis racquet (162.5Hz in this case) the damping associated with its vibrational response will determine the frequency of oscillation (Rao 1995; Meriam and Kraige 1993).

$$\omega_d = \omega_n \sqrt{1 - \zeta^2} \quad (1.5)$$

$\omega_d$  is 148.75Hz in this case, which provides an indication of the damping generated by the tennis grip. Figure 44 shows the change in  $\omega_d$  with respect to subjective increases in gripping tightness.

Looking at figure 44, the resonant peak observed in the first mode of oscillation at approximately 162.5Hz (freely suspended) can be clearly seen in the frequency response of all gripping conditions. The frequency response of the racquet under different gripping conditions shows that with an increase in gripping tightness there is a general decrease in the magnitude at the resonant frequency of the racquet for the first mode of oscillation. The resonant frequencies observed in the racquet's frequency spectrum are shown in table 8 for racquet A and table 9 for racquet B. The tables represent the summary based on the average response spectrum of the tennis racquet. Full analysis of each trail is given in Appendix 4.

Table 8 shows an analysis of the response parameters for racquet A in the case of tennis ball impact, and table 9 shows the same parameters for racquet B. The damping for each of the modes and grip types has been estimated using the half-power bandwidth method (or Quality Factor ( $Q$ )). (The full description and detailed calculation process of the half-power bandwidth method is given in Appendix 3.) The half-power bandwidth method determines the amplitude factor at the resonant peak to establish the damping at the given frequency. The peak frequency and the half-power points (see Appendix 3) are used to determine the associated damping. The half-power points are defined by the power

absorbed by the dampener (in this case the player’s hand) at the given frequency. Any change in the damping parameter will results in changes in the half-power points.

Microsoft Excel® was utilised to determine the peak frequency from the average frequency response for each gripping condition for each mode and the associated values required for the half power bandwidth damping estimation (i.e. half power points).

Gripping Condition	Mode 1		Mode 2		Mode 3		Mode 4	
	$\omega^1$ (Hz)	$\zeta$ (Q)	$\omega^2$ (Hz)	$\zeta$ (Q)	$\omega^3$ (Hz)	$\zeta$ (Q)	$\omega^4$ (Hz)	$\zeta$ (Q)
Free suspension	183.75	0.02041	500	0.01	573.75	0.00436	882.5	0.00425
Light	170	0.11029	(N/A)	(N/A)	573.75	0.00436	881.25	0.00851
Medium	165	0.12879	475	0.70263	573.75	0.00436	881.25	0.00993
Very tight	162.5	0.14615	(N/A)	(N/A)	573.75	0.00436	881.25	0.01135

**Table 8. Evaluation of response parameters of racquet A for tennis ball impacts**

Gripping Condition	Mode 1		Mode 2		Mode 3		Mode 4	
	$\omega^1$ (Hz)	$\zeta$ (Q)	$\omega^2$ (Hz)	$\zeta$ (Q)	$\omega^3$ (Hz)	$\zeta$ (Q)	$\omega^4$ (Hz)	$\zeta$ (Q)
Free suspension	162.5	0.02308	466.25	0.01609	567.5	0.00661	873.75	0.00286
Light	148.75	0.11765	(N/A)	(N/A)	567.5	0.00441	873.75	0.01288
Medium	146.25	0.1282	(N/A)	(N/A)	567.5	0.00441	873.75	0.0172
Very tight	142.5	0.15789	(N/A)	(N/A)	567.5	0.00441	873.75	0.02571

**Table 9. Evaluation of response parameters of racquet B for tennis ball impacts**

The second mode of oscillation has no identifiable peak in most cases which makes damping estimations difficult. A peak was identified in the second mode for lightly gripped racquet A, which gave an estimated of Q of 0.70263, indicating the degree to which the second mode is damped. However, because the resonance peak is indistinguishable in most cases and damping could not be calculated, the remaining

discussion will focus on the first mode of oscillation as these are the vibrations thought to cause the most discomfort for humans (Reynolds *et al.* 1977).

The results have shown that with an increase in gripping tightness there is a decrease in the observed peak at resonant frequency due to an increase in the associated damping. (N.B. The relationship between damped natural frequency and the damping coefficient is shown by equation(1.5).) In order to statistically analyse the relationship between the gripping conditions and the damping of the racquet's first mode of oscillation, each gripping condition was giving a grading (free: 1; light: 2; medium: 3; very tight: 4). Using this grading system for the gripping conditions, correlations are made between the damping of the first mode of oscillation and the gripping tightness. The correlations between the damping estimations (Q) and the grip tightness grade are shown in figure 45 for racquet A and figure 46 for racquet B respectively. Both figures include the correlation evaluation in terms of the *correlation coefficient, R-Squared and P-Value.*

Correlation Coefficient = -0.99757; R-Squared = 99.5146%; P-Value = 0.0024

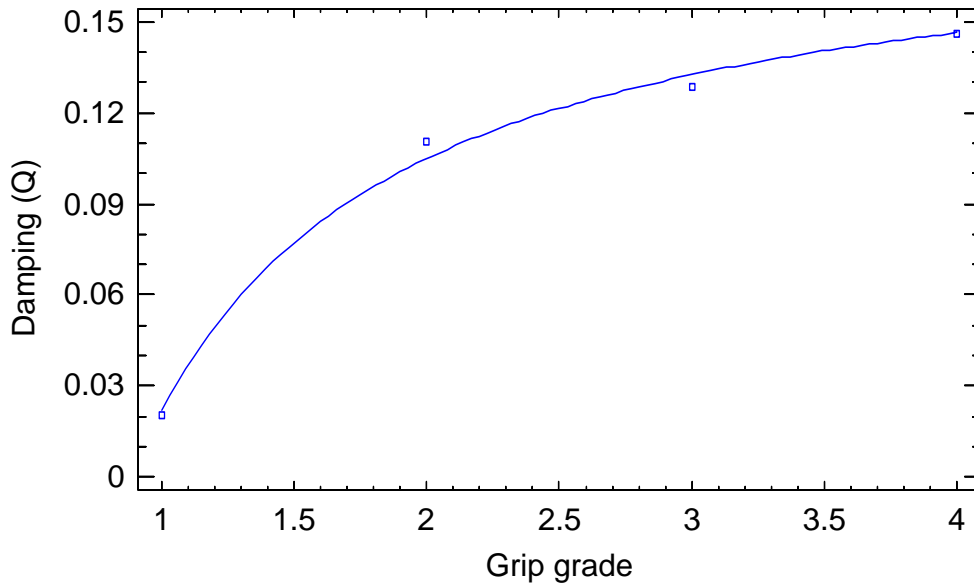


Figure 45. Damping and gripping correlations for racquet A

Correlation Coefficient = -0.990514; R-squared = 98.1118%; P-Value = 0.0095

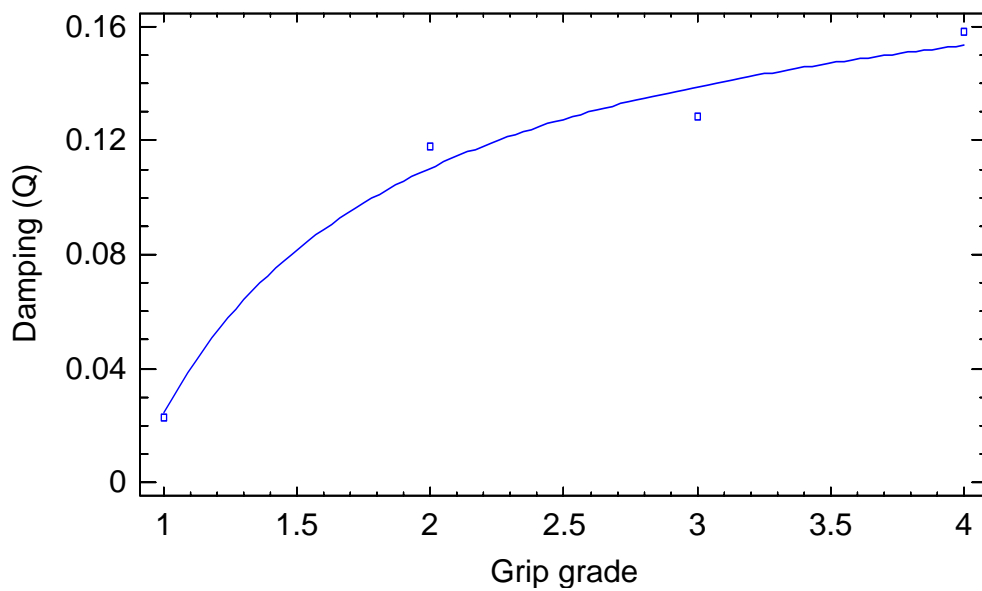


Figure 46. Damping and gripping correlations for racquet B

The correlations indicate a relationship (99%) between the change in gripping tightness levels and the damping of the racquet's first mode of oscillation. However, the correlation between the two parameters was found to be nonlinear. The best correlation between the two parameters involved a reciprocal of the gripping tightness, producing a curve fit with the following equation: (N.B The tennis grip has been subjectively graded in this experiment. This has resulted in a curve fit using only 4 data points. Despite these data points being based on 5 trials the experimental results are still limited in their validity. The results given in this section can therefore only be used as a subjective guide for analysing the relationship between racquet vibration damping and grip tightness. The analysis of the standard deviation of the racquets first mode (given in Appendix 4) shows the variability of each gripping condition. In order to reduce this variability in the analysis, quantification of the grip tightness is required to establish a more significant correlation with the damping of racquet vibrations. This provides the rationale for following chapters.)

$$y = a + b/x \quad (1.6)$$

Previous research has concluded that with an increase in gripping tightness there is a related increase in the rate of vibration decay (Brody 1987; Kotze *et al.* 2000; Hennig *et al.* 1992; Elliot 1982; Wilson and Davis 1995). The relationship between the increase in gripping tightness and vibration damping associated with the racquet's first mode of oscillation has been shown in this experimental investigation (using subjective gripping levels) to be nonlinear. This method of analysing the grip damping phenomena is applicable only to a certain extent as gripping tightness is not constant throughout impact.

If the tennis grip provided a constant racquet boundary condition (i.e. remain at the same gripping tightness level throughout impact) the damping estimates thus far can be used to establish the relationship between the parameters involved in the damping of racquet vibrations. However, chapter 3 that showed the tennis grip varies throughout the impact. With the change of the tennis grip, the damping of racquet vibrations will also vary during impact. This means that a damping estimation based in the time domain must be devised in order to assess accurately the variations in racquet damping in relation to the variations in gripping tightness.

The damping estimates ( $Q$ ) presented thus far, are based on the overall frequency response of the racquet during the entire data collection period. The half-power damping estimation is based in the frequency domain, which does not allow for monitoring of the change in damping parameters over time. The tennis grip is a variable parameter that has been proven to define the magnitude of racquet vibration damping. If correlations between the tennis grip tightness and the damping of racquet vibrations are to be made, then the changes in both of the parameters need to be monitored over time during impact. The half-power method cannot be used for this purpose as it is a frequency based damping estimation. By using a logarithmic decrement method, time reference damping estimations can be calculated.

#### ***4.2.1 Time based damping estimation***

Estimating vibration damping using a logarithmic decrement ( $\delta$ ) allows for the analysis of variations in damping in the time domain. Figure 47 shows the main parameters defining the rate of decay of vibration (Rao 1995; Harris 2002; Beards 1995).

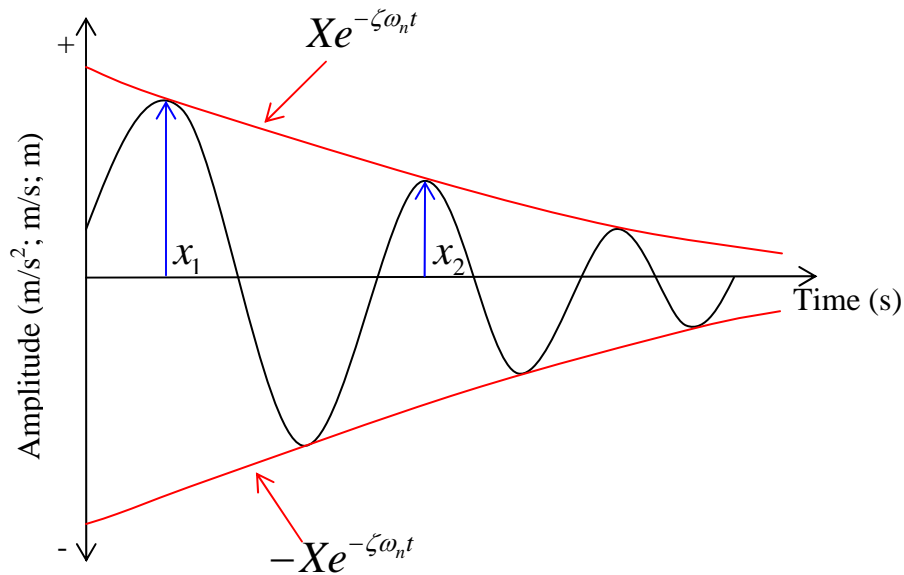


**Figure 47. Decaying vibration**

Figure 47 shows a decaying oscillatory motion in the time domain. The decay of vibration is shown by the lines connecting the peak amplitudes (envelope). The rate of this decay ( $X$ ) is a logarithmic parameter ( $e$ ), which is a function of the damping present in the system ( $\zeta$ ), the natural frequency of the vibration ( $\omega_n$ ) and time ( $t$ ). If damping is constant in the system then the exponential decay of vibration will be constant. However, the damping present in the tennis racquet system during impact is not constant, as shown in chapter 3, and therefore the decay of vibration will vary with time. Mapping the decay of vibration is achieved here using the logarithmic decrement.

Equation (1.7) defines the logarithmic decrement of the oscillating system with a natural frequency of  $\omega_n$ . The damped period of oscillation ( $\tau_d$ ) defines the time between the two successive peaks. It can be deduced from this equation that the variations in the

parameters defining the peak magnitudes will determine the logarithmic decrement of the oscillating system. The natural frequency ( $\omega_n$ ) will remain constant in a linear system and the damped period of oscillation is defined by the damping present in the system. Therefore, variations in damping (due to changes in the tennis gripping tightness in this case) will directly affect the logarithmic decrement. If the logarithmic decrement can be determined for the oscillating system then the associated damping can be estimated (Rao 1995; Inman 1994; Taylor 1994; Thompson 1993) as follows:

$$\delta = \ln \frac{e^{-\zeta\omega_n t_1}}{e^{-\zeta\omega_n (t_1 + \tau_d)}} \quad (1.7)$$

Equation (1.7) can be simplified as equation (1.8) to allow for the logarithmic decrement to be calculated using a vibration signal, where  $x_1$  and  $x_2$  are the magnitudes of the successive oscillation peaks.

$$\delta = \ln \left[ \frac{x_1}{x_2} \right] \quad (1.8)$$

The logarithmic decrement ( $\delta$ ) is defined as the natural logarithm of the ratio of any two successive peak magnitudes. Logarithmic decrement is an expression of the dynamic response of a vibrating structure based on the damping ratio for the specific mode of oscillation as shown in equation (1.9).

$$\delta = 2\pi\zeta \quad (1.9)$$

A rearrangement of equation (1.9) yields the damping ratio ( $\zeta$ ) as follows:

$$\zeta = \frac{\delta}{2\pi} \quad (1.10)$$

The logarithmic decrement is traditionally used for damping estimation of freely suspended structures. This estimation is based on the amplitude of successive peaks and the logarithmic relationship between them. The difference between the two peaks is related to the damping present in the system, as shown in figure 47. This method of estimating the damping present in a system has been applied in this research in order to allow for the decay of vibration to be mapped over time and to show the effects of variable gripping tightness on the level of damping over time.

The amplitudes of two successive peaks in the oscillation signal shown in figure 47 are defined as  $x_1$  and  $x_2$ . In order to map the decay of vibration and estimate the change in damping, both time and amplitude values for each peak must be identified precisely. The damped frequency of the oscillation ( $\omega_d$ ) defines the time between two successive peaks ( $\tau_d$ ). If the frequency of oscillation is 200Hz then the time between the two peaks is 0.005s. If the time and amplitude parameters can be identified, the logarithmic decay of vibration can be mapped over time, allowing for variations in damping to be shown.

As previously stated the decay of vibration depends on the frequency of oscillation and damping characteristics. If damping is constant the rate of decay should also be constant, assuming the structure is linear in nature. The logarithmic decrement calculated between peaks  $x_1$  and  $x_2$  should therefore be equal to the decrement calculated between

peaks  $x_2$  and  $x_3$ . Therefore the decrement between peaks  $x_1$  and  $x_n$  should be constant if the damping present in the system remains constant. However, in this research the damping varies throughout the duration of racquet oscillations as shown by the investigation into gripping pressure distributions. Therefore, the logarithmic decrement calculated between peaks  $x_1$  and  $x_n$  will not be constant. The mapping of the change in damping can be achieved by using the time at which peaks occur in a vibration signal. By using this time value, the changes in damping can be determined over time.

The expression for logarithmic decrement has been derived to describe characteristic variations in racquet damping over time, by using the subjective gripping tightness data presented in this chapter, as shown in the following equation:

$$\delta = \ln \left[ \frac{x_1}{x_2} \right] \quad (1.11)$$

The vibrations of interest in this research are related to the racquet's first mode of oscillation, as these are believed to be the major vibrations contributing to injuries such as tennis elbow (Reynolds *et al.* 1977). A post data collection filtering procedure was devised to isolate the racquet's first mode of oscillation and allow for accurate calculations of the logarithmic decrement, with respect to peak identification.

#### ***4.2.2 Signal processing***

The following signal processing was carried out on the raw vibration signal measured from the accelerometer using the frequency analysis software Autosignal (Systat

Software, USA). The software is capable of a processing data for different purposes depending on the requirements. Figure 48 shows the raw acceleration signal acquired from the tip of the tennis racquet during a service stroke. The explanation of the signal processing is based on this single impact acceleration signal.

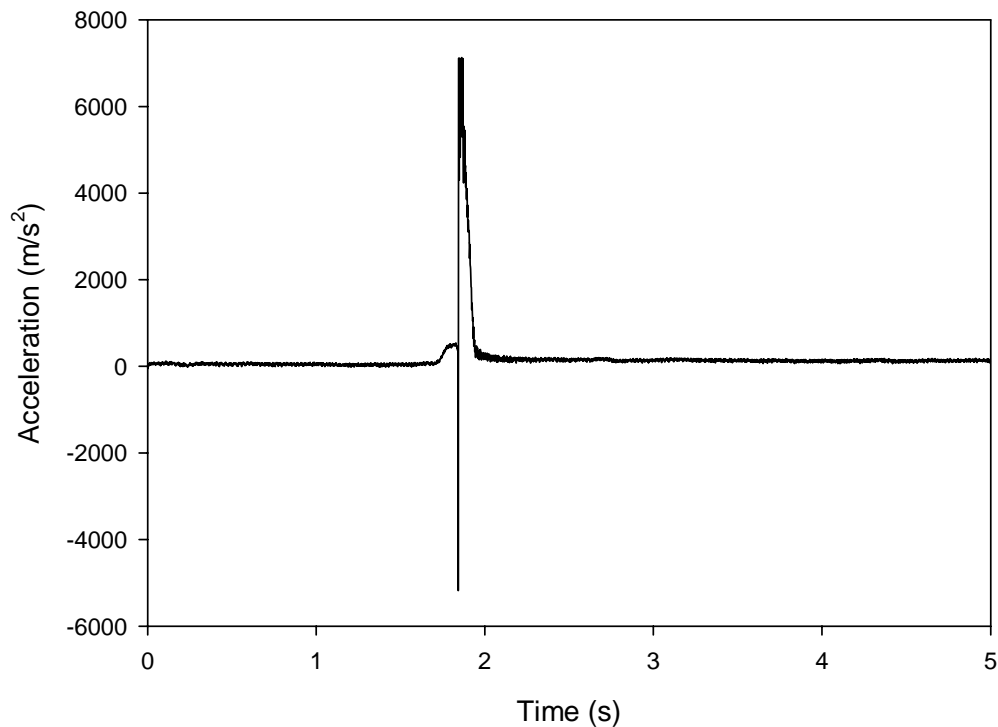


**Figure 48. Sample of raw acceleration data**

**1. Frequency filtering** - A Fourier based filter was used to isolate the frequencies in the 100-200Hz bandwidth. This bandwidth is associated with the racquet's first bending mode (identified in chapter 2), which is the frequency range of vibration that is thought to cause discomfort in tennis elbow sufferers (Brody 1987; Reynolds *et al.* 1977).

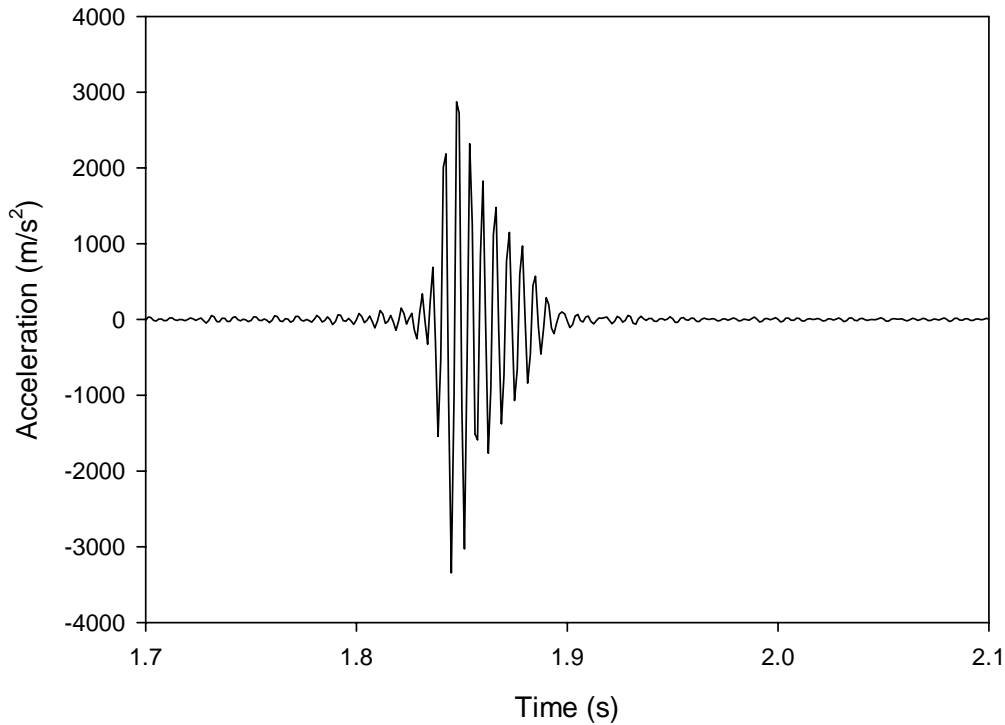


**Figure 49. Sample of acceleration data after frequency filtering**

Figure 49 shows the sample data after the frequency filtering process. The time axis was reduced in the sample to focus on the impact phase of the data and show the vibrations present. By isolating the vibrations in this specific frequency range, the decay of vibrations relating to the racquet's first bending mode can be determined using the logarithmic decrement as a damping function. It is important to understand the relationship between the racquets first bending mode and the grip tightness, as it is vibrations at this frequency that cause most discomfort to humans (Reynolds *et al.* 1977).

2. **Smoothing** – The noise present on the acquired data needed to be minimised in order to accurately measure magnitudes of oscillatory peaks in the time domain. Any noise present in the data can introduce error in the damping calculations due to potential misrepresentation of the oscillatory peaks. A Savitzky – Golay (1964)

smoothing filter was utilised to reduce the noise present in the measurements. This smoothing method is time-based and uses a least squares polynomial curve fit across a moving window.

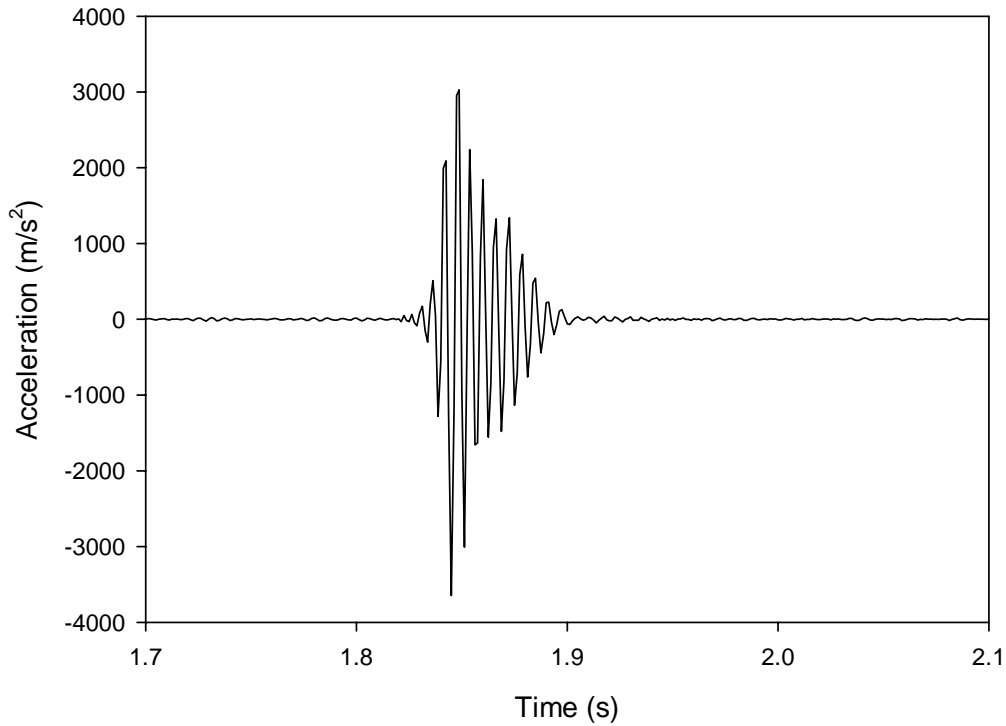


**Figure 50. Sample of acceleration data after smoothing (Savitzky and Golay, 1964)**

Figure 50 shows a sample of the data after the Savitzky – Golay smoothing process has been applied. However, the time based damping estimations are still not possible as the frequencies of interest have not been isolated. If oscillations at different frequencies to those of interest are present in the data then the misrepresentation of peak magnitude and time will introduce an error into the damping estimations.

Table 10 shows the logarithmic decrement calculations for the sample acceleration signal used in the previous signal conditioning (see section 4.2.2). The signal was acquired from

an accelerometer attached to the tip of the racquet during a service stroke. (N.B. Logarithmic decrement calculations have been carried out post-signal conditioning.) An Excel spreadsheet was utilised to estimate damping of the racquet's first mode of oscillation, based on the magnitude ( $m/s^2$ ) and time (s) of each of the oscillating peaks. The first peak ( $x_1$ ) was identified by determining the maximum magnitude of the entire 5 second data collection period. (The five second data collection period was used in chapter 3 during the quantification of grip pressure distribution. The time period was selected as a manual trigger was used. Five seconds was selected to ensure that ball impact occurs during the data collection period.) The maximum magnitude represents the point of impact and can be used for correlations with grip pressure variations in the time domain. The parameters of the oscillating peak (magnitude and time) were then used to yield logarithmic decrement and damping ratio values.

Peak	Peak magnitude ( $m/s^2$ )	Peak time (s)			
$x_1$	2775.993064	2.10875	<b>Peak Ratio</b>	<b>Log Dec (<math>\delta</math>)</b>	<b>Damp ratio (<math>\zeta</math>)</b>
$x_2$	2336.579767	2.115	$(x_1/x_2)$	0.17232	0.027422
$x_3$	1072.266788	2.12125	$(x_2/x_3)$	0.778913	0.123952
$x_4$	799.1227112	2.1275	$(x_3/x_4)$	0.294016	0.046788
$x_5$	529.768201	2.13375	$(x_4/x_5)$	0.411075	0.065416
$x_6$	380.8882735	2.14	$(x_5/x_6)$	0.329933	0.052504
$x_7$	415.2685546	2.14625	$(x_6/x_7)$	-0.08642	-0.01375
$x_8$	129.9496322	2.1525	$(x_7/x_8)$	1.161778	0.184879
	<b>TIME PERIOD (s)</b>	0.04375	<b>AVERAGE</b>	0.437374	0.069601
			<b>RANGE</b>	1.248198	0.198629

**Table 10. Logarithmic decrement calculations for a hand held racquet**

Peak	Peak magnitude (m/s <sup>2</sup> )	Peak time (s)			
$x_1$	5.605079421	0.01716	<b>Peak Ratio</b>	<b>Log Dec (<math>\delta</math>)</b>	<b>Damp Ratio (<math>\zeta</math>)</b>
$x_2$	5.383463344	0.02262	$(x_1/x_2)$	0.040341	0.00642
$x_3$	5.450662489	0.02769	$(x_2/x_3)$	-0.01241	-0.00197
$x_4$	5.165212319	0.03315	$(x_3/x_4)$	0.053791	0.00856
$x_5$	5.003725319	0.03861	$(x_4/x_5)$	0.031764	0.005055
$x_6$	4.682485895	0.04407	$(x_5/x_6)$	0.066354	0.010559
$x_7$	4.439874607	0.04953	$(x_6/x_7)$	0.053203	0.008466
$x_8$	4.216026262	0.05499	$(x_7/x_8)$	0.051733	0.008233
<b>TIME PERIOD (s)</b>		0.03783	<b>AVERAGE</b>	0.040683	0.006474
			<b>RANGE</b>	0.078759	0.012533

**Table 11. Logarithmic decrement calculations for a freely suspended racquet**

Table 10 shows the damping estimate of the racquets first mode of oscillation for a typical tennis stroke (i.e. hand-held). Table 11 shows the damping estimate of the same mode of oscillation but for a freely suspended racquet. The damping estimates in both tables can be used in a comparison of freely suspended and hand-held racquet vibrations.

The average logarithmic decrement ( $\delta$ ) over 8 consecutive peaks for the hand-held racquet was found to be 0.437374. This value equates to an average damping ratio ( $\zeta$ ) of 0.069601 during a 0.0437s time period. As previously stated, the tennis grip represents boundary condition for the racquet structure (i.e. the grip provides a source of vibration attenuation for racquet vibrations). As a result of tennis grip pressure being variable during impact, the damping of racquet vibrations will also be variable. Therefore, the average damping values can be used during impact, only for a freely suspended racquet. Table 11 shows the logarithmic decrement calculations for impact with a freely suspended racquet. A statistical comparison (ANOVA and F-test) of the two data samples was carried out using the statistical analysis software Statgraphics® (StatPoint, USA), to

show the differences between the two gripping conditions. The coefficient of variance for the damping ratio was found to be 94% for the hand held racquet, while the freely suspended racquet resulted in a variance of 63%. This indicates a strong consistency in the damping estimates between peaks  $x_1$  and  $x_8$  for the freely suspended racquet. However, in comparison, the hand-held racquet produces a more inconsistent damping estimate between the same peaks numbers. Box-plots of the hand-held and freely suspended racquet damping estimates are shown in figure 51. The box-plots show the variation in the damping ratio estimates between peaks  $x_1$  and  $x_8$ . The hand held racquet has an inter-quartile range 27 times greater than that of the freely suspended racquet (freely suspended, 0.09653; hand held, 0.003505). An F-test was also carried out on the two sample data sets to determine the differences between their standard deviations. The test indicated (at the 95% confidence intervals) that there was a statistically significant difference between the standard deviations of the two sample data sets. This means that there is a significant difference in damping estimates between successive peaks for hand held and freely suspended racquets.

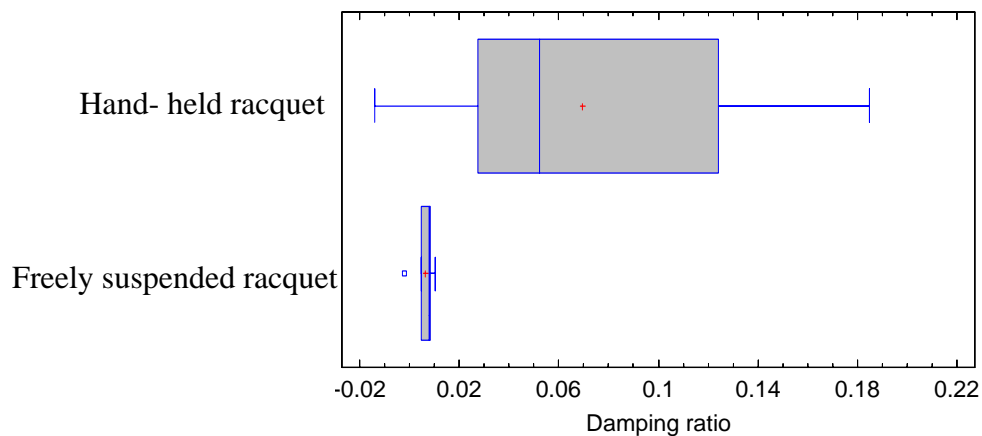


**Figure 51. Damping ratio box-plots for freely suspended and hand held racquets**

For a freely suspended racquet the damping present in the system should theoretically be constant as it is inherent to the racquet and no additional damping is added. In case of a hand-held racquet the damping estimates need to be mapped over time to show the changes in the damping present in the system. The hand produces variable damping of racquet vibrations due to the variations in gripping pressure (identified in chapter 3). The logarithmic decrement can be utilised to determine damping ratio, although the average logarithmic decrement expression of damping may introduce errors into any correlation with grip pressure, due to the variability of tennis gripping pressure.

#### ***4.2.3 Quantifying the effectiveness of the piezoelectric damping system***

The two racquets analysed in chapter 2, are used in this chapter to compare their effectiveness of dampening frame vibrations. As a result of only one of the racquets having the piezoelectric damping system enabled, the effectiveness of the system can therefore be quantified in the comparison. The acceleration data acquired for freely suspended racquet impact tests was filtered and analysed in order to determine logarithmic decrement and damping ratios for each racquet. Only freely suspended ball impact conditions can be used to estimate their effectiveness in the damping vibrations, because hand-held racquet will provide additional damping and therefore change the measured magnitude of vibration damping.

Due to the nature of the experimental set-up (i.e. freely suspended racquet) the average logarithmic decrement ( $\delta$ ) and damping ratio ( $\zeta$ ) values over the first 8 successive peaks were used to estimate the racquet's damping effectiveness. Table 12 shows the average  $\delta$  and  $\zeta$  for racquet A, while table 13 shows the damping values for racquet B.

<b>Trial</b>	<b>Logarithmic Decrement (<math>\delta</math>)</b>	<b>Standard Deviation</b>	<b>Damping Ratio (<math>\zeta</math>)</b>	<b>Standard Deviation</b>
1	0.039653	0.013488	0.00631	0.002146
2	0.043408	0.014117	0.006908	0.002247
3	0.046145	0.034781	0.007343	0.005535
4	0.042349	0.014149	0.006739	0.002252
5	0.040683	0.011997	0.006474	0.001909
<b>AVERAGE</b>	<i>0.0424476</i>		<i>0.0065</i>	
<b>ST DEV.</b>	<i>0.002526</i>		<i>0.000402</i>	

**Table 12. Logarithmic decrement and damping ratio of racquet A**

<b>Trial</b>	<b>Logarithmic Decrement (<math>\delta</math>)</b>	<b>Standard Deviation</b>	<b>Damping Ratio (<math>\zeta</math>)</b>	<b>Standard Deviation</b>
1	0.057241	0.019323	0.009109	0.0037075
2	0.059944	0.02109	0.009539	0.003356
3	0.057306	0.028325	0.009119	0.004507
4	0.05974	0.025321	0.009507	0.004029
5	0.06122	0.06122	0.009742	0.009742
<b>AVERAGE</b>	<i>0.0590902</i>		<i>0.0094</i>	
<b>ST DEV.</b>	<i>0.001753</i>		<i>0.000279</i>	

**Table 13. Logarithmic decrement and damping ratio of racquet B**

The average logarithmic decrement for racquet A was found to be 0.0424476 and for racquet B 0.0590902. These logarithmic decrements yielded damping ratios of 0.0065 for racquet A and 0.0094 for racquet B. Experimental modal analysis conducted in chapter 2 concluded that racquet B had 26% greater inherent damping of the first mode of oscillation than racquet A. The results of chapter 2 support the inherent damping estimates from impact tests carried out in this chapter, as racquet B has shown to have approximately 28% greater inherent damping of the first resonance than in racquet A. To support this finding, a statistical analysis of the difference between the inherent damping estimates, based on the first resonance of the two racquets, was carried out.

A statistical F-test was first carried out (StatPoint, USA) to show the difference of the standard deviations of the damping estimates for the two racquets. The test results showed no statistical difference in the standard deviations of the data sets (at the 95% confidence intervals) indicating that any comparison between the two racquets is valid. A statistical T-test was then carried out (StatPoint, USA) to show the difference between the means (average) of the two damping data sets. The test results showed  $t = -12.1026$  ( $p$ -value = 0.000) (at the 95% confidence interval) for the hypothesis of mean 1 does not equal mean 2. This shows that there is a statistical difference between the damping of racquet A and B and that the 28% effectiveness of the piezoelectric damping system is a valid estimation.

It was stated by the racquet manufacturer that the two racquets were equipped with piezoelectric damping capabilities. However, one of the test racquets had the piezoelectric damping system rendered inactive to allow for its effectiveness to be experimentally analysed. Modal analysis (conducted in chapter 2) is not an indication of the effectiveness of the racquet's damping system as the effect of ball impact was not considered. Modal analysis determines the natural frequencies, associated modal damping and mode shapes. Averaging of single point measurements in modal analysis does not allow for the response of the racquet to be assessed in terms of individual impacts/ excitations. Only the analysis of single response measurements during impact can determine the racquets inherent damping during impact. Therefore dynamic response analysis of the racquet using single impacts/excitations is not possible with the modal analysis measurements as they are based on structural excitation with an impact hammer or shaker and not a ball impact. The response of the tennis racquet needs to be measured

for a single impact, as conducted in this chapter, in order to determine effectiveness of the racquet's piezoelectric damping system.

Similarly, the hand held racquet cannot be used to measure the effectiveness of the piezoelectric damping system due to the influence of the grip on the dynamic response of the racquet. However, freely suspended racquet- ball impacts provide a good estimate of the piezoelectric damping systems effectiveness. The freely suspended racquet ball impact experimental set-up generates a dynamic response of the racquet using an appropriate excitation (i.e. a tennis ball), which is not influenced by any variable boundary conditions (i.e. the tennis grip). The decay of the racquets vibration after the impact with the ball can be mapped and the difference in the measurements will be a valid indication of the piezoelectric damping systems effectiveness. This valid method has been used in this chapter to show that racquet B dampens vibrations at the racquets first resonance 28% more than racquet A. Therefore, it can be concluded that racquet B has the piezoelectric damping system enabled, while racquet A has it disabled.

### **4.3 Conclusions and significance**

The experimental investigation conducted in this chapter has provided results showing the parameters defining the damping of racquet vibration, and the effect of their variability. The effect of the ball's dwell time on the string bed has been experimentally measured using freely suspended and hand held racquets using golf and tennis ball impacts. The addition of the tennis grip to the racquet system limits the recoil of the racquet which in turn generates an increase in the dwell time of the ball on the string bed. The increase in ball dwell time gives rise to drastic damping of the racquet's second

bending mode of oscillation ( $\zeta = 0.70263$ ). This provides further rationale for focusing the investigations on the racquet's first mode of oscillation, as vibrations at this frequency are those which are felt by the player. The first mode of oscillation in hand-held racquets (i.e. 100-200Hz) is thought to generate the greatest amount of discomfort to sufferers of upper extremity injuries such as tennis elbow (Brody 1987; Reynolds *et al.* 1977). The second bending mode of oscillation is drastically damped by the tennis ball and therefore is of little concern regarding the aggravation of tennis elbow.

The half power (Q) damping estimate has been used to determine the effects of grip tightness variations on the damping of the racquet's first bending mode. Despite the grip tightness being quantified in a subjective manner, correlations were established with the damping of racquet vibrations. (N.B. The statistical analysis of the gripping tightness is a subjective guide because only 4 data points have been in the analysis. The correlations given by the analysis will need to be confirmed using more data points in the following chapters with quantified grip tightness.) The best correlation fit was determined to have a non-linear relationship, with the correlation being a reciprocal of the gripping tightness. The nonlinear correlation yielded  $R^2$  values greater than 99% with p-values less than 0.005. It was shown that with a very tight tennis grip, the damping of racquet vibrations was estimated to a damping ratio ( $\zeta$ ) of 0.14615.

The two racquets (A & B) were compared using logarithmic damping estimates, to assess the effectiveness of the piezoelectric damping system incorporated into their design. The damping estimates for both racquets were calculated using the average logarithmic decrement across eight peaks of the racquet's first resonant frequency from a ball impact

excitation of a freely suspended racquet. The results showed that statistically (to the 95% confidence interval) that racquet B was 28% more effective in damping the vibrations of the racquet's first resonant frequency, than racquet A. Based on the experimental analysis it was concluded that racquet B had the active piezoelectric damping system and racquet A had the inactive system. However, it should be noted that this conclusion was not confirmed by the manufacturer and is solely based on the experimental results.

The 28% improved inherent damping of vibrations relating to the racquet's first mode of oscillation has been determined in this research using freely suspended racquets. However, in-order for the damping system to provide a tennis player with reduced vibration absorption, there must be a significant change in the hand-held racquet vibrations.

Due to the player's hand generating far greater vibration attenuation (grip damping) than the piezoelectric system on the racquet (as shown in the hand held test results in figure 51), the effect of the piezoelectric system on racquet vibrations was indistinguishable under hand held conditions. If we consider the estimated logarithmic decrement of the racquet under freely suspended (approximately 0.05) and hand-held (approximately 0.44) conditions, the hand increases vibration attenuation by 880%. With such a great increase in damping generated by the player's hand, the increase in inherent damping by the piezoelectric system is negligible and therefore ineffective when used in its practical manner.

The additional source of racquet vibration attenuation provided by the tennis grip results has been shown as highly subjective depending on the individual player, ball speeds and impact location on the racquet head. Due to the variability of grip damping, the effectiveness of inherent racquet vibration attenuation is indistinguishable under hand held conditions. This proves that the piezoelectric damping system of the tennis racquet is ineffective under hand-held conditions. If future racquet damping systems are to be effective vibration attenuators in practice, they must have an inherent logarithmic decrement similar to that of a hand-held racquet. This would result in a decrease in the magnitude of vibration absorption by the player.

## **Chapter 5**

### **The effect of grip pressure distribution on racquet frame vibrations damping**

Previous chapters have established grip pressure distribution characteristics together with quantification of the relationships between subjective (i.e. non-quantified) grip tightness' and the associated damping of racquet vibrations. This chapter aims to build upon this knowledge by establishing correlations between quantified grip pressures and the damping of racquet frame vibrations (grip damping). By using the data acquired in chapters 3, grip pressure magnitudes in the time domain along with their distribution across the racquet handle can be related to the magnitude of racquet vibration damping. By correlating these parameters (i.e. grip pressure and racquet vibration damping) the levels of vibration transfer to the player can be estimated in terms of the energy absorbed by the player's hand. The overall objective of this chapter is to identify and characterise the effect of grip pressure distribution on the level of tennis racquet vibration damping. In order to describe the mechanics of the transfer of vibration to the player, the specific objectives of this chapter are as follows:

- Relate the magnitude of grip pressure to the magnitude of the racquet's logarithmic decrement
- Relate the distribution of grip pressure across the racquet handle to the logarithmic decrement of racquet vibrations
- Describe the effects of grip damping mechanics and relate them to the tennis player in terms of performance and injury

By achieving these objectives, the mechanics of racquet vibration transfer to the player's hand via the tennis grip can be quantified. By quantifying this transfer of vibration to the

player, vibration attenuation devices can be optimised by incorporating knowledge of the grip damping phenomena in future designs.

### **5.1 Establishing correlations between grip pressure and racquet vibration damping**

Frequency response curves given in this thesis are stated in terms of acceleration ( $m/s^2$ ). However, the important vibrations regarding the players “feel” of the racquets response are defined in terms of displacement. Vibrations at high frequencies may have large magnitudes of acceleration, but with respect to magnitude of displacement there is an exponential relationship between displacement and frequency response, as shown in equation(1.12) (Griffin 1998). Therefore, the magnitude of racquet displacement at the higher frequencies will be far less than that of lower frequency vibrations for the same acceleration.

$$A = (2\pi\omega)^2 D \quad (1.12)$$

Where:

D= Displacement (m)

A= Acceleration ( $m/s^2$ )

$\omega$  = Frequency (Hz)

Displacement of the racquet handle at the racquet’s fundamental frequency is thought to cause the instigation and aggravation of tennis elbow, although no clinic evidence supporting this belief currently exists. Greater racquet displacement equates to a greater

racquet energy, which will therefore be absorbed by the player's hand. However, in order to quantify the relationship between racquet vibrations and grip damping, the use of acceleration as a measure of the racquets frequency response is applicable as relative values regarding the absorption of racquet energy by the player are not under investigation. Moreover, describing grip damping in terms of acceleration is an applicable approach due to the linear relationship between displacement and acceleration (assuming pure translation). The absolute magnitude of racquet energy absorbed by the tennis player is not under investigation in this thesis, therefore the exponential relationship between displacement and frequency (see equation(1.12)) is not considered. However, describing the relationship between grip pressure distribution and racquet vibration damping using acceleration as the measure of frequency response is an applicable approach for model development.

Measurements of grip pressure distribution and racquet vibrations during the impact acquired in chapter 3; have been used in this chapter to analyse the relationship between the two parameters. The decay of vibration, using the magnitude of acceleration ( $m/s^2$ ) with respect to the racquet's first resonance, has been mapped using logarithmic decrement. Five successive peaks were used to show the decay of vibration from the maximum magnitude to the point at which the oscillations have completely diminished. The time period identified for the five peaks was then used to calculate grip pressure data for the same period.

Grip pressure measurements were acquired using the same data acquisition time scale as racquet vibration measurements. Measuring the grip pressure and racquet vibrations

together allows for magnitudes of grip pressure and vibration to be calculated on the same time scale. Using the time of each racquet oscillation peak, pressure values at the corresponding time were calculated. This method allows for magnitudes of vibration and grip pressure to be determined for the same moment in time during impact. By defining the magnitude of grip pressure ( $\text{N}/\text{cm}^2$ ) and racquet vibrations ( $\text{m}/\text{s}^2$ ), relationships between the two can be established. Figure 52 shows how magnitudes of grip pressure and racquet vibration were determined. A sample oscillation signal in the time domain is shown with the corresponding grip pressure measurement (N.B. the grip pressure shown is the summation of all the individual hydrocell pressure measurements on the racquet handle).

It should also be noted that only racquet A was used for grip damping correlations in this chapter. Justification for this is based on the different inherent damping properties the racquets demonstrated (see chapter 4). In order for the grip damping correlations to be viable, the inherent damping of the racquet used must remain constant. Therefore racquet A (deemed in chapter 4 to have the inactive piezoelectric damping system) was used when relating the grip pressure to the damping of racquet vibrations. All related data shown in this chapter is taken from racquet A.

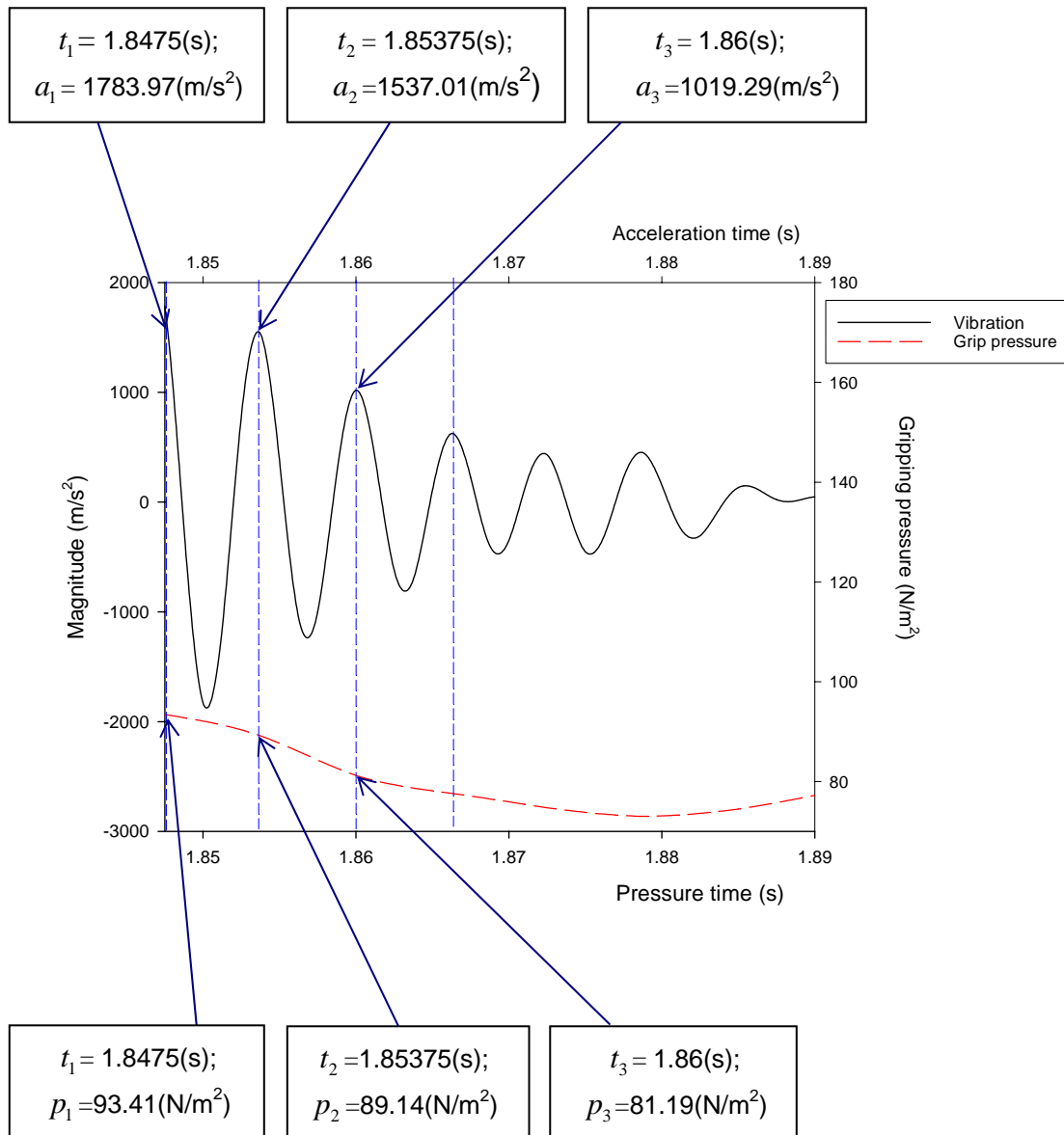


**Figure 52. Definition of vibration ( $a$ ) and pressure ( $p$ ) peak parameters**

The time ( $t$ ) and acceleration magnitude ( $x$ ) parameters for the vibration signal determined from the data shown in figure 52, are shown together with the corresponding pressure measurement ( $p$ ) in table 14. The measurements shown were used to quantify the parameters a) logarithmic decrement and b) the average grip pressure over the same period of time as used for the logarithmic decrement estimate. By using these two

parameters relationships between them can be identified allowing for the damping of racquet vibrations by the tennis grip (grip damping) to be quantified.

<b>Peak time <math>t</math> (s)</b>	<b>Acceleration <math>x</math> (m/s<sup>2</sup>)</b>	<b>Grip pressure <math>p</math> (N/cm<sup>2</sup>)</b>
1.8475	1783.97	93.41
1.85375	1537.01	89.14
1.86	1019.29	81.19
1.86625	624.72	77.60
1.8725	430.22	74.71
1.87875	451.55	73.03
1.885	132.71	74.47
1.89	47.51	77.21

**Table 14. Vibration and pressure measurements used for grip damping correlations**

Chapter 3 established the variability of tennis grip pressure during impact with respect to its distribution across the racquet handle. Chapter 4 established that the change in grip pressure generated a change in the damping of the racquet frame vibrations. However, due to the changes in the distribution of grip pressure across the racquet handle during impact, correlations using logarithmic decrement estimates based on successive peaks may not yield accurate grip damping correlations. This is due to the application of grip pressure at different magnitudes and at different locations on the racquet handle.

As previously stated, the five peaks succeeding the maximum were used to calculate the logarithmic decrement of the vibrations at the frequency corresponding to the racquet's first bending mode. By analysing the vibration measurements it was determined that

vibrations associated with the racquet's first natural frequency, had diminished after approximately five oscillations (depending on the magnitude of grip pressure). Therefore, logarithmic decrement estimates were based on the first five oscillation peaks of the racquet's vibrational response.

The estimated logarithmic decrement was used to show the decay of racquet vibrations at the first natural frequency. Equation (1.13) defines the relationship between damping (logarithmic decrement  $\delta$ ) and the logarithmic ratio of two successive peak magnitudes,  $x_1$  and  $x_2$ :

$$\delta = \ln \left[ \frac{x_1}{x_2} \right] \quad (1.13)$$

As previously explained the variability in the application of grip pressure on the racquet handle, consequently limits the application of this equation to the present investigation. However, equation (1.14) allows non-successive peak magnitudes to be used to estimate damping:

$$\frac{x_1}{x_{m+1}} = \frac{x_1}{x_2} \frac{x_2}{x_3} \frac{x_3}{x_4} \dots \frac{x_m}{x_{m+1}} \quad (1.14)$$

If equation (1.14) is used to determine the decay of vibration at the racquets first natural frequency ( $\omega_n$ ), the integer ( $m$ ) must be included into the equation defining the oscillatory motion, as shown in equation (1.15):

$$\frac{x_m}{x_{m+1}} = (e^{\zeta\omega_n\tau_d})^m = e^{m\zeta\omega_n\tau_d} \quad (1.15)$$

Where:

$x$  = magnitude of acceleration at denoted peak

$m$  = integer

$e$  = base of natural logarithms

$\zeta$  = damping ratio

$\omega_n$  = natural frequency

$\tau_d$  = damped period of oscillation

The integer ( $m$ ) included in equation (1.15) is used in the calculation of the logarithmic decrement, providing the required factoring of the estimate needed resulting from the inclusion of multiple peaks. Incorporating the integer ( $m$ ) into equation (1.13) yields equation (1.16):

$$\delta = \frac{1}{m} \ln \left[ \frac{x_1}{x_{m+1}} \right] \quad (1.16)$$

Equation (1.16) yields a damping estimate in the time domain based on a specified number of peaks. Equation (1.17) is used for the calculation of the logarithmic decrement by applying the integer method, shown in equation (1.16), to the measurement data given in table 14. The calculation is based on peak magnitudes  $x_1$  and  $x_6$  which provides an integer of 5.

$$\delta = \frac{1}{5} \ln \left[ \frac{1783.97}{451.55} \right] = 0.2 \times \ln [3.95077] = 0.27478 \quad (1.17)$$

The logarithmic decrement estimate is based on the integer ( $m$ ) which represents a time period  $x_1$  through  $x_6$ , which can now be used to calculate grip pressures at the corresponding time intervals.

### **5.1.1 Data Exclusion**

The exclusion of certain trials was required to ensure reliable logarithmic decrement damping estimates. Vibrations at the racquets first resonance, which corresponds to its first mode of oscillation, are used to estimate logarithmic decrement. Therefore impact at the node (“sweet spot”) of the associated mode shape would not excite vibrations at this frequency (Brody 1981; Brody *et al.* 2002; Kotze *et al.* 2000) and therefore logarithmic decrement estimates are not possible. This provides a basis for exclusion of certain impact trials. The criterion for the exclusion of certain impact measurements was based on the racquets frequency response, which identifies the resonance frequencies.

Impact at the nodal “sweet spot” was identified by analysing the measured vibration response of the tennis racquet in the frequency domain. Figure 53 shows the frequency response of two separate ball impacts using the same racquet in a forehand stroke. The figure shows the frequency bandwidth of interest corresponding to the racquet’s first bending mode of oscillation (100-200Hz).

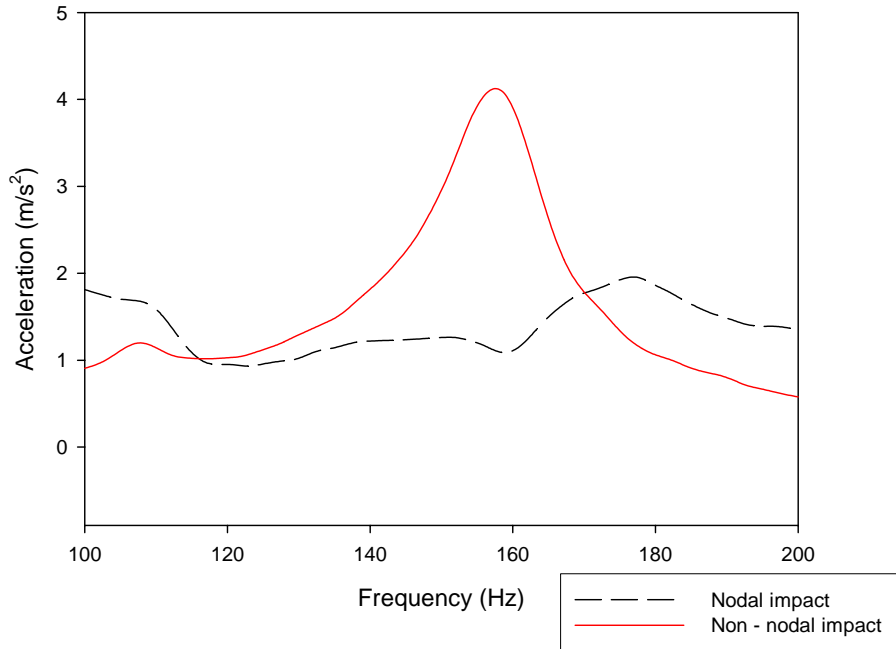


**Figure 53. Frequency response of a tennis racquet with nodal and non-nodal impacts**

Figure 53 shows the frequency responses for two different ball impacts using the same racquet. The impact exciting the resonance peak (approximately 160Hz) can be attributed to a ball impact that does not align with the node of the racquet's first mode. The second frequency response shown in figure 53 has no resonance peak at the corresponding frequency. A ball impact generating this type of racquet response is attributed an impact locations aligning with node of the racquet's first mode. Measurements of racquet vibration during impact displaying no identifiable resonance peak were excluded.

By using the measurements that include the excited racquet's first mode of oscillation, corresponding grip pressure can be estimated. The integer between the two peaks of the vibration measurement used for the logarithmic decrement calculation was also used to establish the relevant magnitudes of the grip pressure. The vibration magnitudes ( $m/s^2$ ) of

peaks  $x_1$  and  $x_6$  were used to estimate the logarithmic decrement estimation and therefore the corresponding pressure magnitudes  $p_1$  and  $p_6$  were used to estimate the grip pressure ( $\text{N}/\text{cm}^2$ ). Grip pressure was estimated by calculating the average between  $p_1$  and  $p_6$ . The sample data set given in table 14 yielded an average pressure magnitude of  $81.51 \text{ N}/\text{cm}^2$ . This example of grip pressure approximation is based on the sum of all the hydrocell pressure measurements acquired in the data acquisition. However, the assumption that pressure estimates based on the pressure distribution across the whole racquet handle will influence the damping of frame vibrations is inaccurate. The application of pressure at relevant locations will have a variable effect on the damping of frame vibrations due to the mode shape of the racquet at the frequency of interest. Defining appropriate pressure measurements related with the damping of racquet vibrations was based on the racquet's mode shape associated with the first resonant frequency.

### ***5.1.2 Defining an appropriate grip pressure***

Not all grip pressure measurements acquired in chapter 3 are applicable with respect to the damping of vibrations at the racquet's first resonant frequency. Pressure applied to the racquet handle out-of-plane from the racquet oscillations will have negligible effects on the damping of the vibrations at the associated frequency, because the racquet is hand-held and the damping associated with the shear type resistance to the racquet movement will be minimal. Therefore, only measurements of pressure in the same plane as the racquet's oscillatory motion at the frequency of interest should be included in the calculation of damping due to the tennis grip effect. (N.B. The author recognises that frictional damping may occur in the tennis grip. However, this research will focus on the

damping associated purely with the changes in grip pressure. Analysis of frictional damping within the tennis grip would be complex due to the many different materials used in the test procedure. The coefficient of friction for the tennis grip would be difficult to determine from the current measurements. Further experiments are required to quantify the magnitude of frictional damping which is outside the scope of this study.)

Figure 54 shows the mode shape of the racquet corresponding to the first bending mode. If we consider the oscillation of the racquet at the frequency of the first mode (figure 54) the displacement is entirely in the z direction as it is a bending mode. Resistive gripping pressure applied to the racquet in the x and y directions will have negligible damping effect on the vibrations at the frequency associated with this bending mode. Application of grip pressure in the z direction will generate resistance to the racquet's displacement in this direction, thus representing a source of damping.

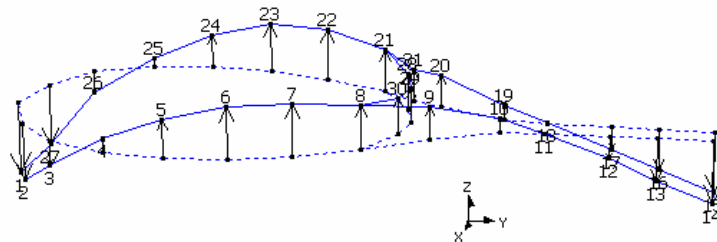


**Figure 54. Mode shape of tennis racquets 1<sup>st</sup> bending mode**

Grip pressures ( $\text{N}/\text{cm}^2$ ) in both the z+ and z- direction will generate a resisting effect on the racquet's displacement. The total pressure in the z direction can be used to establish the resisting effect of the tennis grip on racquet vibrations at the associated frequency of the mode shape. The resistance effect of the tennis grip can be quantified by correlating

the z direction grip pressures and the logarithmic decrement estimates of racquet oscillations at the first resonant frequency.

The forehand grip technique was used to establish the relationship between gripping pressure and the damping of frame vibrations. The different configurations of gripping techniques for different strokes would add significantly to the complexity of the results. Therefore, only the forehand gripping technique was used in the calculation of grip damping.

In summary, the results used to establish the relationship between grip pressure and damping of racquet vibration were ascertained based on the following:

1. Logarithmic decrement has been calculated using post-filtered vibration data based on the frequency of the racquet's first resonant peak. The integer estimation method was used to determine the decay of vibration.
2. The time and amplitude of the oscillation peaks were used to determine the average grip pressure at the corresponding time period.
3. Trials showing no observable resonance peak in the 100-200Hz frequency range were excluded from the analysis as it was deemed that location of the ball impact had aligned with the node of the racquets first bending mode, and therefore no vibrations at the associated frequency had been excited. Damping estimates were therefore not applicable and the data was excluded from the results.
4. Forehand grip pressure data was related to damping results.
5. Racquet A was used in the damping calculations to ensure constant inherent racquet properties.

## 5.2 Grip damping results

The logarithmic decrement estimates were related to grip pressure in different ways to identify the mechanics by which the tennis grip dampens racquet vibrations. This is known as grip damping. The first approach was to relate logarithmic decrement of racquet vibration with the total grip pressure. Figure 55 shows the regression results between the logarithmic decrement and the total grip pressure. The grip pressure used in the regression was estimated by using the sum of all pressure measurements in the forehand grip, irrespective of location on the racquet handle, and determining the average in the same time period used for the logarithmic decrement calculation. (N.B. The lines on displayed on the correlations graphs represent the model line (blue) and the confidence limits at 95% (red).)

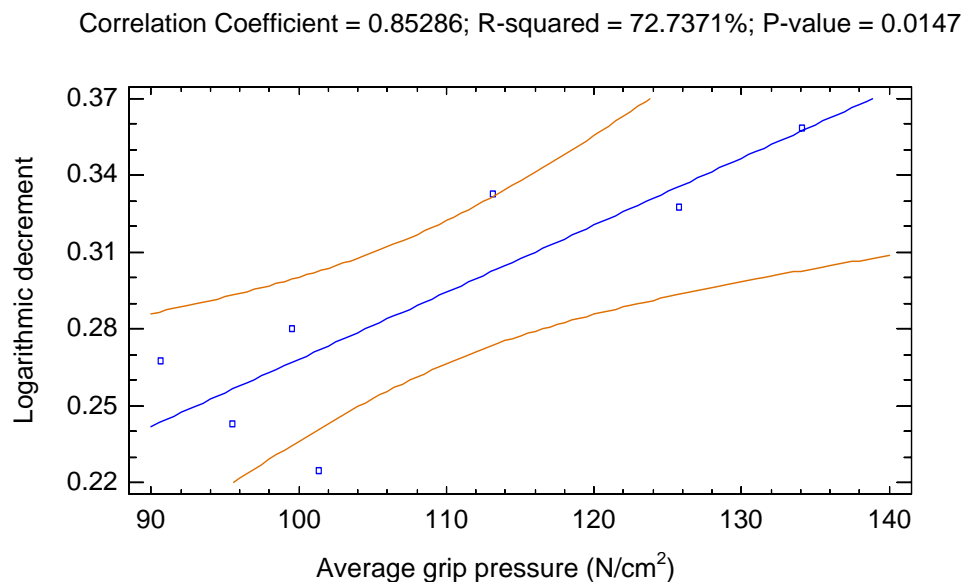


**Figure 55. Damping correlations using the total pressure applied to the racquet handle**

The results from the regression analysis (shown in figure 55), displays a correlation between the two variables with an  $R^2$  value of 72.7%. The p-value is  $>0.05$  making the correlation of 72% between the total pressure and the damping of vibrations associated with the racquet's first bending mode significant to the 95% confidence level. The results show that there is a significant increase in the damping with an increase in grip pressure. An increased rate of decay of vibrations yields an increased logarithmic decrement which represents an increase in damping ratio (see section 4.2.1). The transfer of racquet energy to the player (in the form of vibration) occurs over a certain period of time. A short time period of absorption relates to the greater damping of racquet vibrations by the hand. This is represented by a larger logarithmic decrement (and therefore damping ratio). By absorbing racquet vibrations over a shorter time period, the energy transferred to the players hand will be greater in magnitude than over a longer time period.

### ***5.2.1 Grip damping with respect to mode shapes***

In order to describe the mechanics by which the tennis grip dampens racquet vibrations in terms of absorption with respect to locations on the racquet handle, additional regression analysis between the grip pressure and logarithmic decrement estimates were conducted. As previously discussed in section 5.1.2, mode shapes of a tennis racquet show the direction of displacement along with the location of associated nodes and antinodes. Knowledge of the mode shape for the racquet's first resonant frequency was used to analyse the tennis grip with respect to the distribution of pressure across the racquet handle.

If we consider the tennis grip as a source of resistance to racquet movement over the racquet handle surface, an increase in grip pressure reflects an increase in the resistance effect of the hand. Moreover, an increase in grip pressure provides an increased resistance to the displacement of the racquet handle. The resistance to the displacement of the racquet will be based on two factors. Firstly, the direction of the racquet displacement at the frequency of interest, and secondly the magnitude of pressure applied to the racquet in the same plane. Relationships between damping of racquet vibrations and grip pressure were established using measurements applicable to the displacement of the racquet at the frequency of the first resonant peak. The relationship between grip pressure and vibration damping was also analysed focusing on the locations of grip pressure with respect to the racquet handle. It should be noted that previous research has shown that the tennis grip is not capable of producing sufficient grip pressure to place the racquet under clamped conditions (Brody *et al.* 2002). It was therefore deduced that hand-held gripping conditions are more representative of a freely suspended rather than clamped racquet. The tennis grip is therefore a type of a vibration attenuator that acts as additional damping mass on the racquet and provides a resistance to the racquet displacement. As the mass remains constant (i.e. the hand, forearm and upper arm etc.), the changes in vibration damping during play must therefore be due to the variability of the grip resistance effects (i.e. grip pressure). If grip damping remained constant throughout, the hand-arm system could be considered nothing more than additional mass on the racquet handle. However, the results show that there are variations in racquet vibration damping with respect to changes in grip pressure. The players hand does add mass to the racquet system, but it has a variable effect on the damping of racquet vibrations with respect to the tightness of the tennis grip.

Figure 56 shows the results of the regression analysis involving the logarithmic decrement of racquet vibrations and the measured grip pressure in the z direction. The regression analysis was carried out to show the relationship between the total grip pressure with respect to the displacement of the racquet and the damping of vibrations.

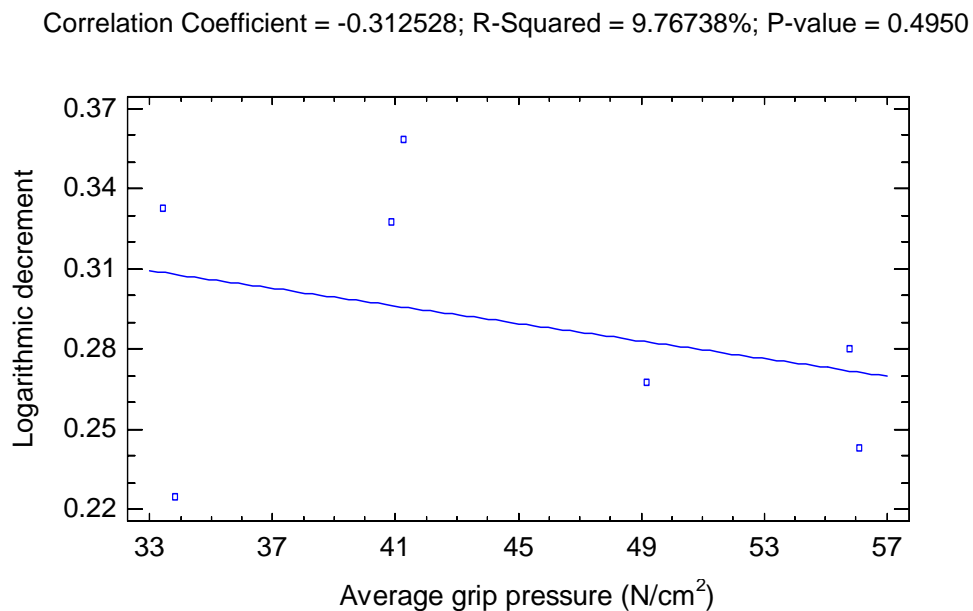


**Figure 56. Damping correlation using the pressure applied to the racquet handle in the z direction**

The results show a weak relationship ( $R^2 = 9.767\%$ ) between the total grip pressure in the z direction and damping at the racquet's first natural frequency. This is in contrast to the strong correlations shown in the earlier regression analysis involving the total pressure applied to the racquet handle in all directions (see figure 55). However, the regression analysis yielded a p-value of 0.495, indicating that the weak correlation between the two parameters was not significant. In order to improve both the significance and correlation levels between the grip pressure in the z direction and damping of racquet vibrations at

the first resonant frequency, additional regression analysis was carried out. The additional regression analysis focused on the location of grip pressure distribution and its proximity to the node location on the racquet handle.

Modal analysis determined that the location of the node on the racquet handle (the handle node) was approximately 163mm (points 11 and 18 shown in figure 54) from the end of the racquet handle (see section 5.1.2). The displacement of the racquet handle at the associated frequency is greatest at the locations closest to the racquet butt and furthest from the handle node (i.e. points 14 and 15 shown in figure 54). When discussing vibration damping, it is important to consider the attachment location of the damping entity (i.e. vibration attenuators, tennis grip etc.). Previous research has shown that vibration attenuators are most effective when they are attached to the structure at locations exhibiting the greatest displacement (i.e. anti-nodes) (Vethecan and Subic 2002). This also applies to the hand-racquet damping interface, as the hand behaves like a vibration attenuator, drastically dampening frame vibrations (Roberts *et al.* 1995; Brody 1987, 1989; Kotze *et al.* 2002; Elliot 1982). The hand acts as a vibration attenuator by attaching to the racquet handle and providing a resistance to its displacement. The degree to which racquet vibrations are attenuated by the hand is related to location of the grip on the racquet with respect to the location of impact and the location of the nodes of the 1<sup>st</sup> mode of oscillation. To examine this hypothesis, regression analysis was carried out using the grip pressure in the z direction and logarithmic decrement estimates, which correspond to the damping of racquet vibrations relating to the 1<sup>st</sup> mode of oscillation.

The pressure applied nearest the node located in the racquet handle (handle node) is 100 mm from the racquet butt (approximately 63 mm from the node location). The pressure applied the furthest distance from the handle node was on the racquet butt (0 mm). The pressures measured on the racquet handle (i.e. from the racquet butt, 0 mm to 100 mm) were divided into two separate sections, upper and lower. Dividing the pressure measurements into the upper and lower handle sections allowed for the effect of the location of pressure application (with respect to the handle node), on vibration damping to be analysed.

Figure 57 shows the regression analysis results for the pressure distributions on the upper handle section, while figure 58 shows results from the pressure distribution on the lower handle section. (N.B. pressure values shown represent the average of the pressure measurements for the upper and lower handle sections, in the z direction, for the same time duration as the logarithmic decrement calculations.)

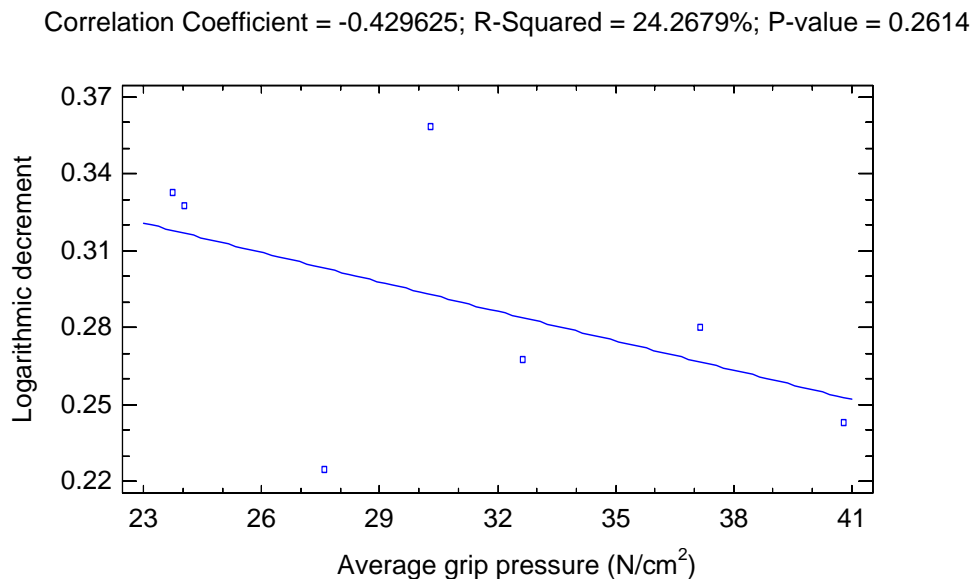


**Figure 57. Damping correlations using the grip pressure applied to the upper handle section**

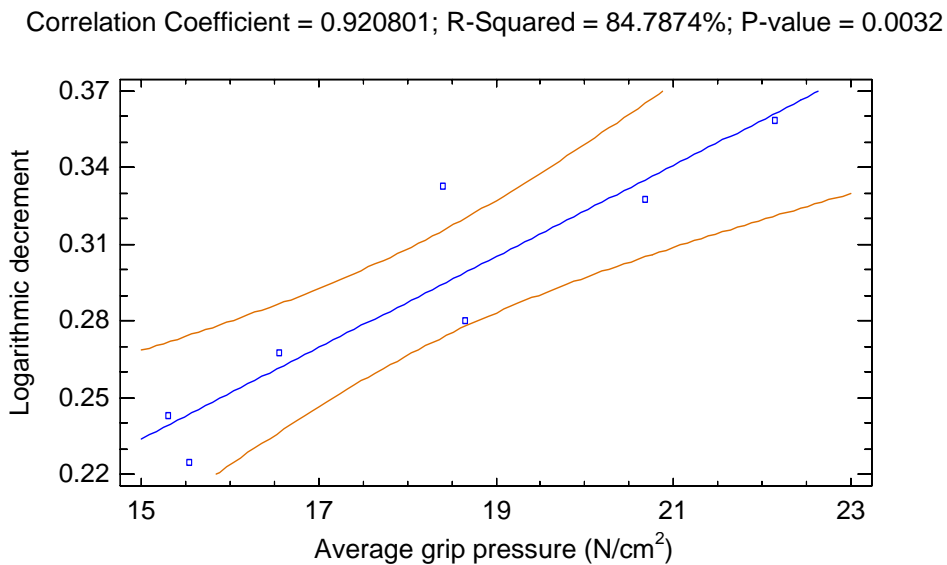


**Figure 58. Linear damping correlations using the grip pressure applied to the lower handle section**

Figure 57 shows an  $R^2$  value of 24.27% and a p-value of 0.261, which indicate weak correlations with no significance between the pressures applied to the upper handle section and the vibration damping relating to the racquet's first mode of oscillation. Contrary to this, the regression results shown in figure 58 show strong correlations ( $R^2 = 84.79\%$ ) between the grip pressure applied for the lower handle section and the vibration damping relating to the racquet's first mode of oscillation. The correlation between the grip pressure on the lower section and the vibration damping, showed significance at the 95% confidence level (p-value = 0.0032). The results of the two regressions for the upper and lower handle sections confirmed that the hand is a vibration attenuator with a varying effect on vibration damping due to the varying locations of the grip on the racquet handle. Variations in gripping pressure at the locations of the handle with the greatest displacement have more influence on the transfer of vibration to the player than changes

in pressure closer to the handle node. The resistance of the grip to the greatest racquet displacement will result in a greater absorption of racquet energy by the player's hand. A greater grip pressure at this location will result in the racquet energy being transferred to the player over a shorter period of time, and it is believed that this causes more discomfort to tennis elbow sufferers, and increased fatigue of not sufferers.

### 5.3 Grip damping model

The regression analysis of the lower handle section shown in figure 58 was calculated using the linear curve fitting model described in equation (1.18), where  $a$  represents the intercept and  $b$  represents the slope of the model. The linear regression analysis yielded the model outlined in equation (1.19), where  $y$  represents the logarithmic decrement of vibrations associated with the racquet's first resonant frequency, and  $x$  represents the pressure applied to the lower handle section in the  $z$  direction

$$y = a + bx \quad (1.18)$$

$$y = -0.03312 + 0.0178063(x) \quad (1.19)$$

The linear model described by equation (1.18) yielded an  $R^2$  value of 84.79%. However, a non-linear regression model was used to optimise both the  $R^2$  and p-values to improve the significance level of the analysis results. The statistic software Statgraphics (StatPoint, USA) was used to compare all possible regression models in the analysis. The optimal model (i.e. the model with the greatest correlation and significance levels) was

found to be that expressed by equation (1.20). The regression analysis yielded the non-linear model given by equation (1.21).

$$y = \left[ a + \left( \frac{b}{x} \right) \right]^2 \quad (1.20)$$

$$y = \left[ 0.849142 + \left( \frac{-5.57305}{x} \right) \right]^2 \quad (1.21)$$

The non-linear regression result of the lower handle section grip pressure in the z direction and the logarithmic decrement damping estimate is shown in figure 59. The non-linear regression analysis yielded optimal R<sup>2</sup> values of 86.2% with a stronger significance level (p-value = 0.0025) than the linear model at the 95% confidence interval.

Correlation Coefficient = -0.928431; R-Squared = 86.1984%; P-value = 0.0025

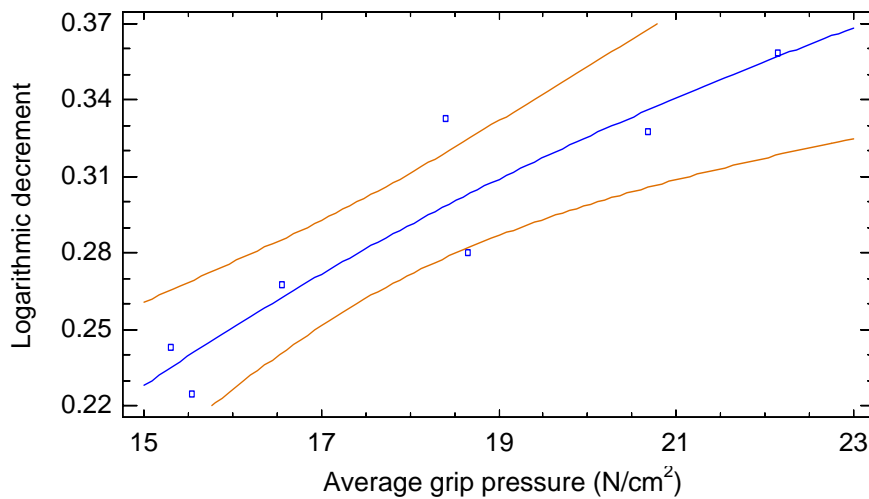


**Figure 59. Non-linear damping correlation using the grip pressure applied to the lower handle section**

Both the linear and non-linear regression models, produced from the analysis of the lower section grip pressure in the z direction and logarithmic decrement, were used to obtain an approximation of damping for a given grip pressure. For a given grip pressure of 20 N.cm<sup>2</sup>, the linear model yielded a logarithmic decrement of approximately 0.323 (eq (1.22)). This equates to an approximate damping ratio of 0.0514. For the same grip pressure (20 N.cm<sup>2</sup>) the non-linear model yielded a logarithmic decrement of approximately 0.325 (eq (1.23)), which equates to an approximate damping ratio of 0.0517.

$$\begin{aligned}
 y &= -0.03312 + 0.0178063(20) \\
 &= -0.03312 + 0.0356126 \\
 &= 0.323006
 \end{aligned}
 \tag{1.22}$$

$$\begin{aligned}
 y &= \left( 0.849142 + \frac{-5.57305}{20} \right)^2 \\
 &= (0.849142 - 0.2786525)^2 \\
 &= 0.5704895^2 \\
 &= 0.325458
 \end{aligned}
 \tag{1.23}$$

Both models yielded similar logarithmic decrement values and associated damping ratio's, however the p-value of the non-linear model (p=0.0025) shows a greater significance level than that of the linear model (p=0.0032). Therefore, the non-linear model is used to determine vibration damping by grip pressure measurements. The development of a reliable non-linear model for this purpose is important because the grip pressure generated is a highly subjective phenomenon.

Each player will generate different pressure distributions in the tennis grip and therefore different magnitudes of vibration attenuation. The measured grip pressure is a subjective phenomenon and is defined by many contributing factors including, individual player grip techniques, racquet swing speed, incoming ball speed and impact location. However, for a specified amount of racquet vibration the model of the tennis grip remains constant (i.e. increase gripping pressure will result in increased vibration damping). Racquet vibration will be absorbed by the player at a magnitude defined by the grip pressure. A tighter tennis grip will result in the transfer of racquet energy to the player (in the form of vibration) over a shorter period of time and at a higher energy level. This relationship between racquet vibrations and grip pressure has been quantified in this thesis and the developed models can be used to show the vibration transferred to the player depending on their grip pressure. The models developed from the measurements of the forehand stroke in this thesis can be applied to all grip pressures. A specified grip pressure measurement in the z direction can be used to estimate the degree of vibration damping and therefore the absorption rate by the player's hand.

#### **5.4 Discussion of findings**

The investigation into the effect of grip pressure distribution on racquet frame vibrations damping, has quantified the relationship between the two parameters. Regression analysis regarding grip pressure and logarithmic decrement describe how a tighter tennis grip will dampen vibrations at a faster rate. The hand is considered the only source of damping in the racquet system (i.e. racquets without string dampeners or active damping systems), and therefore the vibrations not attenuated by the racquet's inherent damping are therefore absorbed by the player's hand. A tighter tennis grip will result in the transfer of

the racquet vibrations over shorter period of time than with a looser grip. The absorption of vibrations over a shorter period of time will result in the player absorbing the racquets energy over a short period of time and therefore at a higher magnitude. The high the magnitude of energy transferred to the player, the greater it is thought the discomfort and rate of fatigue for the player will be.

The grip damping models developed in this thesis can be used to determine the degree of racquet vibration damping by the tennis grip. The exact levels of vibration transferred to the player, are subjective and depend on ball speed and impact location. Therefore precise levels of vibration transferred to the player cannot be modelled. However, the relationship between grip pressure and the transfer of vibration has been described in this investigation and can be used to quantify the levels of vibration transfer to the player for a specified ball impact and grip pressure. The levels of grip damping measured in this research were found to have associated logarithmic decrement values in the range 0.2 – 0.37, for an overall grip pressure or 90 – 140 N/cm<sup>2</sup>.

Two grip damping models have been developed for this purpose, linear and non-linear. Both models had strong correlation and significance levels, for the grip damping relating to the racquets first mode shape. However, the non-linear model had a stronger correlation and significance levels ( $R^2 = 86.2\%$  and  $p=0.0025$ ) than the linear model ( $R^2 = 84.8\%$  and  $p=0.0032$ ). Both models yielded similar grip damping values for a specified grip pressure, but it was concluded that the non-linear model yielded the more accurate estimate of the two.

The transfer of vibrations to the tennis player will occur via the contact locations (see chapter 3). However, the degree to which the vibration is transferred to the player is defined by the location of the grip contact points on the racquet handle and their proximity to the node location of the racquet handle. The further from the handle node the contact location is, the greater the absorption of racquet energy. Moreover, a greater grip pressure at these locations will increase the magnitude of racquet energy absorbed by the player's hand.

## **Chapter 6**

### **Conclusions and recommendations**

## 6.1 Conclusions

The research presented in this thesis aimed to determine the characteristics of vibration damping by the player's hand via the tennis grip. The research has made significant contributions to the current body of knowledge with respect to the quantification of parameters defining the transfer of racquet vibration to the player's hand and arm. The following is a summary of main findings from this research:

- Additional modes of oscillations associated with the racquet frame have been identified and attributed to the vibrations of the strings.
- The distribution of grip pressure within the tennis grip has been describe and contact locations within the tennis grip exhibiting the greatest magnitude of pressure have been identified. It was shown that the contact locations within the grip exhibited pressure values greater than  $60\text{N}/\text{cm}^2$ .
- Variations in grip pressure distribution before, during and after impact have been quantified and related to both the tennis racquet and the player's hand. Grip pressure distribution profiles have allowed for the contraction of forearm muscles and moreover the means of vibration transfer to the player's arm to be hypothesised. Quantification of pressure distribution profiles with respect to different stroke types has allowed for the means of vibration transfer to the player's hand and arm to be hypothesised and related to each stroke. Strokes with medially contracted forearm muscles (i.e. service and forehand) will absorb racquet vibration around this medial area of the forearm. Alternatively, strokes with the lateral forearm muscles contracted (i.e. backhand) will absorb the racquet energy around the lateral areas of the forearm.

- The grip damping phenomena has been quantified by relating the variations in grip pressure distribution to the magnitude of racquet vibration damping during impact. The relationship between the racquet's first mode of oscillation and the location of grip pressure on the racquet handle has been show to be non-linear. The further from the node in the racquet handle grip pressure is applied, the greater the grip damping effect. An increase in grip pressure results in the damping of racquet vibrations over a shorter period of time, therefore increasing the level of racquet energy absorption.

The general and specific outcomes are described in the sections below. The initial objectives are outlined together with in-depth conclusions based on the findings of the research:

### **6.1.1 General outcomes**

- *Establish the inherent structural dynamic properties of the test tennis racquets and examined the influence of strings on frame modes* – Modal analysis was carried out in chapter 2 for both of the tennis racquets used in this research. The results determined the racquet's natural frequencies in the frequency range 0-1000Hz, and the associated damping and mode shapes. Results showed that the addition of the tennis strings to the racquet system also introduced additional modes of oscillation at approximately 568Hz and 894 Hz, with respect to the structure of racquet B. These additional modes were attributed to the excitation of string vibrations.

- *Quantify the tennis gripping tightness* – The tennis grip tightness was quantified in chapter 3 using experimental techniques. The tennis grip tightness is a highly subjective phenomenon which is defined by the swing speed, incoming ball speed, ball impact location, and the individual player. However, under controlled laboratory conditions a gripping force was found to be in the range of 50 – 200 N depending of the location in the tennis grip. The maximum gripping force was generated approximately 0.398 s after impact. Measurement of characteristic grip force variations identified two peaks during impact. These are attributed to both the movement of the racquet in the player’s hand, and the player’s desire to control this movement by increasing the grip tightness.
- *Quantify tennis racquet vibration damping* – Chapter 4 described the different sources of damping of racquet vibration. Ball damping and grip damping were both quantified using experimental techniques. It was found that ball damping is associated with the racquet’s 2<sup>nd</sup> mode of oscillation producing a damping ratio greater than 0.70263. It has been established that the magnitude of ball damping effect is defined by the degree of racquet recoil. A reduction in racquet recoil (caused by the tennis grip) produced a longer ball dwell time and consequently a greater damping of racquet vibrations at the frequency of the racquet’s second mode. Grip damping was quantified using subjective grip tightness. It has been established that with an increase in grip tightness there is an associated small increase in the damping of racquet vibrations. The magnitude of the damping ratios calculated (based on Q estimates) ranged from 0.11029 for light grip tightness, to 0.14615 for a very tight grip. (N.B. These test results were based on only 4 subjective data points and therefore the validity of the analysis could be

questionable. Despite this the result can still be used as a subjective guide to grip damping, and this relationship was investigated in greater detail in later chapters.) Regression analysis of grip damping showed strong correlation and significance levels between grip tightness and the damping of racquet vibrations. The relationship between grip tightness and racquet vibration damping was found to be non-linear. The non-linear relationship was validated by conducting the same tests using both racquets.

- *Quantify the distribution of grip pressure and its effect on the damping of racquet vibrations* – Chapter 5 quantified the distribution of grip pressure and its effect on the damping of racquet vibrations (i.e. grip damping). Using grip pressure measurements ( $\text{N}/\text{cm}^2$ ), the damping effect caused by variations in grip pressure has been modelled. The relationship between the overall grip pressure and the magnitude of vibration damping has been established using logarithmic decrement estimates. Logarithmic decrement estimates ranged from 0.22 – 0.37 for an overall grip pressure of 90 – 140  $\text{N}/\text{cm}^2$ . Grip pressure was related to the mode shape corresponding to vibrations at the racquet's first resonance during impact. The grip damping regression analysis, based on the racquet's mode shape, produced results showing that vibration damping is determined by not only grip pressure, but also the location of the tennis grip on the racquet handle and its proximity to handle node of the mode shape. The further from the handle node the tennis grip is located, the greater the damping of racquet vibrations, and moreover the transfer of racquet energy to the player. The modelling of the grip damping phenomena found the optimal model (i.e. that which produced the strongest correlation and significance levels) to be non-linear. By using a specified grip

pressure of 20 N/cm<sup>2</sup> it was therefore possible to estimate a logarithmic decrement value of 0.325. With an increase in grip pressure there is an associated increase in vibration damping. Increases in damping equate to the absorption of racquet vibrations by the player at a larger magnitude as racquet vibrations are dampened over a short time period. The absorption of the racquet's vibration energy at larger amplitudes (i.e. a tighter tennis grip) is thought to cause discomfort to tennis elbow sufferers and increases fatigue of non-sufferers, in addition to increasing the likelihood of instigating the injury.

- *Relate the transfer of racquet vibration to the contact areas and their associated pressure distributions* – The transfer of vibration to specific areas of the hand was discussed in chapter 5. It was determined that the magnitude of vibration transfer to the player was defined by both grip pressure and the proximity of grip contact points to the racquet handle node. The further from the racquet handle node a grip contact point is, the greater the absorption of transfer of vibration. Moreover, an increase in gripping pressure at this location will generate a greater absorption of racquet vibration than a similar pressure increase closer to the node.

### **6.1.2 Specific outcomes**

- *Identify key locations in the tennis grip with the greatest magnitudes of grip pressure* – Pressure sensitive film was used in chapter 3 to qualitatively analyse the tennis grip. The pressure film allowed for the distribution of pressure across the player's hand to be described, by identifying the contact points with the greatest magnitudes of contact pressure within the tennis grip. The main contact

locations in the tennis grip were found to be at the following locations on the player's hand for a continental tennis grip:

- MP joint of the index, 3<sup>rd</sup> and 4<sup>th</sup> fingers
  - Distal phalanx of the thumb
  - Middle phalanx of all phalanges around the middle IP joint
  - Middle metacarpals of the 3<sup>rd</sup> and 4<sup>th</sup> fingers.
- 
- *Evaluate grip pressure distribution characteristics for different stroke types in the time domain* – Tennis grip pressure distributions were quantified in chapter 3 using hydrocell pressure sensors. Grip pressures were quantified in terms of contact locations on the player's hand and the distribution across the racquet handle. Characteristics distributions of grip pressure were established for the forehand, service and backhand tennis strokes. The results showed opposing pressure distributions between upper and lower handle sections for all stroke types. This opposing distribution is attributed to the movement of the racquet in the player's hand and the player's resistance to this movement both before and after impact. The magnitudes of grip pressure were found to be greater than 60 N/cm<sup>2</sup>, similar to those measured using the pressure sensitive film. By establishing the distribution of pressure in the tennis grip it was possible to hypothesise specific hand movements for each stroke type. This allowed for further assumption of the required muscle contractions required in order to resist racquet movement. By suggesting hand movements and their related muscle contractions it was possible to describe the means of racquet vibrations energy transfer to specific locations on the player's forearm. It has been hypothesised that

the racquet energy will be transferred to the medial forearm locations for forehand and service strokes and lateral forearm locations for backhand strokes. This is based on the contracted muscles in the forearm before, during and after impact.

- *Describe the effect of player perception* – Player perception was addressed in chapter 2. In laboratory controlled conditions (i.e. stationary hand-held racquet – moving ball) it was possible to estimate the player’s grip reaction time to the incoming ball. The grip reaction time was calculated using the time of initial increase in grip force in relation to the time of impact. It was established that the player required approximately 0.398 s to prepare the racquet for impact in terms of grip stiffness characterisation. The increase in grip stiffness is required to give control over the rebound ball in terms of speed and direction. It was determined that the player requires an approximate time of 0.498s to generate the required grip stiffness to control the impact. However, this time estimate was based on stationary hand-held racquet conditions and therefore may increase with the introduction of a moving racquet scenario because of the need to generate racquet speed.
- *Determine the effectiveness of the piezoelectric damping system on the Head Intelligence racquet* – An experimental test procedure was developed in chapter 4 to estimate the damping effectiveness of a given racquet. Two racquets were used to test the effectiveness of the piezoelectric damping system. It was unknown which of the two racquets had the damping system embedded before the research commenced. The experimental tests in chapter 4 established that racquet B had the system embedded, and from this it was possible to compare the damping of the two racquets (racquet A having the same dimensions but no piezoelectric

damping system). By comparing the results of the two racquets, it was concluded that a racquet with piezoelectric damping system was 28% more effective at dampening the racquet vibrations than a racquet without this type of system.

The research has established that the tennis grip is a highly variable parameter with respect to the transfer of racquet vibrations to the player. The magnitude of grip pressure is subject to the individual player, incoming ball speeds, impact location and racquet swing speeds. Consequently the levels of vibrations transferred to the player are also subject to these defining factors. In this research, the relationship between grip pressure and the damping of racquet vibrations has been quantified and modelled. The grip damping models developed in this thesis were found to be applicable for determining the levels of vibration absorption by the tennis grip for any racquet or stroke type, provided grip pressure measurements and the inherent damping of the racquet are known.

This research has quantified grip damping in tennis racquets. However, the tennis racquet can be thought of as a simple beam structure that is used to strike a moving object. Therefore the grip damping models established in this thesis can be applied to other racquet and bat sports, where transfer of sports equipment vibration to the athlete is of concern with respect to injury, fatigue and performance.

## **6.2 Recommendations**

The effect of the tennis player's hand grip on the rate of vibration absorption has been quantified in this research. This information can be used in the development of vibration attenuation systems for tennis racquets. Vibration attenuation systems are designed based

on the freely suspended racquet system. However, this thesis has found the racquet to behave quite differently when gripped by the player during impact. With the introduction of the player's hand to the racquet system the natural frequency of the tennis racquet is decreased together with a change in vibration damping. The player's hand is the best vibration attenuator at present however, it is this absorption of racquet energy that is thought to cause upper extremity discomfort. Future designs need to accommodate the effect of vibration absorption by the hand with respect to the proximity of the tennis grip to the racquet handle node. By simply altering the locations of the racquet nodes and varying the natural frequencies, the levels of vibrations absorption by the player's hand can be reduced.

The piezoelectric damping system tested in this research represent a new generation of vibration attenuation systems that aim reducing the levels of racquet shock and vibration absorbed by the tennis player. The 28% effectiveness of this system for freely suspended racquets, determined in the research, is an indication of how effective such systems can be. The increased vibration attenuation by the piezoelectric system was indistinguishable with hand held racquets, due to the 880% vibration absorption of the tennis grip. If a vibration attenuation system is to be effective in the reduction of vibration absorption by the player, tests should be able to distinguish between different racquets under hand held conditions. In order to optimise such systems, the design needs to incorporate the effect of the hand on the racquet structure, in terms of changes in node location, natural frequency and grip damping effects.

Further research needs to focus on quantifying the relationships (if any) between the levels of racquet vibration absorption by the hand and the magnitude of discomfort and injury status with respect to tennis elbow. Clinical research to date has not proved that tennis elbow is caused by racquet vibrations but it is still thought by many to be a major contributor to the injury. Clinical evidence needs to be discovered to provide precise magnitudes of racquet vibration absorption by the player and determine if this causes aggravation and instigation of the tennis elbow injury.

This research has focused on the damping of racquet vibrations by the player's hand during impact. Future research need to quantify the relationship between the tennis grip and the behaviour of the racquet regarding its axis of rotation in the grip. The changes in the location of the racquet COP needs to be related to the gripping pressures. Quantifying this relationship will allow for models to be established regarding the transfer of shock forces to the player's hand.

Research into the biomechanics of the player's arm, hand and wrist during impact together with muscle behaviour is essential if contributing factors to tennis elbow injuries are to be reduced. The racquet-hand system with respect to racquet vibrations has been investigated in this research; however the biomechanics of the lower arm needs to be considered as well in order to determine the effects of shock and vibration transfer on the player.

## References

Baker, J.A. & Putnam, C.A. (1979) Tennis racquet and ball responses during impact under clamped and free-standing conditions. **Research Quarterly**, 50, pp.164-170.

Beards, C.F. (1995) **Engineering Vibration Analysis with Application to Control systems**. 1<sup>st</sup> ed. London, Edward Arnold.

Brannigan, M. & Adali, S. (1999) Mathematical modeling and simulation of a tennis racquet. **Medicine and Science in Sports and Exercise**, 1, pp.44-53.

Brebner, J.T. & Welford, A.T. (1980) Introduction: an historical background sketch. In: Welford, A.T. ed. **Reactions Times**, New York, Academic Press, pp.1-23.

**Brüel & Kjær**, Nærum, Denmark.

Brody, H. (1979) Physics of the tennis racket. **American Journal of Physics**, 47 (6), pp.482-487.

Brody, H. (1981) Physics of the tennis racket II: “sweet spots”. **American Journal of Physics**, 49 (9), pp.816-819.

Brody, H. (1987) Models of tennis racket impacts. **International Journal of Sport Biomechanics**, 3, pp.293-296.

Brody, H. (1989) Vibration damping of tennis rackets. **Journal of Sports Biomechanics**, 5, pp.293-296.

Brody, H. (1997) The physics of tennis III: The ball-racket interaction. **American Journal of Physics**, 65(10), pp.981-987.

Brody, H., Cross, R. & Crawford, L. (2002) **The physics and technology of tennis**. Solana Beach, California, Racquet Tech Publishing.

Cassel, E. & McGrath, A. (1999) **Lobbing the injury out of tennis – a review of literature**. Report#144. Monash University, Australia.

Cavanagh, P.R., Hewitt, F.G.Jr. & Perry, J.E. (1992) In-shoe plantar pressure measurement: a review. **The Foot**, 2, pp.185-194.

Chadwick, E.K.J. & Nicol, A.C. (2001) A novel force transducer for the measurement of grip force. **Journal of Biomechanics**, 34, pp.125-128.

Cottey, R., Kotze, J., Lammer, H. & Zirngil, W. (2006) An extended study investigating the effects of tennis rackets with active damping technology on the symptoms of tennis elbow. In: Moritz, E.F. & Haake, S.J. ed. **6<sup>th</sup> International Conference on the Engineering of Sport, 2006, Munich**, pp.391-369.

Crawford, L. (2000) Head's Intelligence technology – the shocking truth. **Racquet TECH**.

Cross, R. (1997) The dead spot of a tennis racket. **American Journal of Physics**, 65, pp.754-764.

Cross, R. (1998a) The sweet spot of a baseball bat. **American Journal of Physics**, 66 (9), pp.772-779.

Cross, R. (1998b) The sweet spot of a tennis racket. **Sports Engineering**, 1 (2), pp.63-78.

Cross, R. (1999) Impact of a ball with a bat or racket. **American Journal of Physics**, 67 (8), pp. 692-702.

Cross, R. (2001) Customising a tennis racket by adding weights. **Sports Engineering**, 4, pp.1-14

Cross, R. (2004) Centre of percussion of hand-held implements. **American Journal of Physics**, 72 (5), pp.622-630.

David, J. & Cheeke, N. (2002) **Fundamentals and Applications of Ultrasonic Waves**. Boca Raton, Florida, CRC Press LCC.

Dossing, O. (1988) Structural testing part I: Mechanical mobility measurements. **Brüel & Kjør**, Denmark.

Elliot, B. (1982) Tennis: the influence of grip tightness during the tennis stroke. **Medicine and Science in Sports and Exercise**, 14 (5), pp.348-352.

Ewins, D.J. (1984) **Modal testing: Theory and Practice**. Wiley, Research Studies Press.

Gade, S., Herlufsen, H. & Konstantin-Hansen, H. (2005) Application note: how to determine the modal parameters of simple structures. **Brüel & Kjør**, Denmark.

Giangarra, C.E., Conroy, B., Jobe, F.W., Pink, M. & Perry, J. (1993) Electromyographic and cinematographic analysis of elbow function in tennis players using single- and double- handed backhand strokes. **American Journal of Sports Medicine**, 21 (3), pp.394-399.

Grabiner, M. (1983) Resultant tennis ball velocity as a function of off-centre impact and grip firmness. **Medicine and Science in Sports and Exercise**, 15, pp.542-544.

- Griffin, M.J. (1998) Part VI – General Hazards – Vibration. In: Stellman, J.M. ed. **Encyclopedia of Occupational Health and Safety**. 4<sup>th</sup> Ed, Chapter 50. International Labour Office.
- Grollman, S. (1969) **The human body: its structure and physiology**. 2<sup>nd</sup> ed. New York, Macmillan.
- Harris, C.M. (2002) **Shock and Vibration Handbook**. 5<sup>th</sup> ed. New York, McGraw-Hill.
- Hatze, H. (1976) Forces and duration of impact, and grip tightness during the tennis stroke. **Medicine and Science in Sport**, 8 (2), pp.88-95.
- Hatze, H. (1998) The centre of percussion of tennis rackets: a concept of limited applicability. **Sports Engineering**, 1, pp.17-25.
- Hennig, E.M., Rosenbaum, D. & Milani, T.L. (1992) Transfer of tennis racket vibrations onto the human forearm. **Medicine and Science in Sports and Exercise**, 24 (10), pp.1134-1140.
- Inman, D.J. (1994) **Engineering Vibration**. Englewood Cliffs, New York, Prentice Hall.
- Iwatsubo, T., Kanemitsu, Y., Sakagami, S. & Yamaguchi, T. (2000) Development of a racket with an “Impact Shock Protection System”. In: Haake, S.J. & Coe, A. ed. **Tennis Science and Technology**, London, Blackwell Science, pp.101-108.
- Kamien, H.A. (1990) A rational management of tennis elbow. **Sports Medicine**, 9 (3), pp.173-191.
- Kawazoe, Y., Tomosue, T., Yoshinari, K. & Casolo, F. (2000) Predictions of impact shock vibrations of a racket grip and player’s wrist joint in the forehand drive. In: Subic,

A. & Haake, S.J. ed. **3<sup>rd</sup> International Conference on the Engineering of Sport, 2000, Sydney**, pp. 1-8.

Kawazoe, Y. & Yoshinari, K. (2000) Predictions of impact shock of the players wrist: comparisons between two super large sized rackets with different frame mass distribution. In: Haake, S.J. & Coe, A. ed. **Tennis Science and Technology**. London, Blackwell Press, pp.91-99.

Kotze, J., Mitchell, S.R. & Rothberg, S.J. (2000) The role of the racket in high-speed tennis serves. **Sports Engineering**, 3, pp.67-84.

Kotze, J., Lammer, H., Cottey, R. & Zirngibl, W (2003) The effects of active peizo fiber rackets on tennis elbow. In: Miller, S. ed. **Tennis Science and Technology 2**, London, ITF.

Knudson, D.V. & White, S.C. (1989) Forces on the hand in the tennis forehand drive: application of force sensing resistors. **International Journal of Sports Biomechanics**, 5, pp.324-331.

Knudson, D.V. (1991) Forces on the hand in the tennis one-handed backhand. **International Journal of Sports Biomechanics**, 7, pp.282-292.

Lammer, H. & Kotze, J (2003) Materials and tennis rackets. In: Jenkins, M. ed. **Materials in Sport**, Cambridge, England, Woodhead Publishing Ltd, pp.391-369.

Li, F-X., Fewtrell, D. & Jenkins, M. (2004) String vibration dampers do not reduce racket frame vibration transfer to the forearm. **Journal of Sports Sciences**, 22, pp.1041-1052.

Meriam, J.L. & Kraige, L.G. (1993) **Engineering Mechanics: Dynamics**. 3<sup>rd</sup> ed. New York, Wiley & Sons. Inc.

Mogk, J.P.M. & Keir, P.J. (2003) Crosstalk in electromyography of the proximal forearm during gripping tasks. **Journal of Electromyography and Kinesiology**, 13, pp.63-71.

Morris, M., Jobe, F.W., Perry, J., Pink, M. & Healy, B.S. (1989) Electromyographic analysis of elbow function in tennis players. **American Journal of Sports Medicine**, 17 (2), pp.241-247.

Nirschl, R.P. (1986) Soft-tissue injuries about the elbow. **Clinics in Sports Medicine**, 5 (4), pp.637-652.

Ollivierre, C.O. & Nirschl, R.P. (1996) Tennis elbow: Current concepts of treatment and rehabilitation. **Sports Medicine**, 22, pp.133-139.

**Orthopaedic Website for Health Professionals** [On-line] <http://www.auscast.org>, July 5<sup>th</sup>. 2005.

Orlin, M.N. & McPoil, T.G. (2000) Plantar pressure assessment, **Physical Therapy**, 80 (4), pp.399-409.

**Paromed Medizintechnik GmbH**, Munich, Germany.

**Pediatric Advisor** [On-line] 2005, <http://www.med.umich.edu>, 5<sup>th</sup> July. 2005.

Perttunen.J.R. & Komi, P.V. (2001) Effects of walking speed on foot loading patterns. **Journal of Human Movement Studies**, 40, pp.291-305.

**Polytec GmbH**, Waldbronn, Germany.

Rao, S.S (1995) **Mechanical Vibration**. 3<sup>rd</sup> ed. Reading, Massachusetts, Addison Wesley.

Reynolds, D.D., Standlee, K.G. & Angevine, E.N. (1977) Hand-arm vibration: Part III Subjective response characteristics of individuals to hand induced vibrations. **Journal of Sound and Vibration**, 51, pp.267-282.

Roberts, P.E., Brody, H., Dillman, J.C. & Groppe, J.L. (1995) The biomechanics of tennis elbow: An integrated approach. **Clinics in Sports**, 14, pp.47-57.

Robinson, E.S. (1934) Work of the integrated organism. In: Murchison, C. ed. **Handbook of general experimental psychology**, Worcester, MA, Clark University Press.

Rosenbaum, D. & Becker, H-P. (1997) Plantar pressure distribution measurements: Technical background and clinical applications. **Foot and Ankle Surgery**, 3, pp.1-14.

Savitzky, A. & Golay, M.J.E. (1964) Smoothing and differentiation of data by simplified least squares procedures. **Analytical Chemistry**, 36, pp.1627-1639.

**Sensor Products Inc.**, East Hanover, NJ, USA

Scahff, P.S. (1993) An overview of foot pressure measurement systems. **Clinics in Podiatric Medicine and Surgery**, 10, pp.403-415.

Sinclair, D. (1975) **An introduction to functional anatomy**. 5<sup>th</sup> ed. Oxford, Blackwell Scientific Publications.

Sports Marketing Surveys USA. (2003) **Tennis Consumer Technology Report**, commissioned by HEAD Sport AG.

**StatPoint Inc.**, Virginia, USA.

Stroede, C.L., Noble, L. & Walker, H.S. (1999) The effects of tennis racket string vibration dampers on racket handle vibrations and discomfort following impacts. **Journal of Sport Science**, 17, 397-385.

**Sytsat Software Inc.**, Point Richmond, USA.

Taylor, J.L. (1994) **The vibration analysis handbook – A practical guide to solving rotating machinery problems**. Tampa, FL, Vibration Consultants Inc.

**The Tennis Server** [On-line] <http://www.tennisserver.com>, 20<sup>th</sup> June. 2005.

Thompson, W.T. (1993) **Theory of vibration with applications**. 4<sup>th</sup> ed. Englewood Cliffs, NJ, Prentice-Hall.

**Vibrant Technology Inc.**, Scotts Valley, USA

Vethecan, J.K. & Subic, A.J. (2002) Vibration attenuation of tennis racquets using tuned vibration absorbers. **Sports Engineering**, 5, pp.155-164.

Welford, A.T. (1980) Choice reaction time: Basic concepts. In: Welford, A.T. ed. **Reactions Times**, New York, Academic Press, pp.73-128.

Wilson, J.F. & Davis, J.S. (1995) Tennis racket shock mitigation experiments. **Journal of Biomechanical Engineering**, 117, pp.479-484.

Zequera. M.L., Solomonidis, S.E., Vega, F. & Rondon, L.M. (2003) Study of plantar pressure distribution on the sole of the foot of normal and diabetic subjects in the early stages by using a hydrocell pressure sensor. In: Leder, R.S. **25<sup>th</sup> Annual Conference of the IEEE Engineering in Medicine and Biology Society, 2003, Cancun, Mexico**, pp.1874-1877.



# Appendices

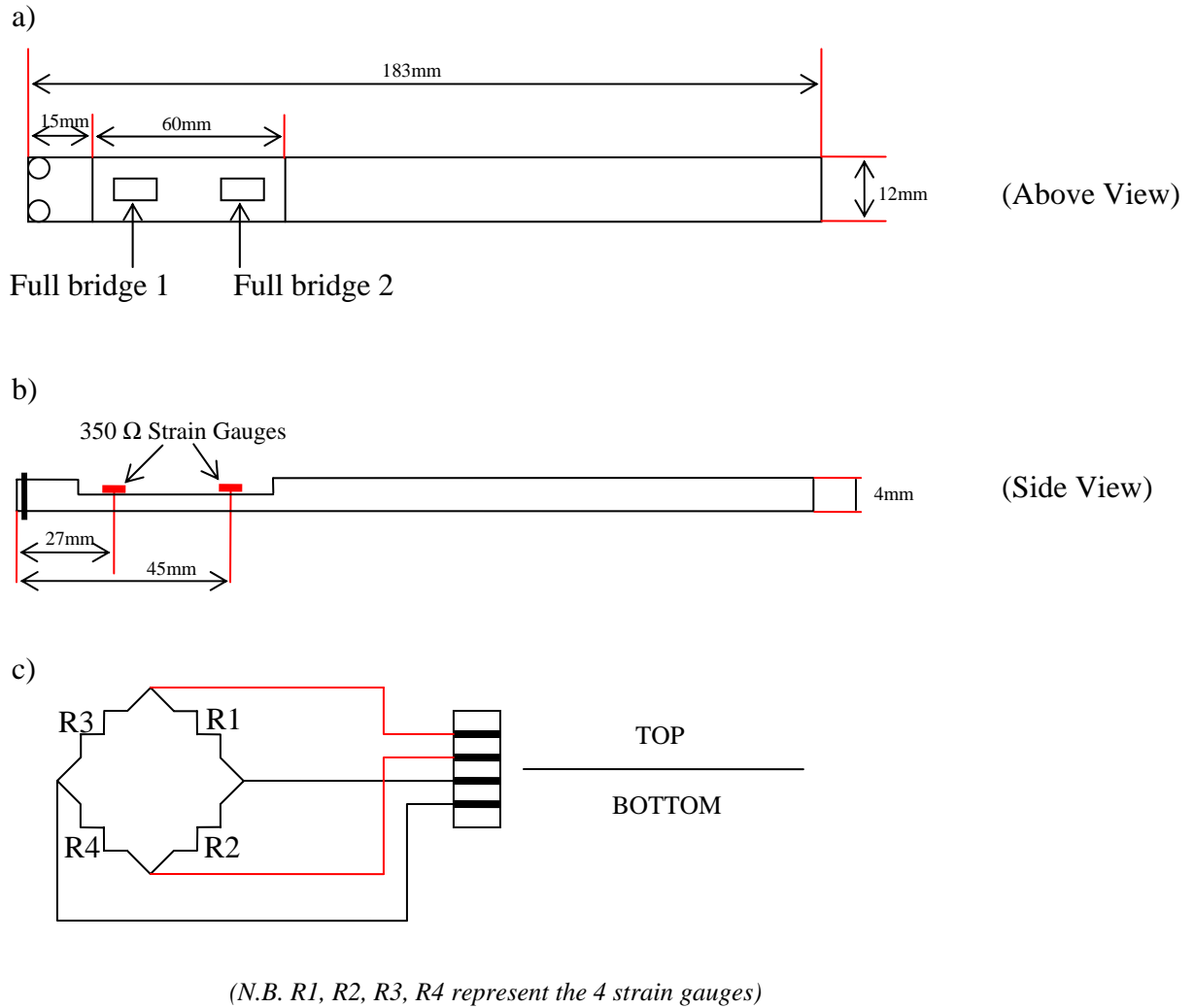
## 8.1 Appendix 1

### 8.1.1 *Development of a strain gauge cantilever system for the measurement of tennis gripping forces*

The following instrumentation was used in the set-up of the stain gauge cantilever system:

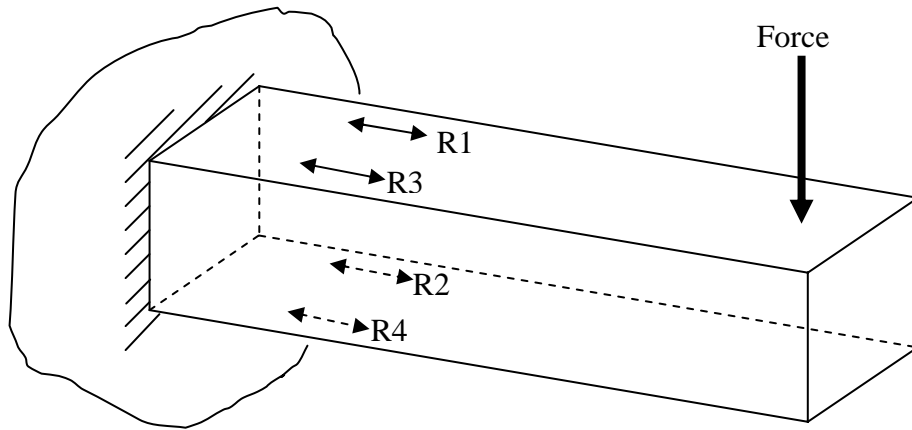
- 16 x 350 $\Omega$  Strain gauges (J2A-09-S033P-350)
- Lightweight PCB 352C65 accelerometer (mass – 2.28g)
- National Instruments DAQ card

Four cantilever beams have been manufactured from steel to the dimensions shown in figure 60a) and b) together with the attachment of the two full bridge strain gauge configurations to the cantilever. Full Wheatstone bridge configurations were used as the circuit provides temperature compensation. Temperature compensation is necessary to eliminate the effect of temperature variations on voltage change and heat effects of the tennis grip. The trough on the cantilever beam was included in the design to isolate the bending of the beam. The beam bending was isolated to ensure all bending of would be measured by the strain gauges and therefore reduce the degree of error introduced in the experiments. The strain gauges are attached to the beam trough in two locations (figure 60) with full Wheatstone bridge configurations.



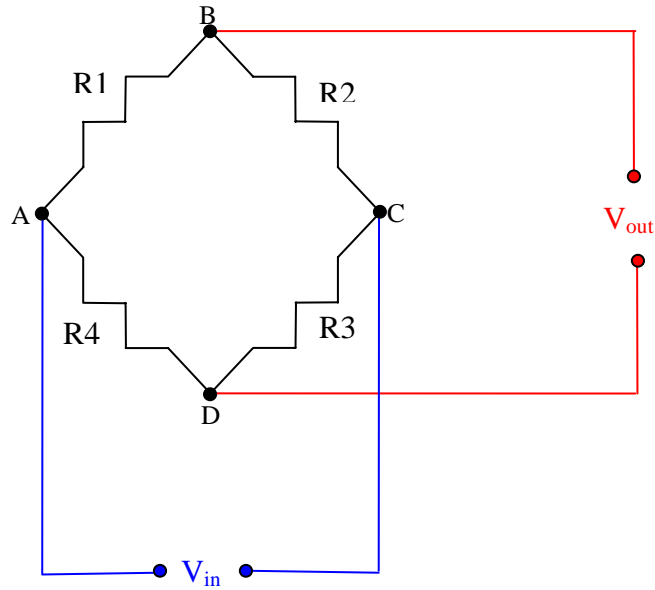
**Figure 60. Schematic of the cantilever beam and circuit diagram**

Figure 60.c) shows the full Wheatstone bridge strain gauge circuit diagram for the cantilever beam. 350 $\Omega$  parallel strain gauges were bonded to both the top and bottom of the cantilever beam in the bend isolating trough. Figure 61 shows the orientation of the full Wheatstone bridge on the cantilever beam.



**Figure 61. Full Wheatstone bridge orientation on a cantilever beam**

Gauges R1 and R3 are attached to the top of the beam while gauges R2 and R4 are attached to the bottom of the beam. Strain imparted on the beam is obtained by measuring the variations between the upper and lower gauges. The circuit diagram shown in figure 62 represents the four resistances of the strain gauges (R1:R4) and the four terminals (A: D) where an excitation voltage ( $V_{in}$ ) is supplied and a response voltage ( $V_{out}$ ) is measured.  $V_{out}$  is the total strain measured by the full Wheatstone bridge and can be calibrated to show the loading of the beam.



**Figure 62. Wheatstone bridge circuit diagram**

Equation (1.24) shows the calculation of voltage variations between terminals A and B ( $V_{AB}$ ). Similarly, equation (1.25) gives the expression of voltage variation between terminals A and D ( $V_{AD}$ ).

$$V_{AB} = \frac{R_1}{R_1 + R_2} V_{in} \quad (1.24)$$

$$V_{AD} = \frac{R_4}{R_3 + R_4} V_{in} \quad (1.25)$$

The overall variation of voltage can be determined using equation (1.26). The measured voltage ( $V_{BD}$ ) is proportional to the overall strain imparted to the beam at that location.

$$V_{BD} = V_{AB} - V_{AD} = \left( \frac{R_1 R_3 - R_2 R_4}{(R_1 + R_2)(R_3 + R_4)} \right) V_{in} \quad (1.26)$$

By measuring the variation of ( $V_{BD}$ ), the applied force (N) to the cantilever beam can be estimated. The estimation of the applied force is calculated from the difference between the two strain gauge measurements. The measurement is independent of the loading location on the cantilever and represents the cumulative force on the beam.

Four cantilever beams were used in the experiments to monitor the gripping dynamics, which are the variations in gripping force during impact together with approximate magnitude of force. The four beams are labelled A: D to enable an analysis of gripping dynamics with respect to variations in gripping force during impact. Each of the four beams has two full Wheatstone bridge strain gauge configurations attached within the bend isolation trough, as shown in figure 60.

The two full bridge configurations on each cantilever beam were labelled channel 1 and channel 2. The difference between the measured variations from each full bridge (channel 1 and 2) was calibrated to produce an expression for the force on the cantilever beam in (N). The calibration of the beams is explained in section 8.1.1.1.

Once the strain gauge configurations were attached to the cantilevers, the beams were attached to a manufactured test racquet handle butt. The handle butt was manufactured from an aluminium alloy (AI7075) and was designed to attach to the end of the racquet handle. The handle butt was used to attach the four cantilever beams to racquet handle. Both the racquet butt and racquet handle had milled grooves to allow for the displacement of the cantilever beams during hand-held conditions. Figure 63 and figure

64 show the dimensions for the manufactured test racquet handle butt. Figure 63 shows the dimensions of the handle butt from an end view. The butt was an elongated octagon with two sides of 20mm in length and two sides of 15 mm in length, with an addition four sides of equal length (12mm). The longer sides of 15mm and 20 mm were used as attachment points for the cantilever beams. Figure 64 shows the dimension of the racquet butt from a side view, focusing on the surface for the cantilever beam attachment. A section of 12mm x 60mm was milled out to of the butt to allow for the displacement of the beam during loading. The cantilever beams were attached to the racquet butt using two screws 5mm from the end of the manufactured racquet butt. The butt itself was attached to the racquet handle using 4 screws, 67mm from the end of the butt on the four smaller sides of the octagon shape.

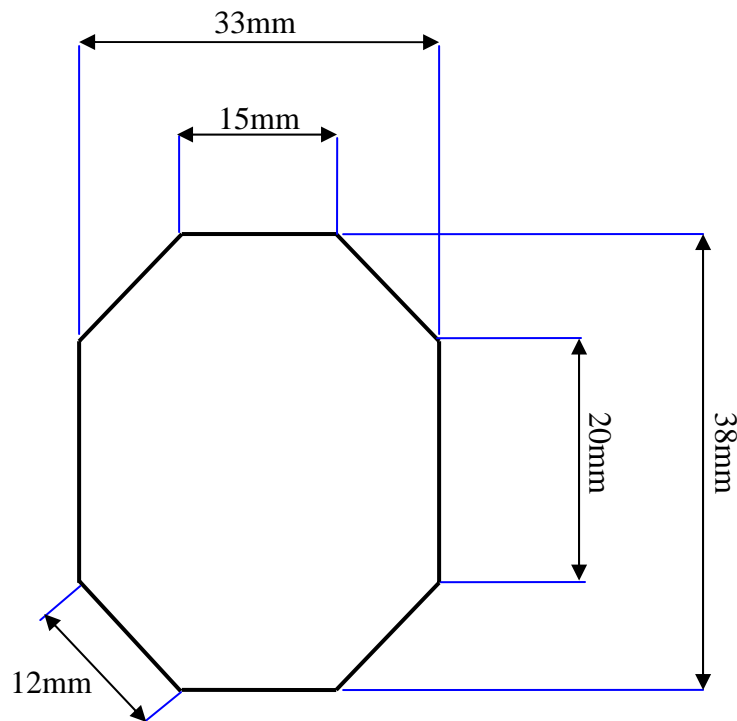
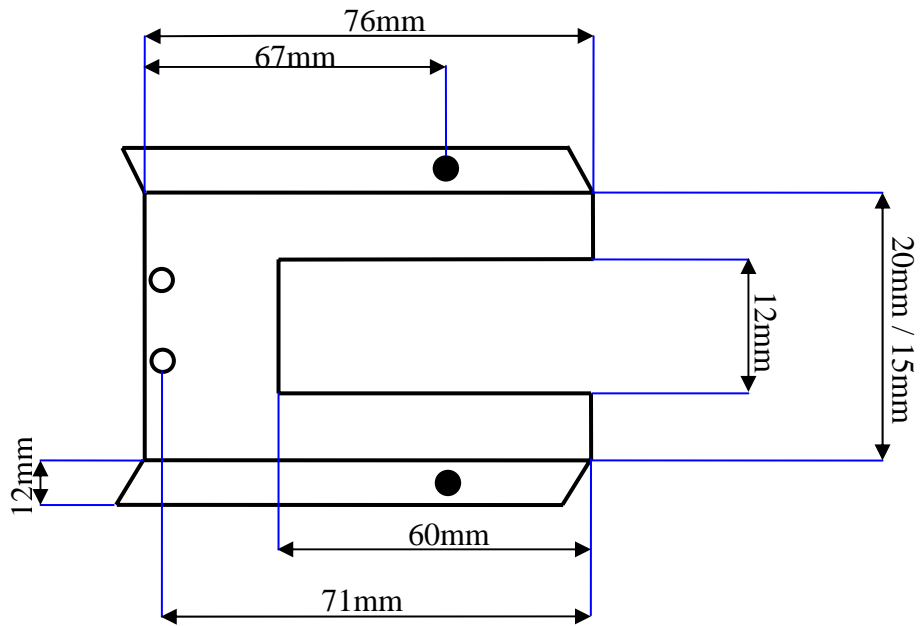
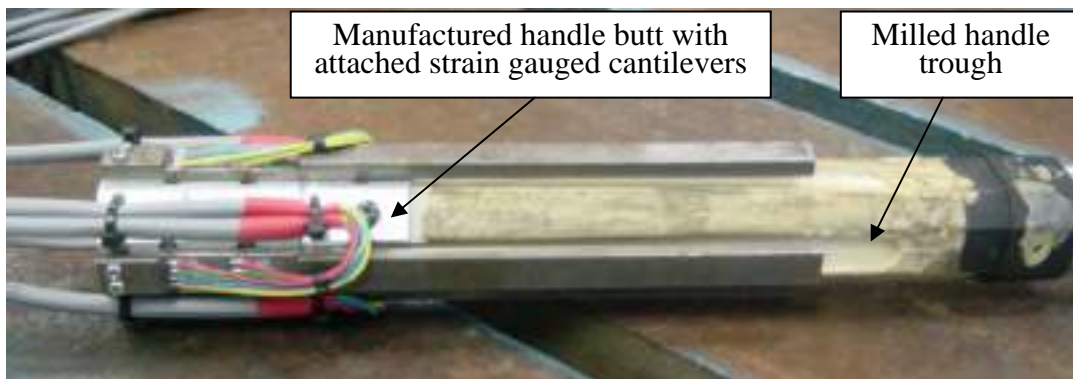


Figure 63. Test racquet handle butt (end view dimensions)



**Figure 64. Test racquet handle butt (side view dimensions)**

A trough was milled in the racquet handle to align with the cantilever beams. The trough is required to allow for the displacement of the beams under loading conditions figure 65 shows milled sections of the racquet handle and the test handle system after the attachment of the manufactured butt and strain gauge cantilevers.



## **Figure 65. Hand grip cantilever test system**

### *8.1.1.1 System calibration*

Before the hand grip cantilever test system was used to acquire real time gripping data, calibration of the strain gauge configuration was required. The test racquet was firstly made rigid by clamping the top of the racquet to a table. Rigidity was needed to prevent any displacement of the racquet when calibration weights were loaded onto the cantilever beams. Each beam was individually calibrated by measuring the change in voltage with increase in load, from each of the full bridges (channel 1 and channel 2) on the cantilever. The calibration of each beam was done by placing calibration weights onto a plate (1.21kg) to load the beam. The known weight was recorded together with the output voltage for Ch1 and Ch2. The weights were increased by 0.5kg increments until 10kg was loaded onto the cantilever beam. The weights were then removed in 0.5kg increments and a second voltage was recorded for each load interval. The average of the two voltages was used to calculate the difference between the two channels for a given load. The calculated difference between the two channels for each load was graphed to find the equation for the gradient of the strain relationship. The equation for the gradient of each beam is shown in figure 66, together with the calibration chart. The calibration chart shows the raw data points for each of the beams A: D. Each of the raw data plots is accompanied with a regression plot from which the gradient equation has been determined. The gradient equations have been used to calibrate the acquired data from a raw voltage (mV) measurement to a force unit (N).

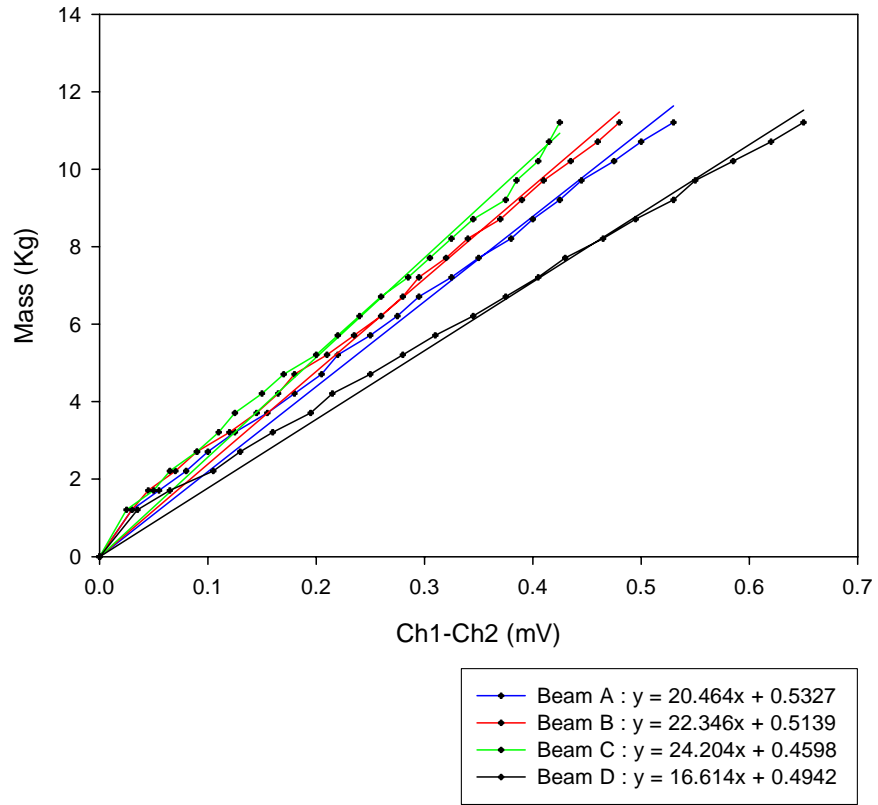
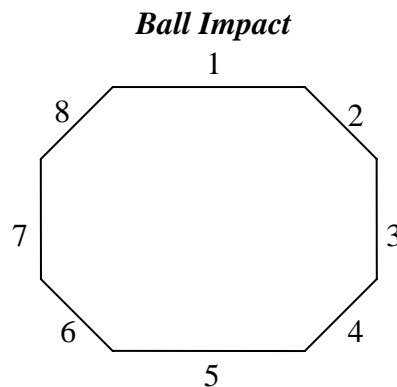


Figure 66. Calibration chart for beams A: D

## 8.2 Appendix 2

### 8.2.1 Locations of hydrocell pressure sensor attachments on the racquet handle

Up to twenty one individual hydrocell pressure sensors are required here to analyse the variations in pressure distribution at the important contact locations determined in section 3.1. The contact locations of interest were all the phalanx from the MP joint to the distal bones, the thumb and the 3<sup>rd</sup> and 4<sup>th</sup> bones of the metacarpal system. Figure 67 shows the numbers of the racquet handle sides for the configuration of the hydrocell locations and the contact locations of interest. Table 15 describes the locations of the hydrocell attachment on the racquet handle for the continental forehand, and table 16 describes the hydrocell locations for the service and backhand strokes. The tables describe the attachment locations in terms of the side number (see figure 67) and the distance from the racquet butt to the centre of the hydrocell. (N.B. Hydrocells 2, 3 and 11 were removed from the data collection due to technical problems with the voltage signal.) Before the pressure sensors are attached to the racquet, the gripping material is removed from the handle, so that the measurements of gripping pressure would not be affected by the deformation of the gripping material.



**Figure 67. Racquet handle side configuration**

<b>Hydrocell</b>	<b>Side</b>	<b>Distance (mm) (from butt 0mm)</b>
1	7	74
2	2	54
3	N/A	N/A
4	1	10
5	1	11
6	1	99
7	8	10
8	7	46
9	1	83
10	1	37
11	N/A	N/A
12	2	30
13	6	50
14	7	19
15	4	68
16	6	65
17	8	62
18	8	111
19	1	58
20	4	93
21	5	12

**Table 15. Hydrocell attachment locations for the continental forehand grip**

<b>Hydrocell</b>	<b>Side</b>	<b>Distance (mm) (from butt 0mm)</b>
1	2	53
2	N/A	N/A
3	N/A	N/A
4	7	16
5	5	47
6	1	67
7	8	15
8	4	12
9	1	87
10	5	13
11	N/A	N/A
12	1	100
13	8	38
14	6	20
15	8	62
16	2	54
17	8	45
18	6	43
19	6	65
20	3	63
21	5	85

**Table 16. Hydrocell attachment locations for the service and backhand slice grips**

## 8.3 Appendix 3

### 8.3.1 *Half power bandwidth damping calculation*

The half power damping calculation method (often referred to as the Quality Factor (Q)) is an estimation of the damping associated with the modes of oscillation of a structure. The estimation of damping is based in the frequency domain and can be used with any expression of magnitude (i.e. acceleration ( $\text{m/s}^2$ ), velocity ( $\text{m/s}$ ), displacement ( $\text{m}$ )). The method can be used with either frequency response function or frequency response measurements.

The half power estimation uses the points at either side of the resonant frequency for an identified mode. The half power points are calculated by finding the frequencies at magnitudes equal to that of the resonance  $\times 0.707$  (or 3dB below the peak magnitude) (Taylor 1994; Thompson 1993; David and Cheeke 2002). The half power points are chosen because they identify the frequency range that needs to be excited to produce the resonance/mode peak. This frequency range is known as the mode's amplification factor. A mode is referred to as a single frequency, but in-order for this mode to be excited there must be adequate excitation of frequencies both greater and smaller than the peak frequency. A large frequency bandwidth means excitation of a greater number of frequencies is required to excite the mode of the system. The further apart the half power points are from the resonant frequency (i.e. the wider the resonant peak) the greater the associated damping of the vibrations at the resonant frequency. A sharp resonance peak means that the excitation of fewer frequencies is required for the excitation of the system mode and therefore there is less associated damping.

Figure 68 shows an example of a resonance peak obtained from a frequency response analysis. A peak magnitude is identified along with the half power magnitude (*peak magnitude*  $\times 0.707$ ). The peak frequency is identified as  $\omega_n$  and the corresponding half power frequency are identified as  $\omega_1$  and  $\omega_2$ .

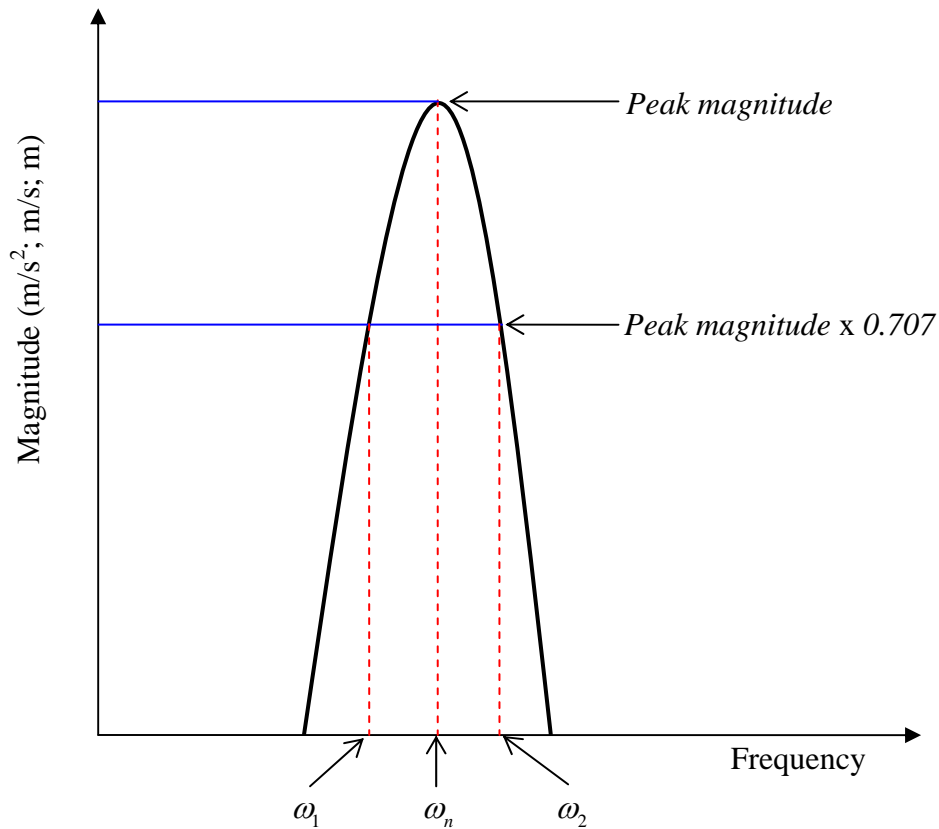


**Figure 68. Half power damping parameter identification**

Once the parameters of the half power damping estimation have been identified they are applied to the equation (1.27).

$$Q = \frac{\omega_2 - \omega_1}{\omega_n} = \frac{1}{2\zeta} \quad (1.27)$$

Equation (1.27) shows the expression of Q using the half power points. The equation also shows the relationship between the half power damping estimation and the damping ratio of the mode. Figure 69 shows an example frequency response and the identification of the half power damping estimation parameters.

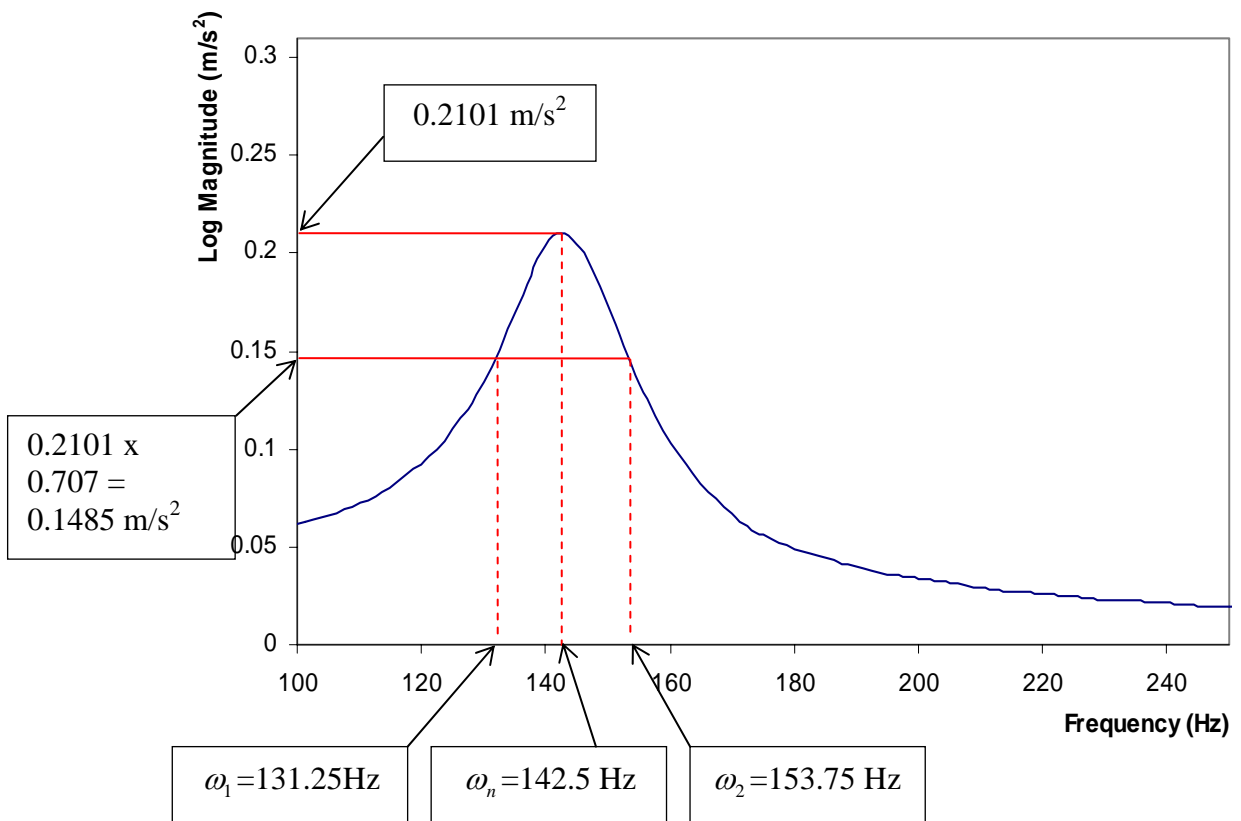


**Figure 69. Example of half power damping parameter identification**

The half power damping parameters identified in figure 69 have been used in equation (1.28) to estimate the Quality factor using the half power bandwidth technique.

$$\begin{aligned}
Q &= \frac{\omega_2 - \omega_1}{\omega_n} \\
&= \frac{153.75 - 131.25}{142.5} \\
&= \frac{22.5}{142.5} \\
Q &= 0.15789
\end{aligned}
\tag{1.28}$$

Equation (1.29) shows the expression of the modes damping ratio by using the Quality factor estimation in equation (1.28).

$$\begin{aligned}
\zeta &= \frac{1}{2Q} \\
&= \frac{1}{2(0.15789)} \\
&= \frac{1}{0.31578} \\
\zeta &= 3.1668
\end{aligned}
\tag{1.29}$$

The half power bandwidth damping estimation (Quality factor) is based in the frequency domain. As a result of the damping estimation being based in the frequency domain, correlations with time based variables are not possible. The estimation is an expression of the damping present in the system assuming that the parameters defining the dynamic response of the system remain constant throughout the data collection period. Variable defining parameters may result in variation in the rate of decay of vibration and this is not considered when using the half power bandwidth damping estimation. If time based variables are included in the investigation, then time based damping estimation should be utilised.

## 8.4 Appendix 4

### 8.4.1 Subjective Gripping data

The data presented in this appendix shows the response of the two racquets A and B during ball impacts. A summarised for of the results is presented in chapter 4 together with a discussion of the findings. The variation of modes 2-4 is very little so the data presented here is focused on the first mode ( $\omega^1$ ). Table 17 shows the response data for racquet A during ball impacts while table 18 shows the data for racquet B. Both tables show the frequency resonant frequency for the first mode of oscillation under different gripping conditions together with the associated half-power damping estimation. The tables also include the standard deviations and averages of the two response parameters.

<b>Grip Condition</b>	<b>Trial</b>	<b><math>\omega^1</math> (Hz)</b>	<b>Standard Deviation</b>	<b>Average</b>	<b><math>\zeta</math> (Q)</b>	<b>Standard Deviation</b>	<b>Average</b>
Free	1	183.75	0	183.75	0.020408163	0	0.020408
Free	2	183.75			0.020408163		
Free	3	183.75			0.020408163		
Free	4	183.75			0.020408163		
Free	5	183.75			0.020408163		
Light	1	170	1.629801	170.25	0.095588235	0.027067	0.124698
Light	2	168.75			0.111111111		
Light	3	168.75			0.133333333		
Light	4	172.5			0.166666667		
Light	5	171.25			0.116788321		
Medium	1	162.5	1.976424	165	0.138461538	0.007364	0.127322
Medium	2	167.5			0.126865672		
Medium	3	163.75			0.129770992		
Medium	4	166.25			0.120300752		
Medium	5	165			0.121212121		
Tight	1	162.5	1.629801	162.25	0.146153846	0.020001	0.149539
Tight	2	142.5			0.157894737		
Tight	3	141.25			0.132743363		
Tight	4	142.5			0.157894737		
Tight	5	145			0.155172414		

**Table 17. Response data of racquet A for tennis ball impacts**

<b>Grip Condition</b>	<b>Trial</b>	$\omega^1$ (Hz)	<i>Standard Deviation</i>	<i>Average</i>	$\zeta$ (Q)	<i>Standard Deviation</i>	<i>Average</i>
Free	1	162.5	0	162.5	0.023076923	0	0.023077
Free	2	162.5			0.023076923		
Free	3	162.5			0.023076923		
Free	4	162.5			0.023076923		
Free	5	162.5			0.023076923		
Light	1	148.75	1.629801	149	0.117647059	0.013336	0.120865
Light	2	150			0.1		
Light	3	147.5			0.127118644		
Light	4	147.5			0.13559322		
Light	5	151.25			0.123966942		
Medium	1	146.25	2.338536	146.25	0.11965812	0.007161	0.129927
Medium	2	143.75			0.139130435		
Medium	3	150			0.133333333		
Medium	4	146.25			0.128205128		
Medium	5	145			0.129310345		
Tight	1	141.25	1.530931	142.5	0.17699115	0.015726	0.156139
Tight	2	142.5			0.157894737		
Tight	3	141.25			0.132743363		
Tight	4	142.5			0.157894737		
Tight	5	145			0.155172414		

**Table 18. Response data of racquet B for tennis ball impacts**